FACULTY OF ENGINEERING
AND ARCHITECTURE

Light emission from a stack of chiral and nematic dye-doped liquid crystal

Yu-Tung Hsiao
Student number: 02001774

Supervisors: Prof. dr. ir. Kristiaan Neyts, Prof. dr. ir. Jeroen Beeckman
Counsellor: Frederik Van Acker

Master's dissertation submitted in order to obtain the academic degree of
European Master of Science in Photonics

Academic year 2021-2022

GHENT
UNIVERSITY

Statement of confidentiality

Confidential up to and including 20/06/2042

This master dissertation contains confidential information and/or confidential research results proprietary to Ghent University or third parties. It is strictly forbidden to publish, cite or make public in any way this master's dissertation or any part thereof without the express written permission of Ghent University. Under no circumstance may this master dissertation be communicated to or put at the disposal of third parties. Photocopying or duplicating it in any other way is strictly prohibited. Disregarding the confidential nature of this master dissertation may cause irremediable damage to Ghent University. The stipulations mentioned above are in force until the embargo date.

FACULTY OF ENGINEERING
AND ARCHITECTURE

Light emission from a stack of chiral and nematic dye-doped liquid crystal

Yu-Tung Hsiao
Student number: 02001774

Supervisors: Prof. dr. ir. Kristiaan Neyts, Prof. dr. ir. Jeroen Beeckman
Counsellor: Frederik Van Acker

Master's dissertation submitted in order to obtain the academic degree of
European Master of Science in Photonics

Academic year 2021-2022

GHENT
UNIVERSITY

Acknowledgements

First and foremost, it's a great honor of me to study in University of Ghent. I would like to thank Professor Kristiaan Neyts, Jeroen Beeckman and Tsung-Hsien Lin, who have introduced me to the wonderful world of liquid crystal field and provided me with this immensely rewarding research opportunity, and who continued to inspire me with the brilliance. I am immensely grateful to PhD student Frederik Van Acker, my supervisor, who has so patiently guided me throughout the past year and teaching me many lab techniques. I could not have hoped for a better mentor. Special thanks to Sunqian Liu, my friend and PhD student in our lab, who is always there helping me and solving my problems and accompany me in those days in the laboratory.

I would like to thank all the other members of the liquid crystals and photonics lab in UGent and liquid crystal photonics lab in National Sun Yat-sen University who have offered me support along the way: Brecht Berteloot, Migle Stebryte, Qiming Sun, Xiangyu Xue, Yera Ussembayev and Inge Nys from UGent; Hung-Chang Jau, Duan-Yi Guo, Ting-Mao Feng, Li-Min Chang, and Guan-Wu Lin from National Sun Yat-sen University. I am also thankful for the companionship of the other undergraduates, Birger Deserrano, Yu Nung Huang, Kaiwen Chen, Ruqi Shi, Yancan Wu and Yao Tung Chang.

I would like to thank all of my wonderful friends who have made my National Sun Yat-sen University and UGent experience the best it could have been.

Most of all, I would like to thank Mom, Dad and my brother Bo-Chian for their unconditional love, support, and encouragement that has led me here today. I am forever grateful for their presence in my life. This thesis is dedicated to my family.

Yu-Tung Hsiao June 2022

Permission of use on loan

The author gives permission to make this master dissertation available for consultation and to copy parts of this master dissertation for personal use. In all cases of other use, the copyright terms have to be respected, in particular with regard to the obligation to state explicitly the source when quoting results from this master dissertation.

June 2022

Abstract

Cholesteric liquid crystal-based laser is characterized as easy fabrication, self - assembly, small structure size and high tunability. In the past literature, the optical phenomenon of the defect structure was mainly observed by simulating or by measuring the transmission spectrum, and a few of them successfully excited the defect laser. It is needless to say to make a high-quality tunable defect mode laser. That is why I try to make defect mode laser but still keep the tunable characteristic of cholesteric liquid crystal.

Laser is made of a material with optical gain placed between two reflectors. For the gain I use photo-luminescent dye-doped liquid crystal layers. Light emitting organic molecules can effectively provide gain when the material is excited with a short laser pulse. For two reflectors, I make reflective cholesteric liquid crystal film which can spontaneously form a periodic grating and reflect specific wavelength as one-side mirror. And, as for the other side mirror, I use metal coating substrate as a mirror. Layers with gain and layers which effectively reflect light can be combined to realize lasing in an organic stack. I successfully made the organic stacks by depositing polymerized cholesteric liquid crystal layer which is designed at proper reflective wavelength. From the results, I assumed that I measured the photo-luminescence and lasing of my sample. Furthermore, by applying voltage, I investigated the wavelength shift. However, there is a problem in wavelength modulation. The voltage cannot be continuously applied for a long time. In the future, it would be interesting to conduct further experiments to confirm the results and solve the modulation problems.

Keywords: Cholesteric liquid crystal film, light emission, wavelength modulation

摘要

膽固醇液晶雷射具有結構尺寸小、可調控性佳等特點。尤其膽固醇液晶製作出的缺陷雷射，還兼具有低雷射閾值的優點。在以往的文獻中，主要通過模擬或測量透射光譜來觀察缺陷結構的光學現象，少數成功地激發了缺陷雷射。更不用說，製作高品質的可調缺陷雷射。因此，本論文目標希望能製備缺陷雷射並期達成可連續調控的波長的效果。

雷射是由兩個反射器及具有光學增益的材料製成。我們利用可以自發形成周期性光柵並反射特定波長的膽固醇型液晶膜製作其中一面反射鏡，而另一反射鏡利用金屬塗佈而成的玻璃基板製成。將上述兩反射鏡堆疊中間灌入光致發光染料摻雜的液晶層我們即完成樣品製作。我們發現當材料被脈衝雷射激發時，染料有效地提供增益並激發雷射產生。此外，通過施加電壓，我們觀察到了微幅的波長位移。然而，在波長調控上發生無法長時間連續施加電壓調控的問題。在未來，我們將做進一步的實驗來確定及改善初步的結果。

關鍵詞：膽固醇液晶薄膜、發光元件、發光波長調製

Light emission from a stack of chiral and nematic dye-doped liquid crystal

Yu-Tung Hsiao

Supervisor(s):Kristiaan Neyts, Jeroen Beeckman, Tsung-Hsien Lin, Frederik Van Acker

Department of Electronics and Information Systems, Ghent University, Technologiepark-Zwijnaarde 126,9052, Gent, Belgium

***Abstract*— Cholesteric Liquid crystal-based lasers are characterized by their easy fabrication, self-assembly, small structure size and high tunability. Additionally, with the advantage of lower threshold condition, I would like to make a tunable cholesteric liquid crystal-based defect mode laser. To demonstrate the simulation results of the defect mode appearance done by Frederik Van Acker, I made my own sample and measured it with our laser measurement setup. In this research, by optimizing fabrication process, I successfully made the organic stacks by depositing polymerized cholesteric liquid crystal layer which is designed at proper reflective wavelength. From the results, I assumed that I measured the photo-luminescence and lasing of my sample. Furthermore, by applying voltage, I investigated the wavelength shift.**

Keywords—Cholesteric liquid crystal film, light emission, wavelength modulation

I. INTRODUCTION AND PROPOSED METHOD

In recent years, many researchers have stepped into the cholesteric liquid crystal based laser field. Cholesteric Liquid crystal-based lasers are characterized as easy fabrication, self-assembly, small structure size and high tunability. There are two main kinds of applications in laser field: One is cholesteric liquid crystal band edge mode laser. The laser happens at the edge of bandgap owing to the zero group velocity in this area; the other is cholesteric liquid crystal defect mode laser. It gives rise to the resonance in specific wavelength in the photonic bandgap by designing the defect structure in the cholesteric liquid crystal layer. Due to the advantage of the lower threshold[1], I would like to make a defect mode laser. The continuous tunability has not been fully presented, so here I hope to fully present the wavelength-tunable defect laser through simulation and experiments.

The schematic of our tunable defect mode laser sample is designed as below figure. I use mirror and cholesteric liquid crystal film as our resonant cavity. Then, I fill in liquid crystal E7 and Dye mixture. E7 is supposed to help changing phase retardation by applying different AC voltage to tune the position of the defect mode. As for dye, it acts as the gain media. The simulation results based on our designed structure are made by Frederik Van Acker. It is demonstrated that the defect mode laser can be found in our designed structure. In this research, I will make the cell and use the experimental methods to verify the results of the tunable laser. It is expected that by applying different voltages I will obtain a laser spectrum shifted in the photon energy gap.

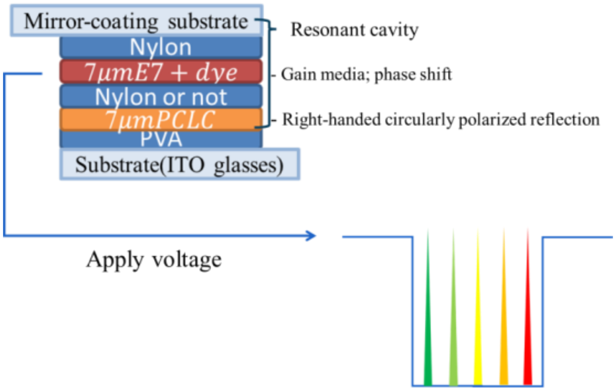

Figure. 1 Schematic of the designed structure

II. SIMULATION

Based on the simulation results from one of my supervisors PhD student Frederik van Acker, I believed that it is possible to make a defect mode laser according to our designed structure. The laser occurs at the position where the lowest threshold appears. The results are shown as below figure. 2. I found three data and they are represented as long band edge, short band edge, and defect mode in the band gap. I demonstrated that I can obtain defect mode laser at 1/4 wave plate condition (controlled by liquid crystal layer).

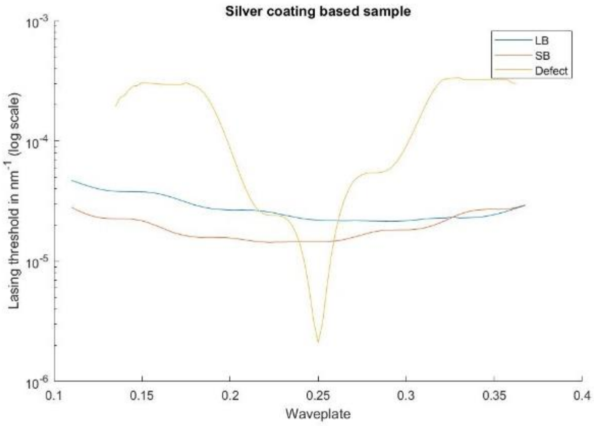

Figure. 2 laser threshold simulation with silver-coated based sample

I further simulated the position where the lowest threshold happened. X represents the position in the sample. 0 is the place where the glass substrate surface locates closed to the position of CLC film. 1 is the place where the mirror surface exists closed to the position of liquid crystal film. I detected that the lowest threshold occurs when defect mode forms and the gain are located at the edge of mirror-based substrate. Based on the simulation results, I am capable of detecting defect mode laser with our designed structure. I can obtain the best property of defect mode laser at the position of liquid crystal layer by silver coated mirror-based sample. The following experiments are conducted in order to demonstrate the simulation results I get.

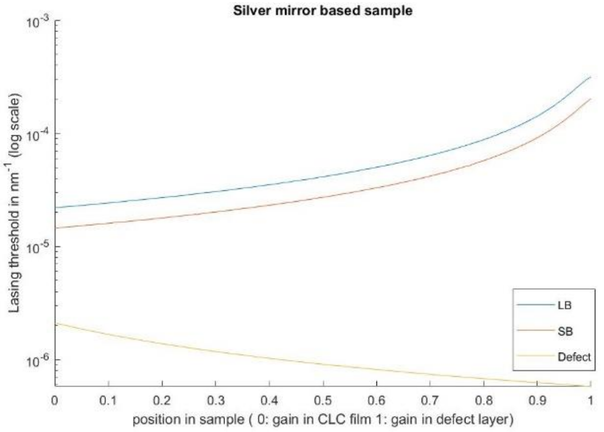

Figure. 3 the position where lowest laser threshold occurs

III. MATERIALS AND EXPERIMENT

In the research, two kinds of mixtures- cholesteric liquid crystal and dye doped in liquid crystal are prepared as below shown.

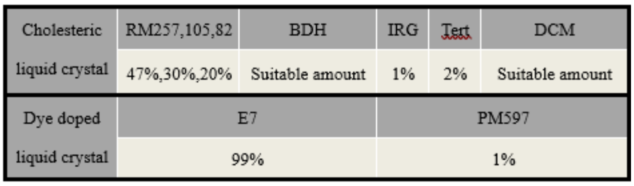

Cholesteric	RM257,105,82	BDH	IRG	Tert	DCM
liquid crystal	47%,30%,20%	Suitable amount	1%	2%	Suitable amount
Dye doped	E7		PM597		
liquid crystal	99%		1%		

Figure. 4 Composed ratio of two mixtures in this research

I divided our fabrication process into a four step: preparation of the cells, fabrication of one-side cholesteric liquid crystal film by the recipe of Cholesteric liquid crystal in Figure. 4, preparation of mirror-based cholesteric liquid crystal film and filling in the cells with dye and E7 mixture as the recipe of the dye-doped liquid crystal. The schematic of process flow is shown below.

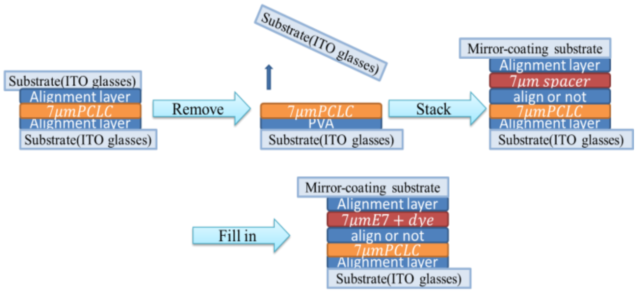

Figure. 5 Schematic of process flow

I utilized polarized optical microscopy to view the optical performance of my sample and spectrometer to detect the wavelength. Laser measurement system is shown in Figure. 6. Nd-YAG pulsed laser which generates laser light at 532nm is the pumping laser source. The laser beam is then passing through the half wave plate, polarized beam splitter and lenses and ND filter. And then, the laser light is focused on the sample and excited the laser dye. I further detect the laser signal at 45 degree of the pumping laser emission direction. By the filter, the emission laser beam can be blocked. The spectrometer detects only the signal from the excitation of our sample. Finally, to investigate the variation of applying different voltages, I utilize function generator to apply voltage.

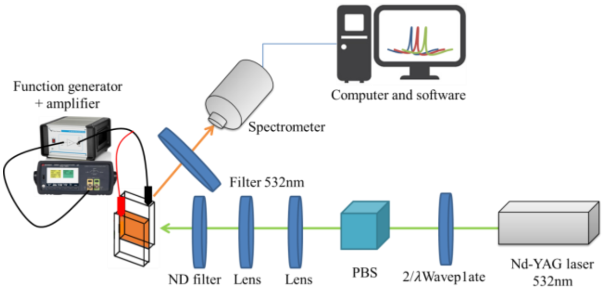

Figure. 6 defect mode laser measurement system

IV. RESULTS AND DISCUSSION

A. Sample Fabrication and Optimization the sample process

- Two side substrates with different alignment layers

To obtain the high quality of the Cholesteric Liquid Crystal film, I have to lift one-side substrate off perfectly. The following figure is the schematic process of getting rid of substrate.

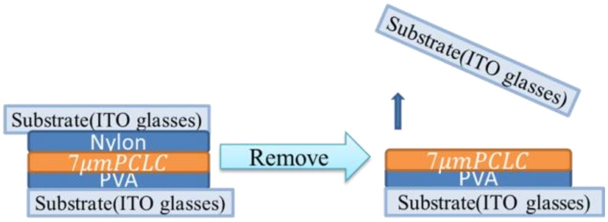

Figure. 7 Schematic of removal of various alignment layers

I stack up PVA based substrate and PVA based substrate to make our cell. Based on the difference of alignment layers, chemical interactions between the alignment layers and liquid crystal molecules are supposed to differ from each other and give rise to the different anchoring energies. The structure of our sample is shown in Figure. 8. I discovered that after the removal of the one side substrate, I then get a perfect complete film without damaged parts.

Figure. 8 Films with PVA & nylon coating substrates

- The method to solve investigation problems of CLC bandgap

It is not enough to get the complete cholesteric liquid crystal film. In my experiment, perfect CLC planar texture film without inclination lines for acting as a good reflective material is indispensable. If there are many defects in the liquid crystal film itself, the laser emission will be affected by internal defects and cause scattering and affect the resonance quality, so that the full width at half maximum (FWHM) of the laser is not narrow enough to affect the color purity. As the figure. 9 shown, there are a lot of inclination lines on my first made CLC film. I fill in the cholesteric liquid crystal in vacuum environment to avoid the air bubbles formed in the cell. And, according to the reference[2], the inclination lines will vanish and shrink with time. I placed our sample in the oven and cooled down my sample from isotropic phase for one night. The result reveals that the inclination lines decreased a lot, as shown in figure. 10.

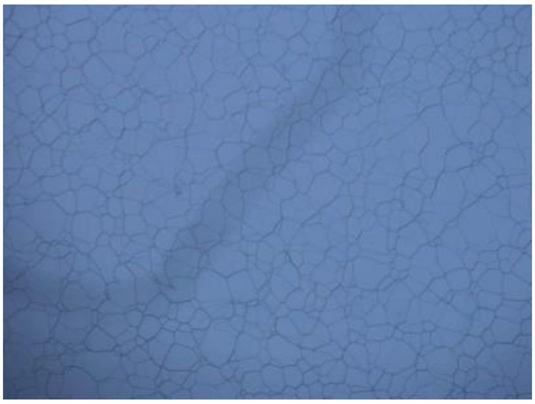

Figure. 9 Reflective image under POM

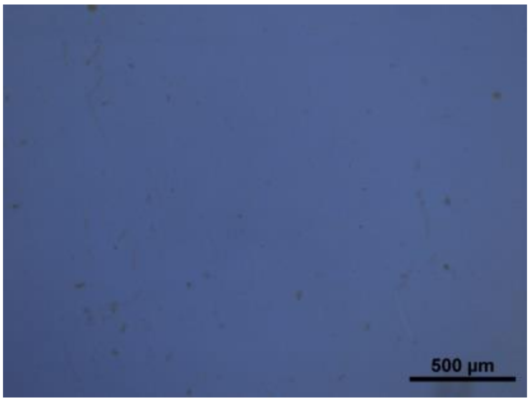

Figure. 10 Reflective image under POM

- Spin coat the alignment layer on mirror based substrate

I first made our sample without the alignment layer: PVA coating on the mirror-based substrate, as shown in figure 11①. I observed the image under the polarized optical microscopy (POM), shown in figure. 12①. I discovered that there are large amounts of big and small black dots in the microscopy image. These dots have the birefringence appearance and the property can be demonstrated that they are liquid crystal molecules in disorder. I, then, coated the alignment layer on the mirror-based substrate. This helps to improve the arrangement of the liquid crystal molecules.

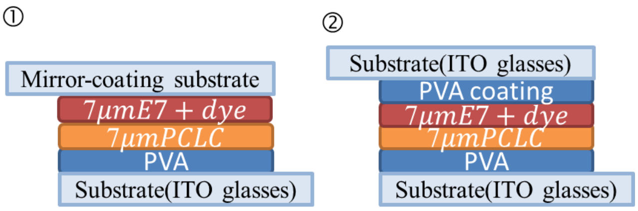

Figure. 11 Side-view of layers in our sample

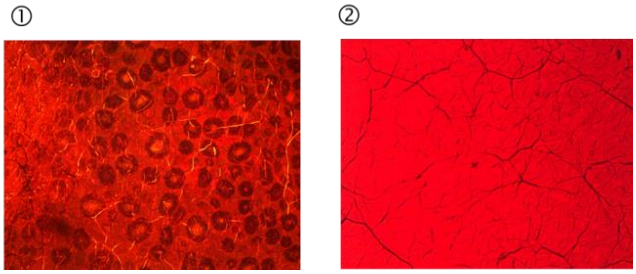

Figure. 12 POM image of the optical performance

- Well-controlled the reflective wavelength of the cholesteric liquid crystal film

I discovered that the wavelength changed when I filled in dye doped liquid crystal layer. And, the value of the wavelength shifts around 110nm. So, to compensate the wavelength shift, I need to take account of this variation. Based on the formula below[3], I can control the reflective wavelength easily.

$$\lambda=n\cdot p\cdot\cos\theta$$

As the formula, the wavelength is decided by two parameters: average refractive index of liquid crystal and the value of pitch (controlled by the concentration(c) and the helical twisting power (HTP) of chiral dopants I added). After several trial and error, I finally obtained the reflective wavelength around 540-595nm like Figure. 13 shown which is at the emission range of the gain media: photo-illuminance dye.

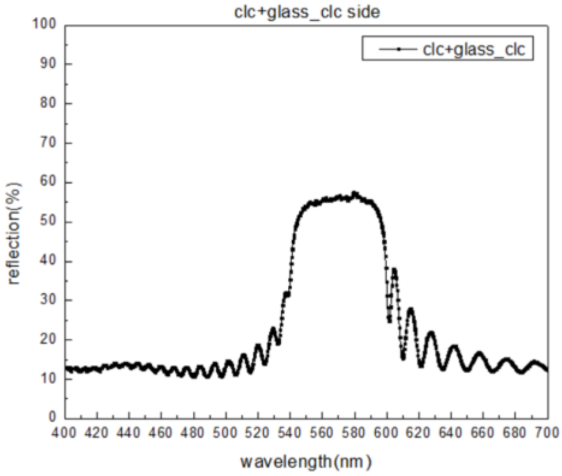

Figure. 13 Reflective spectrum of sample

B. Laser property measurement

The sample is well-prepared from those optimization steps. I further measure the laser signals and do the analysis with the sample. I measured my sample with the laser measurement setup. The results are shown as below. From the figure.14, I observed the light emission happened at wavelength around 586-593nm. And, the full width at half maximum (FWHM) at 586nm is 4.8nm and at 593nm is 5.5nm, respectively. They are roughly in the bandgap. I can assume that maybe the light emission appears at the defect mode position.

To check if I am measuring the spontaneous amplification or lasing emission, I further measure input pump intensity and output light emission signal of the sample. As shown in Figure15, I measured the dependence of the lasing pulse energy on pump pulse energy at 532 nm. From the figure, I suppose that I get the low spontaneous emission at low pump intensity. Then, with the increasing of the pumping energy, I further got extra high laser emission. By analyzing the peak of the laser, the threshold would be detected. Before achieving the threshold, the points have low slope. After reaching threshold, the laser intensity increased dramatically and the slope became steep we may assume that the laser is produced after the threshold energy. The results point out that I am measuring laser action. According to the results above, I assume that I measured the laser action inside the band gap where is referred as defect mode. This is a preliminary result. And, Further experiment should be done to certain laser emission and the corresponding input power of laser.

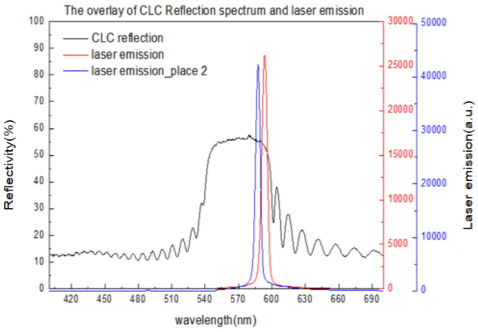

Figure. 14 Overlay of CLC spectrum and laser emission

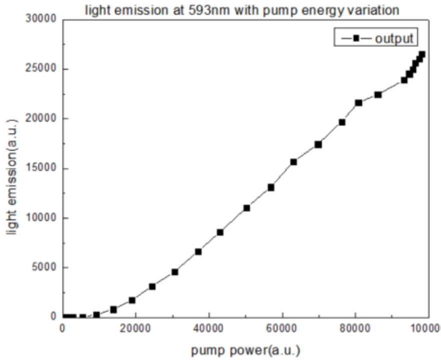

Figure. 15 Dependence of lasing pulse energy on pump pulse energy at 532 nm

C. Mirror application for higher laser intensity

I deposited the silver on the glass substrate as a mirror. Silver reflects more than 99% of the emission light. To confirm the importance of the amplitude of reflection in the cavity on laser emission performance, samples with and without silver layer at the back surface are evaluated. The results of the output energy measurements based on pump energy variation are shown in figure.16. The slope of the curve corresponds to the slope efficiency but the absolute value could not be obtained. The black line (with silver mirror) has higher slope efficiency. The laser emission of the sample with silver substrate increases faster compared to the sample without silver. I demonstrated that the sample with the mirror truly enhances our laser performance.

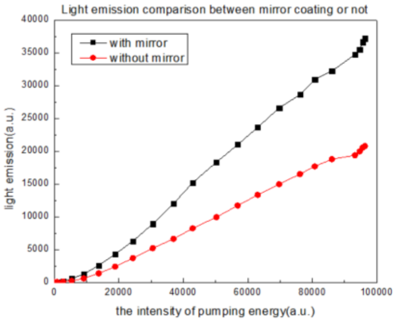

Figure. 16 Laser performance comparison between the samples with silver or not

D. Lasing wavelength modulation by voltage control

For the purpose of making a tunable laser, I applied a voltage on my sample by a function generator and 10X amplifier. I measured two points. At point1, the wavelength located at 588.7nm without voltage and shifted to 586.1nm with 1KHz 10 Volt. At point 2, the wavelength located at 588.7nm without voltage and shifted to 586.5nm with 1kHz 9 Volt and to 586.1nm with 1kHz 10 Volt, as shown in Figure17. By employing 10 Volt, the wavelength blue shifts 2.6nm accompanied by the decay of laser intensity. Liquid crystal in the sample acts as a phase retarder. By applying the voltage, the liquid crystal molecules rotate and give rise to the phase shift. Further, they change the resonance condition in the resonant cavity. Finally, I detect the laser emission wavelength shifts.

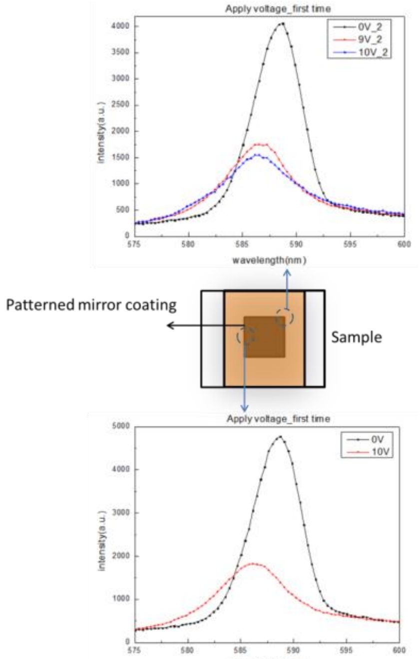

Figure. 17 Schematic diagram of sample and the laser shift with different voltages

I discovered that the wavelength shift only occurred in specific places which are near the edge of the patterned coating mirror. In the center of the patterned mirror, I could not observe the wavelength shift of the output light emission by the electric field. This experiment had a problem with stability. Initially, I could observe the laser wavelength shift when I applied the voltage. However, after several repetitions, the shift of the wavelength was reduced and finally disappeared. Repeatability is important to make a reliable component. I repeatedly applied voltage on the sample, but I was not able to get the wavelength shift anymore. With higher voltage, the laser emission fixed at the sample wavelength.

E. The reliability of the voltage application

The problem in voltage application should be solved. Multi-frequency LCR meter is microprocessor-based impedance measuring instrumentation. This device offers LCR components or electronic circuits tested under actual working conditions. I use this device to check the problem in my sample under the working voltage and frequency. The device revealed that the cell without applying voltage has the capacity value about 603pF. But, when I connected the sample which had already applied voltage for several times, I investigated that the capacity dropped to 11pF which means that the contact with the electrodes is lost. Simultaneously, I tested the sample without coating mirror on the glass substrate and with the voltage application. The capacity value I obtained is about 924pF. I realized that the mirror coating on the substrate played an important role on the voltage application. In the future, it would be interesting to conduct further experiments to confirm the results and solve the modulation problems.

V. CONCLUSIONS

I designed the stack of chiral and nematic dye-doped liquid crystal and I was convinced that it is possible to obtain defect mode laser based on the simulation results by my supervisor Frederik Van Acker. In this research, I improved and optimized the process of making the Cholesteric liquid crystal film so as to obtain high quality resonator. And further, I filled in the dye-doped liquid crystal layer at proper reflective wavelength and solved several fabrication problems. After several trial and error, I made a good usage of my sample and successfully measured laser emission signal by our laser measurement system.

From the results, I assumed that I measured the photo-luminescence and lasing of my sample. Furthermore, by applying electric field, I investigated the several nanometers wavelength shift. I speculated that I measured the tunablility of my sample at the defect mode position. However, there are still some problems when it comes to wavelength modulation. The voltage cannot be continuously applied for a long time. In the future, it would be interesting to conduct further experiments to confirm the results and solve the modulation problems.

VI. REFERENCES

[1] S. M. Jeong *et al.*, "Defect mode lasing from a double-layered dye-doped polymeric cholesteric liquid crystal films with a thin rubbed defect layer," *Applied physics letters,* vol. 90, no. 26, p. 261108, 2007.

[2] F. Zhang and D.-K. Yang, "Evolution of disclinations in cholesteric liquid crystals," *Physical Review E,* vol. 66, no. 4, p. 041701, 2002.

[3] H. Kozawaguchi and M. Wada, "Helical twisting power in cholesteric liquid crystal mixtures. I. Experimental results," *Japanese Journal of Applied Physics,* vol. 14, no. 5, p. 651, 1975.

Contents

List of figures

Chapter 1 Introduction

1.1 Introduction of liquid crystal

The liquid crystal phase is a phase with both liquid and crystalline properties, and it has special properties. For example, it orients solid crystal-way but with conventional liquid-like flowing. Due to the weak force between molecules, liquid crystals are easy to control by external fields such as temperature[1], electric field, or optical field. Thus, liquid crystal is applicable to act as tunable devices and sensors. In this section, the origin, the composition, and the associated properties of liquid crystals will be introduced one by one.

1.1.1 Origin and citation on history

The history of liquid crystal research can be traced back as early as 1850AD. The Prussian doctor-Rudolf Ludwig Karl Virchow and his colleagues discovered an unusual substance in the extract of nerve fibers and soap water. They observed optically anisotropic property. Few years later, in 1888, Friedrich Reinitzer, an Austrian botanist extracted Cholesteryl benzoate from plants which is a white crystalline substance of organic matter at room temperature and he found two phase transitions points of cholesteryl benzoate in his research. The first phase change occurs at 145.5°c when heating up. At this temperature, the crystal state turns into colorful and turbid liquid state. Afterwards, when the temperature is heated up to 179°c, the second phase change occurs. It turns to transparent liquid state. The following year, Otto Lehmann, a German physicist, built a polarized microscope with a heating system so as to further investigate the changes of this material during the process of heating and cooling. He discovered that the turbid pasty liquid possessed liquid fluidity and crystal-specific birefringence.

According to the special properties, this unique phase was named as "Fliessende Krystalle" in German. Also, it is translated as "Liquid crystal" in English which means flowing crystalline. Followed by the two researchers- Friedrich Reinitzer and Otto Lehmann' discovery and definition of liquid crystal, this research in liquid crystal realm was continued by George William Gray. He dedicated himself to synthesizing materials with different compositions which have the liquid crystal characteristics. With the demands of the electronic flat panel displays, the researches and applications in liquid crystal realm especially in nematic liquid crystals is growing rapidly. In this century, liquid crystal-based displays play the important roles in our daily life. Liquid crystals not only act as a main material in liquid crystal based displays, they are also applicable in the field such as adaptive optics[2], nonlinear optics[3], and photonic crystals[4].

1.1.2 The classification of liquid crystal

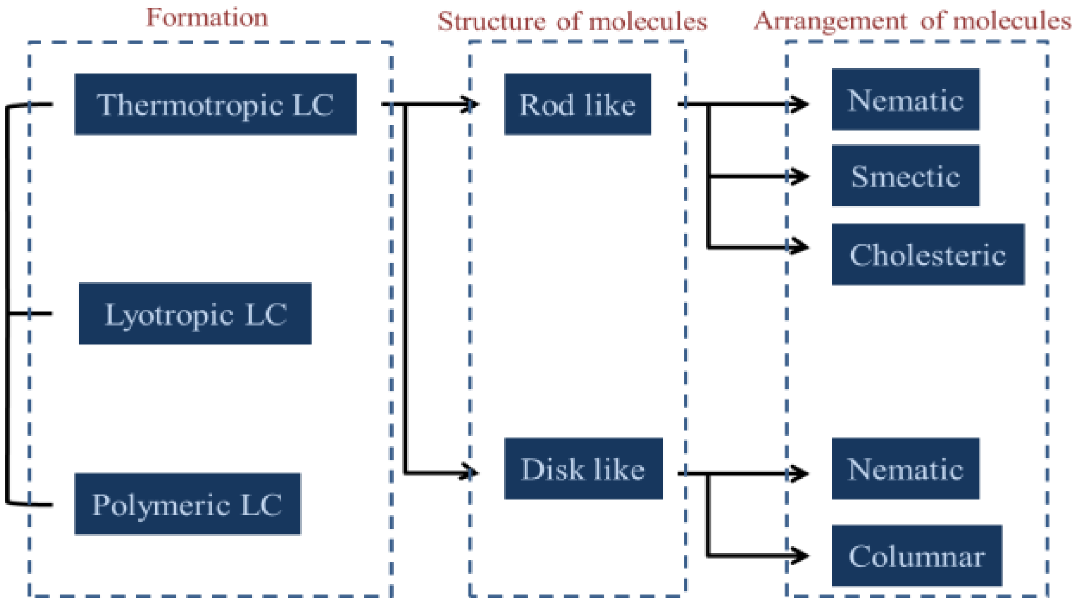

Figure1- 1The classification of liquid crystal

Based on different formation conditions, as shown in Figure1-1, we can separate them into three orders of liquid crystal which are thermotropic liquid crystal, lyotropic liquid crystal and polymeric liquid crystal. For lyotropic liquid crystal, the molecules are randomly distributed in the solvent and form isotropy phase at low concentration. However, as the increase of the concentration, the molecules will be closely arranged according to their own geometric shape to form anisotropic arrangement which means that they have certain orientation. For polymeric liquid crystal, they are polymer fibrils and are formed liquid crystal phase under certain range of temperature and pressure. As for thermotropic liquid crystal, when at low temperature, the van der Waals force between liquid crystal molecules gives rise to the formation of regular arrangement as crystalline solid. Conversely, when the temperature increases to a certain extent, the molecules get enough kinetic energy and break binding energy. At the same time, the liquid crystal state (the intermediate state between solid and liquid in some materials) is formed. As mentioned above, this type of liquid crystals are controlled by temperature to determine the existence of liquid crystal states, and are relatively simple to use, so they are widely used in academic research and industrial applications. Also, in our research, we focus on this type of liquid crystal.

According to their structures and arrangements, the thermotropic liquid crystal molecules can be differentiated into several types, as depicted in Figure1-1. On the basis of structures, we can categorize into two types- rod-like and disk-like molecules respectively. In our experiment, we use rod-like molecules. For this type of molecules, they are formed by a rigid core (polar groups) and flexible tail (long carbon chains). The following introduces the three common arrangements of rod-shaped thermotropic liquid crystal including nematic, sematic, and cholesteric liquid crystal phase, as shown in Figure1-2 below.

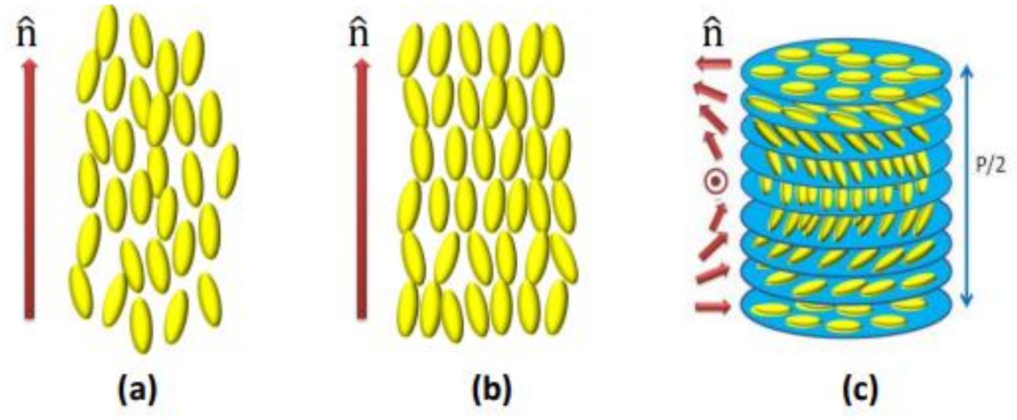

Figure1- 2 Scheme of different arrangements thermotropic liquid crystal. (a) nematic phase, (b) smectic phase, and (c) chiral nematic phase

1. Nematic phase

The molecular orientation property of rod-like nematic liquid crystals is shown in Figure1-2(a). There are two mainly characteristics[5]:

(1) The molecules tend to align along one certain direction when they are arranged. And, the direction is defined by the director n̂. We can not distinguish between head and tail by n̂ or -n̂, so we usually use n̂ to represent the direction of the liquid crystal axis.

(2) The nematic liquid crystal state is fluid which means the position of molecules is without ordered.

2. Smectic phase

The smectic liquid crystal has the arrangement order of both solid crystal and nematic liquid crystal. That is, it has one dimensional regular layered structure and also the orientational direction of molecules have a specific angle with each layer, as shown in Figure1-3. Compared with nematic phase, the arrangement of smectic liquid crystals is closer to that of solid crystals, so it has a higher order of arrangement. Furthermore, this phase is more viscous than other two phases. According to different arrangements of the molecules, we can classify smectic liquid crystal into smectic A and smectic C as shown below. For smectic A, the long axes of molecules are parallel to the normal direction of layers as shown in Figure1-3(a). As for smectic C, we can investigate a tilting of the molecules in respect of the plane of layers as shown in Fiqgure1-3(b).

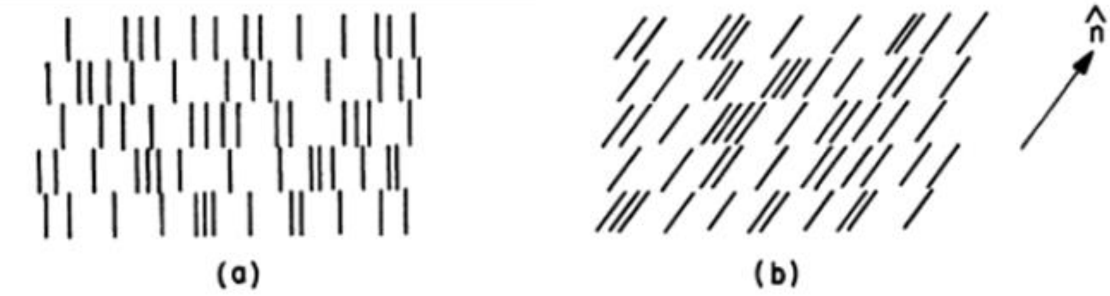

Figure1- 3 Schematic arrangement of (a) smectic A and (b) smectic C[5]

3. Cholesteric phase

Liquid crystal molecules in the phase of cholesteric liquid crystal will arrange like a helical structure as Figure1-4(a) shown. Due to the poor coplanarity of chiral substances, when the liquid crystal molecules are arranged in space, the upper and lower molecules will be staggered by a small angle to achieve the lowest free energy. Also, we can use free energy formula to explain this arrangement. Based on Oseen-Frank theory, the free energy of cholesteric liquid crystal can be expressed by the following equation[6]

$$F=\frac{1}{2}\{k_{11}[\nabla\cdot\hat{n}]^2+k_{22}[\hat{n}\cdot(\nabla\times\hat{n})+q_0]^2+k_{33}[\hat{n}\times(\nabla\times\hat{n})]^2\}$$

$$-\frac{1}{2}\varepsilon_0\left(\varepsilon_\perp+\Delta\varepsilon sin^2\varphi\right)E^2 \qquad \text{(Eq1-1)}$$

Where $\hat{n}$ is the director, and q_0 represents the chirality. Furthermore, by Landau's theory, the steady state occurs when the free energy reaches minimum. Therefore, owing to the value of k22 is positive, to meet the minimum, the term $\hat{n}\cdot(\nabla\times\hat{n})+q_0$ should be 0. The director of the molecules can be rewritten as

$$\hat{n}=-\sin(q_0z)\,\hat{x}+\cos(q_0z)\hat{y} \qquad \text{(Eq1-2)}$$

From the above, it demonstrated that the molecules are periodically arranged along the z-axis direction as shown in Figure 1-4(a). Thus, chiral nematic liquid crystal is known as a one-dimentional periodic structure. The length when the liquid crystal molecules rotate 360° is called a pitch (p). The pitch is decided by two parameters-the concentration(c) and the helical twisting power(HTP) of chiral dopants, and is given by the following equation[7]

$$\mathrm{HTP}=\frac{1}{p\times c} \qquad \text{(Eq1-3)}$$

Since the refractive index exhibits a periodic helical distribution along the z-axis, just like the multilayer film structure, the cholesteric liquid crystal will produce Bragg reflection when there is incident light (the detailed explanation about Bragg reflection of Cholesteric liquid crystals will be elaborated in photonic crystal part 1.2.2). The reflective spectrum is shown in Figure1-4(b)[8]. Because the cholesteric liquid crystals selectively reflect either right-handed or left-handed polarized light, so the reflection measured by the unpolarized white light source is up to 50%. And, the definition of the central reflective wavelength and bandwidth are expressed in the equations below

$$\lambda=\mathrm{n}\cdot \mathrm{p}\cdot \cos\theta \qquad \text{(Eq1-4)}$$

$$\Delta\lambda=\Delta\mathrm{n}\cdot \mathrm{p}\cdot \cos\theta \qquad \text{(Eq1-5)}$$

Where n is average refractive index ($\mathrm{n}=\frac{n_e+n_o}{2}$) which is based on the host nematic liquid crystal, $\Delta\mathrm{n}=n_e-n_o$, and θ is the angle between the axis of rotation and the incident light. This optical characteristic is the same as the photonic energy gap of the photonic crystal, so the cholesteric liquid crystal is regarded as a one-dimensional photonic crystal (More introductions about photonic crystals will be elaborated in 1.2.1).

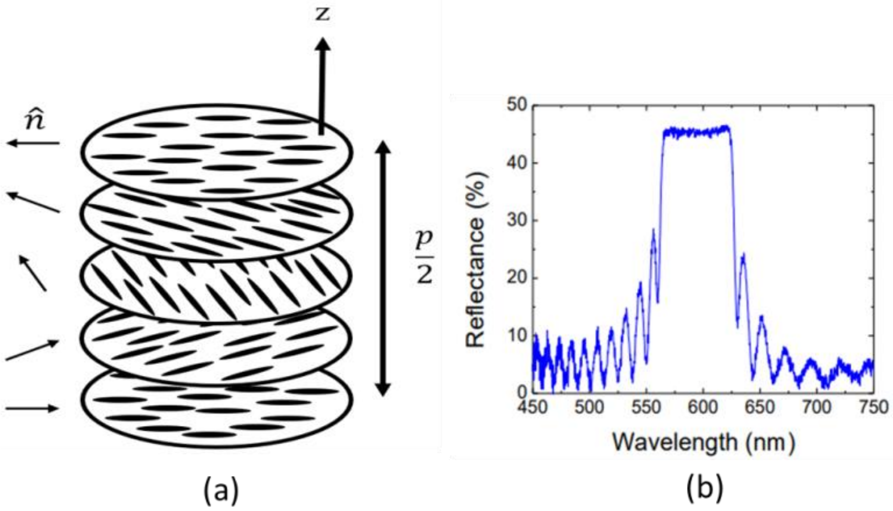

Figure1- 4 (a) Schematic of the arrangement of cholesteric liquid crystal (b) Optical reflective spectrum

In addition, the most common of the cholesteric liquid crystal texture is planar texture. It happens when the rotating axis of cholesteric liquid crystal is perpendicular to the substrates as shown in Figure1-5. To fabricate this planar texture, we can easily mix liquid crystal molecules with chiral dopants, and modulate them in the visible band. Finally, inject them into a double-sided horizontally aligned liquid crystal cell. The boundary force given by the substrates on both sides will make the liquid crystal molecules naturally spirally arranged. Moreover, by controlling the handedness of chiral dopants, we can decide the reflection band. The handedness of chiral dopant impacts the handedness of periodic structure of cholesteric liquid crystal. Right-handed chiral dopants lead to right-handed twisted helical structure. Otherwise, the left-handed chiral dopants are vice versa. Because the reflection of cholesteric liquid crystal depends on their helical structure, the handedness of chiral dopant also impacts the reflection of the light[9]. For instance, for right-handed chiral nematic liquid crystal, the reflection is right-handed circular polarization, and there is no Bragg reflection for left-handed circular polarized light.

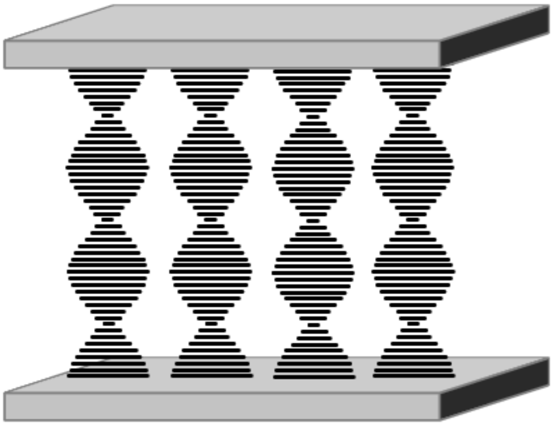

Figure1- 5 Scheme of a planar texture

1.1.3 Basic related properties

Due to the structure and the arrangement of liquid crystal that we introduced in previous paragraph, liquid crystal molecules have good optical properties and electro-optics applications. In the following chapter, we will introduce birefringence, dielectric anisotropy, and finally elastic deformation theory. Based on basic background knowledge, it can be easier for us to choose the appropriate liquid crystal material and do our research precisely.

1. Birefringence

Owing to the geometrical anisotropy of the rod-like liquid crystal molecules when the light propagates through the liquid crystal with different incident angles and polarizations, it will sense different effective refractive indices which lead to different phase velocities. For analyzing easily, we divide the propagation electromagnetic wave into two orthogonal linearly-polarized waves. When these two electromagnetic waves are incident on anisotropic liquid crystal molecules and propagate, they will experience different refractive indices. For the polarized light parallel to the long axis of the molecules, it will sense n_e(Extraordinary refractive index). And, for the polarized light parallel to the short axis, it will sense n_o(Extraordinary refractive index), as shown in

Figure1-6. Rod-like nematic liquid crystals is a positive uniaxial crystals, and the refractive indices can be written as the following equation

$$\frac{x^2}{{n_o}^2}+\frac{y^2}{{n_o}^2}+\frac{z^2}{{n_e}^2}=1 \tag{Eq1-6}$$

If polarized light is not incident along x or y axis, it will sense two refractive indices. This property is called birefringence. Figure1-6 perfectly explains the refractive index anisotropy of positive uniaxial crystals. Moreover, if the light is oblique incident into nematic liquid crystals with an angle, the induced refractive index will change toward n_{eff}. We can use the equation below to define the effective refractive index n_{eff}

$$n_{eff}(\theta)=\frac{n_o n_e}{\sqrt{{n_e}^2 cos^2\theta+{n_o}^2 sin^2\theta}} \tag{Eq1-7}$$

As shown in Figure1-6, depending on the incident direction of the light, the incident condition can be divided into the following three categories:

I. The k vector of the incident electromagnetic wave parallel to the x axis

One of the oscillation direction of wave is on the x-z section, so its refractive index is n_e (the long axis of the ellipsoid). The other polarization is on x-y section, the refractive index is supposed to be n_o (the short axis of the ellipsoid).These two polarized lights see different refractive indices and give rise to propagate in different phase velocities. The phase difference (δ) when encounters liquid crystals can be calculated by the following formula

$$\delta=\frac{2\pi(n_e-n_o)d}{\lambda} \tag{Eq1-8}$$

where d equals to the thickness of liquid crystal layer and λ is the wavelength of the incident light. Through this formula, we can further realize the change of the polarization state when the light passes through the liquid crystal molecules.

II. The k vector of the incident electromagnetic wave parallel to the z axis

When the electromagnetic wave passes through the crystal, the oscillation directions of these two orthogonal polarized lights are parallel to the x axis and y axis respectively. So, both of the refractive index is n_o. Therefore, the phase velocity of two polarized lights after passing through this ellipsoid is consistent, and there will be no difference in the polarization state.

III. The k vector of incident electromagnetic wave have an angle θ with the z-axis

When the wave travel at the angle θ with the z axis, the refractive index sense by the incident wave are n_{eff} and n_o. By the above formula, we can calculate the phase difference below between the two orthogonal polarizations after passing through the liquid crystals which is

$$\delta = \frac{2\pi(n_{eff}-n_o)d}{\lambda} \qquad \text{(Eq1-9)}$$

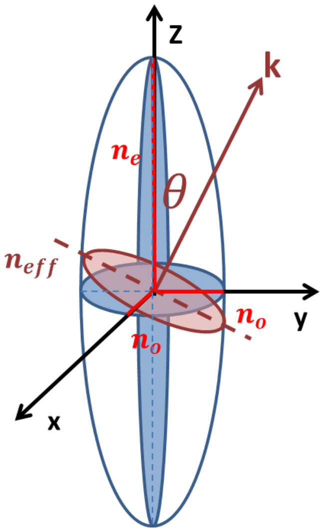

Figure1- 6 Schematic of index ellipsoid of nematic liquid crystals

2. Dielectric anisotropy

The distribution of charge-clouds of nematic liquid crystals which is induced by electric field is not the same in different directions. That’s why nematic liquid crystal presents dielectric anisotropy. We define the dielectric constant in short axis of molecules as $\varepsilon_\perp$ and the dielectric constant in long axis as $\varepsilon_\parallel$. Owing to the dielectric constant difference, the induced moment of force parallel and perpendicular to the orientation of the molecules are different. It controls the alignment of the molecules. The dielectric anisotropy$\Delta\varepsilon$ is defined as($\varepsilon_{\parallel}$-$\varepsilon_{\perp}$). For positive $\Delta\varepsilon$, the liquid crystal is referred to positive liquid crystal. On the contrary, for negative $\Delta\varepsilon$, the liquid crystal is known as negative liquid crystal. As a result of dielectric anisotropy, the director of liquid crystal in the space can be dominated by applying voltage. The contribution of the electric field to the free energy per unit volume of the liquid crystal molecules in space is expressed as below

$$F_e = -\frac{1}{4\pi}\int D \cdot dE = -\frac{\varepsilon_{\perp}}{8\pi}E^2 - \frac{\Delta\varepsilon}{8\pi}(n \cdot E)^2 \qquad \text{(Eq1-10)}$$

According to Landau's theory, the steady state of the liquid crystals occurs when it reaches the minimum free energy. With regard to negative liquid crystal, when the voltage is applied above the critical voltage, the director of molecules tends to orient along the axis which is perpendicular to the electric field so as to maintain the lowest free energy state. But for positive liquid crystal, the liquid crystal molecules have the tendency to align along the direction parallel to the electric field. The schematic of the difference after applying the voltage are shown as Figure1-7.

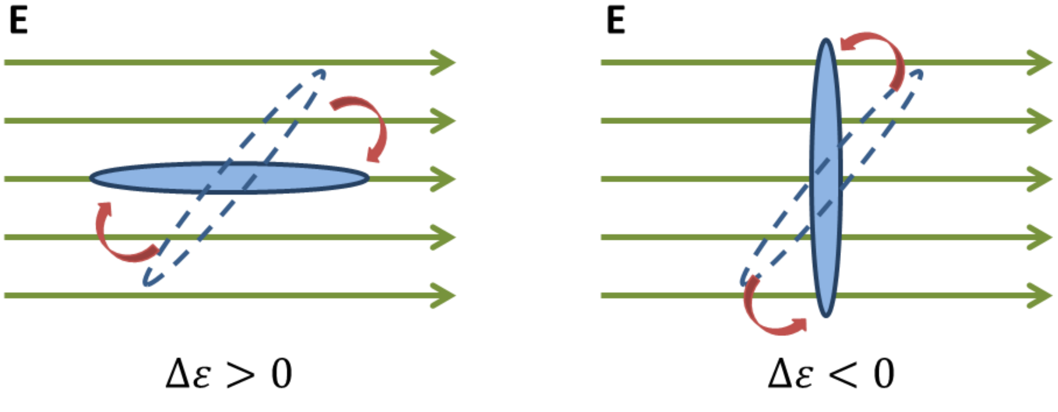

Figure1- 7 Schematic of the relationship between the dielectric anisotropy and electric field

3. Elastic deformation theory (Elastic constant)

In 1948, F.C Frank and his colleagues gave the explanation of liquid crystal arrangement by introducing the thought of surface energy and finally compiled the theory of continuous elasticity structure deformation[10]. By applying electric field or giving the alignment on the surface, we will change the arrangement of the liquid crystals and further result in the deformation. There are three kinds of deformation forms-splay, twist, and bend respectively, as shown in Figure1-8. And the corresponding elastic constants are K11, K22, and K33. Based on the Oseen-Frank theory, these three parameters offer the free energy of the molecules and give rise to the state that liquid crystals exist. The elastic free energy can be expressed as the equation below

$$f_{elastic} = \frac{1}{2}[K_{11}(\nabla \cdot n)^2 + K_{22}(n \cdot \nabla \times n)^2 + K_{33}(n \times \nabla \times n)^2] \qquad \text{(Eq1-11)}$$

In the equation, the first term is due to splay deformation, the second one comes from twist deformation, and the third one is given by bend deformation. To be more precisely,

$$f_{splay} = \frac{1}{2}\mathrm{K}_{11}[\nabla \cdot \hat{\mathrm{n}}]^2 \qquad \text{(Eq1-12)}$$

$$f_{twist} = \frac{1}{2}K_{22}[\hat{\mathrm{n}} \cdot (\nabla \times \hat{\mathrm{n}})]^2 \qquad \text{(Eq1-13)}$$

$$f_{bend} = \frac{1}{2}K_{33}[\hat{\mathrm{n}} \times (\nabla \times \hat{\mathrm{n}})]^2 \qquad \text{(Eq1-14)}$$

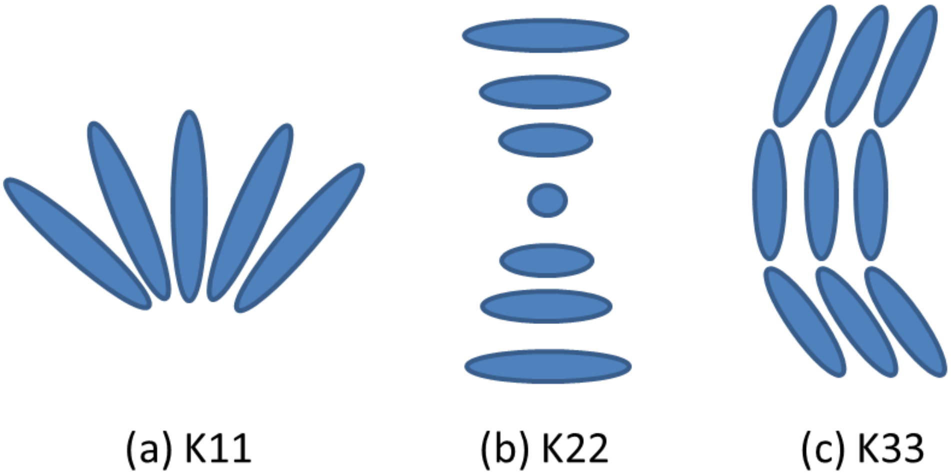

Figure1- 8 Schematic diagram of (a) splay, (b) twist, and (c) bend deformation and elastic constants

1.2 Introduction of theory

According the introduction in the previous section, we know that liquid crystal is easy to control the arrangement and change the alignment by external electric field. Because it is good at modulating, we think of using it as a tunable laser. So, in this section, we will first talk about the theory of general laser, what is photonic liquid crystal laser, and how to use our organic material-cholesteric liquid crystal to make cholesteric photonic crystal laser.

1.2.1 Laser introduction

When applying an external electric field, the electron will be excited to an excited state, and owing to the instability, it drops to ground state in short time and release the energy as light form. For this type, the intensity, direction and amplitude of the released photons are inconsistent with each other which called spontaneous emission, as shown in below figure; and, when the photons generated by spontaneous radiation collide with the electrons in the exited state, the electrons will be induced to generate stimulated emission. In this type, the photons will possess the same intensity, direction and amplitude as the incident light, as shown in below. This poses to the amplification of the light. In the design, the gain medium is used for extending the existed time of the electrons in excited state so as to enlarge the amounts of electrons to return to the ground state at one time, and emit a large number of photons simultaneously. When the number of electrons in excited state is more than the number of electrons in the ground state, population inversion is reached which leads to the light amplification and leads to laser amplification.

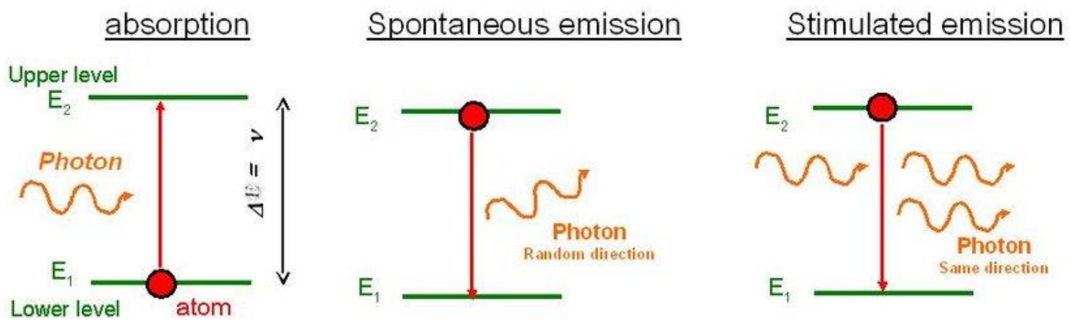

Figure1- 9 The schematic of the absorption, spontaneous emission and stimulated emission[11]

A laser is an acronym of Light Amplification by Stimulated Emission of Radiation. Generally speaking, there are three important elements that constitute the laser-pumping source, gain medium and the optical resonator. The gain material is placed between reflective elements such as mirrors and the material is excited by pumping source. Due to the external energy, the gain medium releases photons. The photons oscillate back and forth in the optical resonator and then form a standing wave in between. When the gain of light in the resonant cavity is greater than the loss, the laser can be generated from the end of the partial reflective mirror, as shown in Figure1-10.

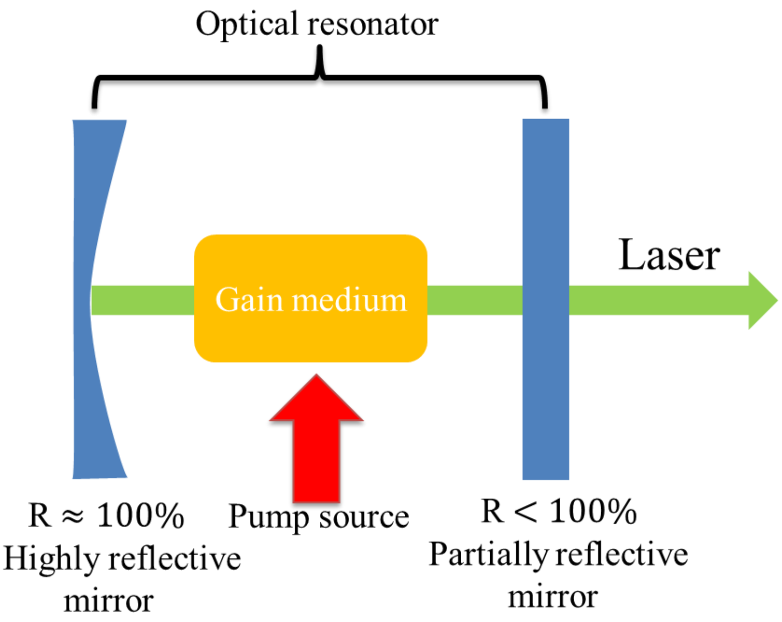

Figure1- 10 Schematic of the basic structure of laser

We use lasing threshold to define the lowest excitation energy when the laser produce. Above the laser threshold, the laser output is generated by stimulated emission which has dramatically increasing laser power. But, below the laser threshold, the output of laser is dominated by spontaneous emission which rises slowly with raising external energy. To get the value of the lasing threshold, we define the balance between the gain of the laser medium and the sum of the loss generated in one round trip in laser's optical resonator. This phenomenon at the steady state can be characterized as

$$R_1 R_2 \exp(2g_{threshold}\ell)\exp(-2\alpha\ell) = 1 \qquad \text{(Eq1-15)}$$

Where $R_1 \; and \; R_2$ are the reflectivities of the two mirrors, $\exp(2g_{threshold}\ell)$ is the round-trip of the gain, $\exp(-2\alpha\ell)$ is the loss part, α is the parameter of optical loss such as control losses and distributed losses (absorption or scattering) and ℓ is the length of the gain medium (the length of the optical resonator). Under the assumption that the optical loss is the constantα_0, we can describe the threshold as[12]

$$g_{threshold} = \alpha_0 - \frac{1}{2\ell}\ln(R_1 R_2) \qquad \text{(Eq1-15)}$$

From the equation above, we realize that to minimize the threshold, we are supposed to lower the distributed losses and higher the mirror’s reflectivity.

1.2.2 Photonic crystal

The concept of photonic liquid crystal was proposed in 1987 by S. John and E. Yablonovitch[13]. Due to the periodic structure with different refractive indices, the photonic liquid crystals are formed. According to the arrangement, it can be divided into 3 types of photonic crystals, one-dimensional, two-dimensional and three dimension of image, respectively, as shown in Figure1-11[14]. When the periodic size of the arrangement is about the same scale as the electromagnetic wave, the photonic crystal can affect the motion of the photons, such as the color of the peacock feather, butterflies wings or opals, this is unique optical phenomenon in photonic crystal. Usually, we can know the effect of photonic crystal on different electromagnetic wave frequencies through the dispersion relationship diagram in Figure1-12. From this figure, we can see two very important optical properties. The first is that electromagnetic waves cannot propagate in a certain frequency band. The second is that group velocity of the edge of photonic bandgap will approach zero. When light propagate through these periodic crystals, it gives rise to develop multiple reflections. These reflective lights interact with each other, and produce destructive and constructive interference light. When the ranges of constructive interference are not continuous, the light cannot pass through this area and cause Bragg reflection. (For the Bragg reflective wavelength, we have already mentioned in the section Cholesteric phase liquid crystal. $\lambda = n \cdot p \cdot \cos\theta$) That is to say, the light of specific wavelength will be reflected after entering the photonic crystal and this region is known as photonic bandgap as Figure1-12 shown.

The fabrication of photonic crystals can be divided into self-assembly or not. For not self-assembly way, some studies made photonic crystals structure by semiconductor materials. This process involves multiple times of photoresist, photolithography and photoresist removal which is process-complicated and time-comsuming As for organic fabrication like liquid crystal based photonic crystal, we add chiral substance, and automatically present one-dimensional periodic refractive index distribution. Its structure can form a photonic bandgap. Moreover, chiral nematic liquid crystals also pose to several advantages such as self-assembly, small volume. Nevertheless, as for modulating the reflective wavelength, chiral nematic liquid crystals have wide tunable range of wavelength. We can easily control this by adjusting the arrangement or structure of this periodic helix chiral nematic liquid crystal structure. Therefore, it is a useful material when it comes to making a laser.

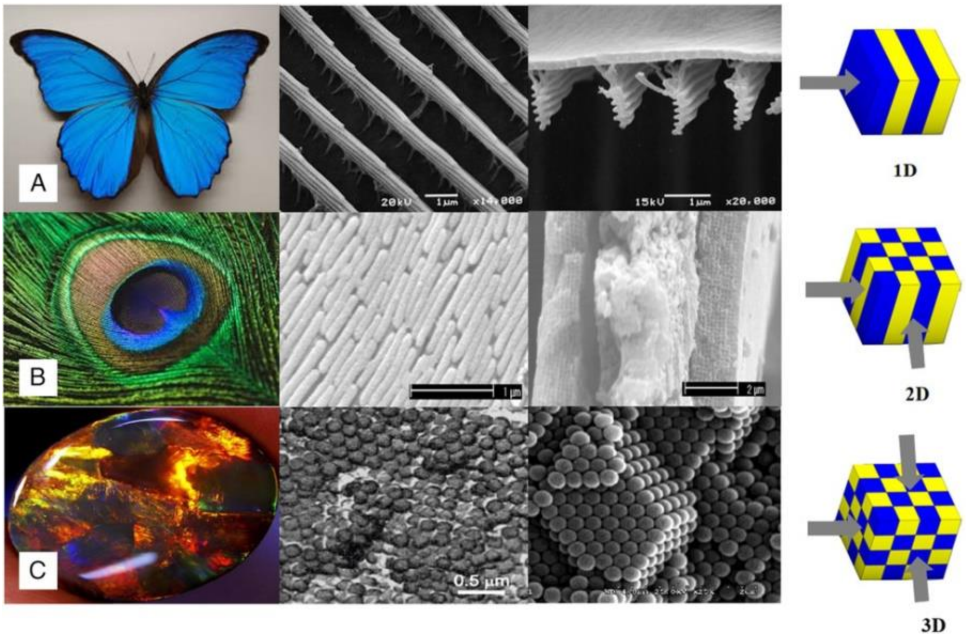

Figure1- 11Schematic of different dimensions of photonic crystals[14]

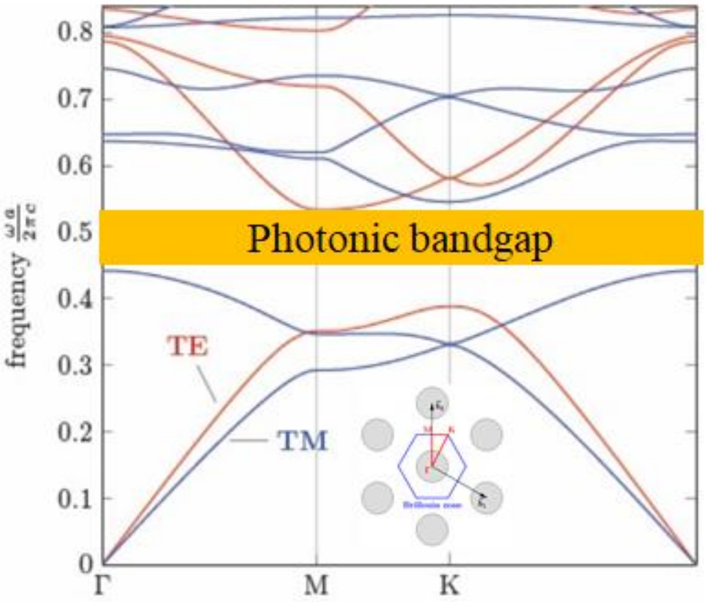

Figure1- 12 Dispersion relationship[15]

1.2.3 Photonic crystal laser

The characteristic of photonic bandgap edge can be used to replace the cavity of general laser structure because the group velocity is close to zero. We will elaborate in the following section. Due to the magnetic field given by Maxwell's equation shown below, we can realize the propagation form of the light in photonic crystals

$$\left\{\nabla \times \frac{1}{\epsilon(r)} \nabla \times\right\} \mathrm{H(r)} = \frac{\omega^2}{c^2} H(r) \qquad \text{(Eq1-16)}$$

Where electric permittivity ϵ can be written as periodic functions of position $\epsilon(r) = \epsilon(r+a)$. By taking account of the distribution of electric permittivity, the mathematical solutions of H(r) are found. Based on a series of calculation, we can get the dispersion relation of photonic crystals as shown in Figure1-13. In the figure, we realize specific wave vectors $(\vec{k})$ are related to angular frequencies (ω) and describe the modes which exist. In the Figure1-13, it shows that the edge of photonic bandgap exists $\frac{d\omega}{d\mathrm{K}} = 0$ which means the group velocity (V_g) is close to zero. The slower the group velocity is, the longer the luminescent material interacts. This leads to long optical path in the structure and the photons in the layer form a standing wave. Therefore, it is incredibly suitable to act as a resonator in the lasers. Compared with general laser structure, photonic crystal laser has its advantage of small size about nano-scale.

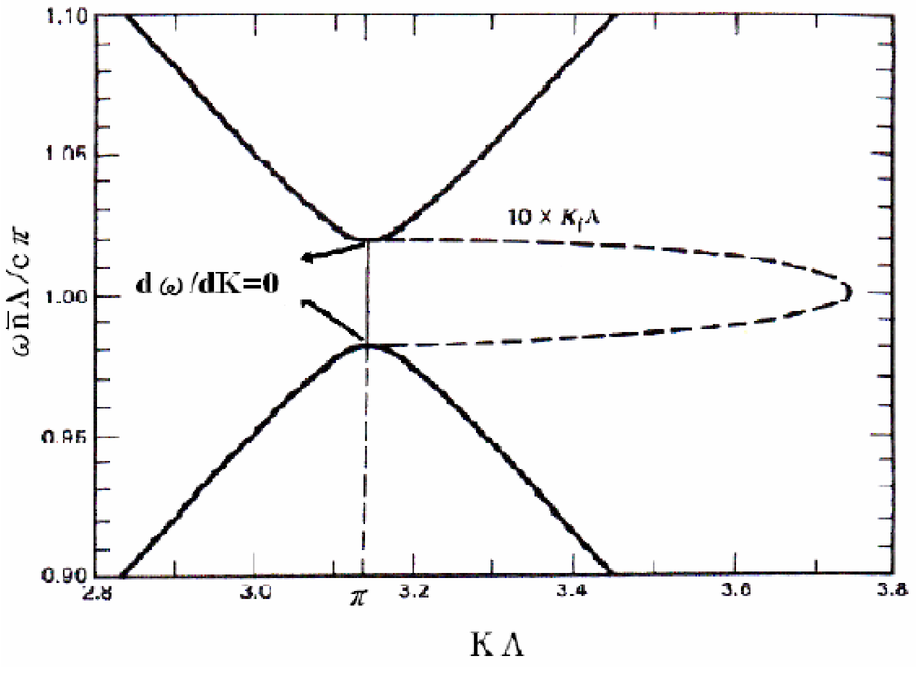

Figure1- 13 Dispersion relation of photonic crystals[16]

In the field of photonic crystals, cholesteric liquid crystals, one-dimensional periodic structures, can form a photonic bandgap so it benefits for affecting photons movement. It can reflect circularly polarized light of specific wavelength as mentioned in section 1.1.2. Therefore, it also is applicable for laser. There are two main kinds of applications in lasing: One is cholesteric liquid crystal band edge mode laser. The lasing happens at the edge of bandgap owing to zero group velocity in this area. I will then introduce in next section. The other is cholesteric liquid crystal defect mode laser. It gives rise to the resonance in specific wavelength in the photonic bandgap by designing the defect structure in the cholesteric liquid crystal layer. It will be illustrated in section 1.2.5.

1.2.4 Cholesteric liquid crystal band edge mode laser

Due to cholesteric liquid crystal's characteristics- self-arrangement and good tunability, the application of cholesteric liquid crystals in lasers has been researched for a long time[17]. Liquid crystal molecules are helically arranged to form a one-dimensional stacking photonic crystal structure. Like in other photonic structures, the photons meet a forbidden energy gap. The input light at a specific frequency and with specific circular polarized light cannot pass through the structure. We call this photonic band gap. And, we will obtain relatively high gain at the edge of the energy gap (the edge on both sides of the photon energy gap, as shown in Fig1-14[18]) because the group velocity Vg at this place approaches zero.

From the previous section, we know that the position of the energy band edge has the standing wave condition to form a resonant cavity. By adding the laser dye whose emission wavelength covers the position of the energy gap edge into cholesteric liquid crystals as a gain medium, like Figure 1-15, a laser can be formed at the edge of band gap. This kind of laser is named as Cholesteric liquid crystal band edge mode laser.

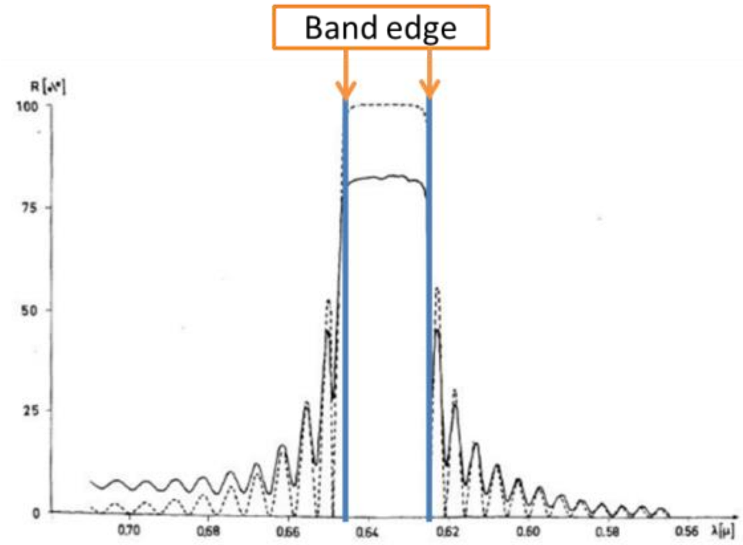

Figure1- 14 Reflective spectrum of CLC (Solid curve: measured data; dashed curve: simulated result)

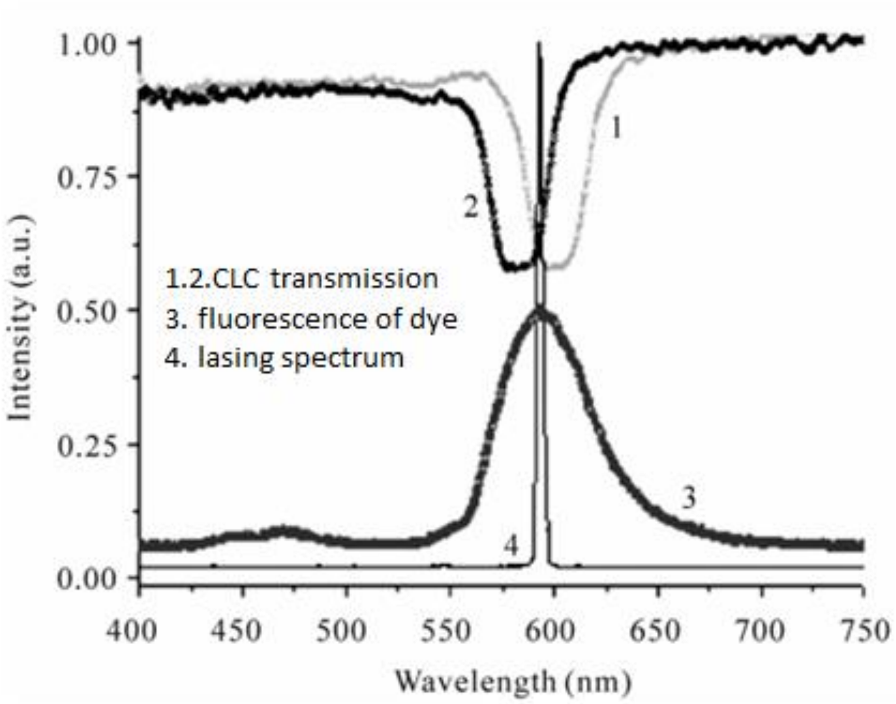

Figure1- 15 Cholesteric liquid crystal band edge mode laser.[19]

At present, there are many types of lasers on the market, such as common helium-neon gas lasers, semiconductor lasers, and solid-state crystal lasers. These lasers have their own advantages. For example, gas lasers have stable light quality and high coherence and are often used for experimental interference diffraction observations.

Semiconductor lasers (electron lasers) are small in size and low in power consumption, and have been widely used in commercial applications such as reading light sources for CD players. Solid-state crystal lasers have the characteristics of high output power and are useful in biomedicine, industry, and academics. However, a problem with these lasers is that wavelength modulation is not easy. Cholesteric edge mode lasers are more convenient. Furthermore, they have various ways to modulate laser wavelengths. Many methods to control the wavelengths have been proposed in the past few years [19-21].

Here, we illustrate two main methods to control the cholesteric liquid crystal band edge mode laser. First method is to modulate the laser wavelength by electrically pulling the polymer network. The polymers are added in the Cholesteric liquid crystal which is doped with laser dyes. After photo-polymerization by UV light, a polymer network is formed in between the liquid crystals molecules as Figure1-16 shown. Then, we apply DC electric field (parallel to the helical axis) to form a gradient distribution of the internal helical pitch like Figure1-17 left. The ions are attracted by the voltage which attached to the polymer branches and pull the network to form a pitch gradient. This poses to widen the photon energy gap and change the position of the band edge[20, 21]. By modulating the magnitude of the DC electric field, the laser wavelength can be freely switched in the wide spectral range from around 600nm to 670nm as Figure1-17 right shows.

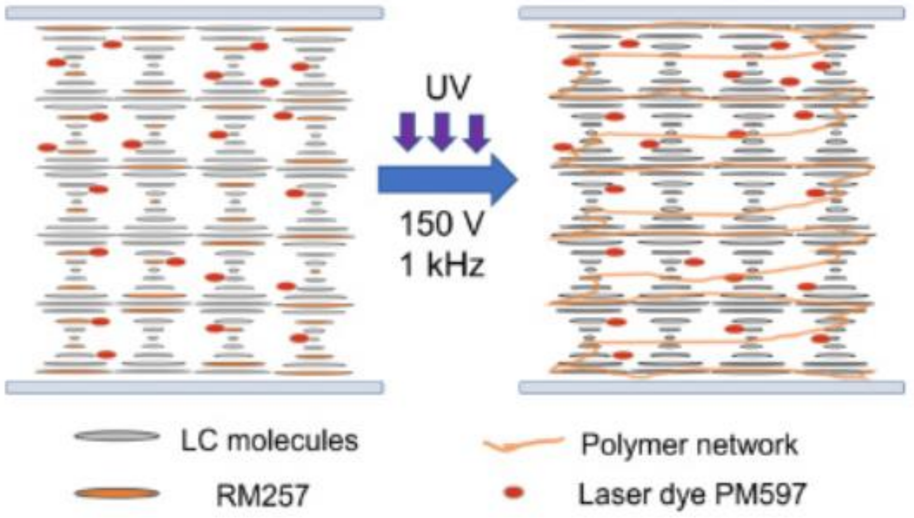

Figure1- 16 Formation of polymer- stabilized cholesteric liquid crystals[21]

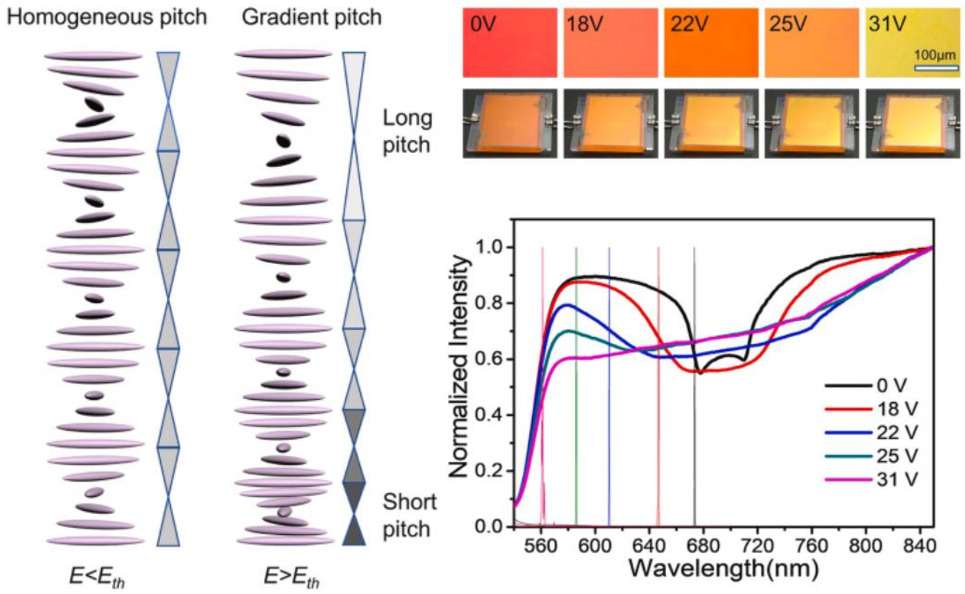

Figure1- 17 (Left) the schematic of the pitch distribution under different DC fields (Right) The microscopy images, transmission and laser emission of dye- doped PSCLC under certain DC voltages

The second is to incorporate photo-isomerization material in the Cholesteric liquid crystals. This material changes the molecular structure when illuminated, and then stretches the helical pitch of cholesteric liquid crystals to modulate the reflected wavelength as illustrated in the Figure1-18 left. In turn, it causes the laser which produces in the edge of the bandgap shifts as shown in Figure1-18 right[19]. We name this as photo tunable Cholesteric liquid crystals band edge laser.

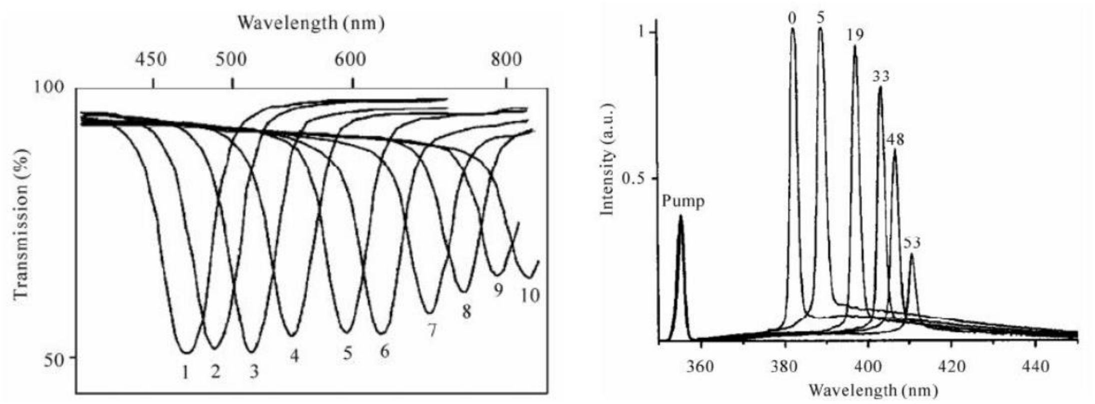

Figure1- 18 (Left) Transmission spectra which is irradiated under different times. (Right) Laser emission from the CLC under different exposure time.[19]

1.2.5 Cholesteric liquid crystal defect mode laser

There is other kind of Cholesteric liquid crystal lasers which we call defect mode lasers. Normally speaking, to form this type of lasing, we will find ways to break periodic helically arranged liquid crystal molecules and leads to structural discontinuity. Defects in special periodic structures can cause resonances at specific wavelengths in the photon energy gap. The methods adopted in the past literature can be roughly summarized into several types.

A. Sandwich a layer of isotropic material or anisotropic layer in the middle of two helical structure[22, 23], as shown in Figure1- 19(a).
B. Divide the original continuous spiral structure into two layers and create a dislocation angle between the upper and lower layers, also known as phase jump[24], as illustration in Figure1- 19(b).
C. Control the length of the pitch to form pitch difference (pitch jump)[25], as the picture shows in Figure1- 19(c).

Similarly, these defect structures can also modulate the wavelength of the defect laser by controlling the thickness of the isotropic layer, the pitch length, and the dislocation angle, respectively.

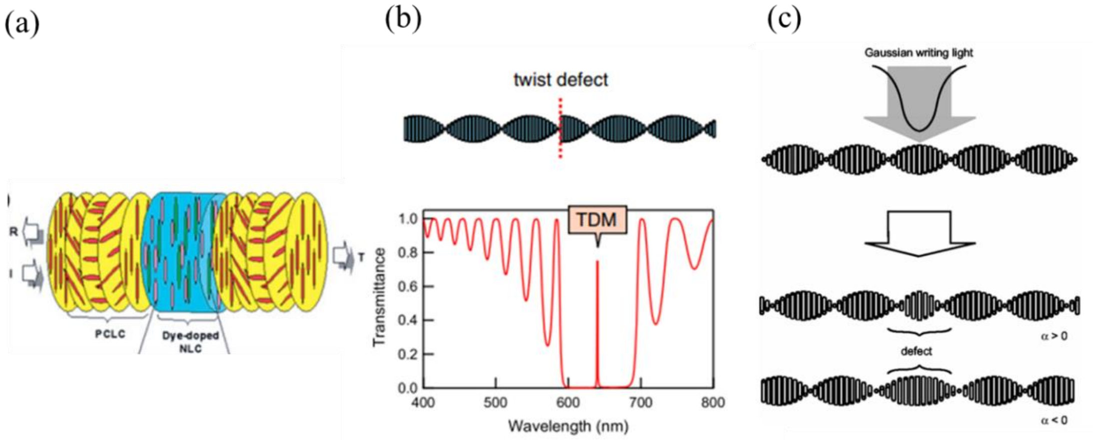

Anisotropic layer in between Phase jump Pitch jump

Figure1- 19 Different kinds of defect modes (a) layered defects (b) phase jump (c) pitch jump[22, 24, 25]

There are more teams doing the researches in the layer defects mode laser so I will use this type of defect mode laser to explain defect mode laser. In 2007, Jeong et al. and his colleagues use spin coating method to place isotropic layer between two polymerized cholesteric liquid crystal films[23], as shown in Figure1-20. According to the Figure1-20 (c), I realize the reflective spectrum of the defect structure. At the same time, the author also simulate reflection spectrum for right-handed circularly polarized light by numerically using 4×4 Berreman method which is shown in Figure1-20 (b). The dip which occurs in the simulation results and measured data demonstrate that there has a single resonance mode in the photonic bandgap.

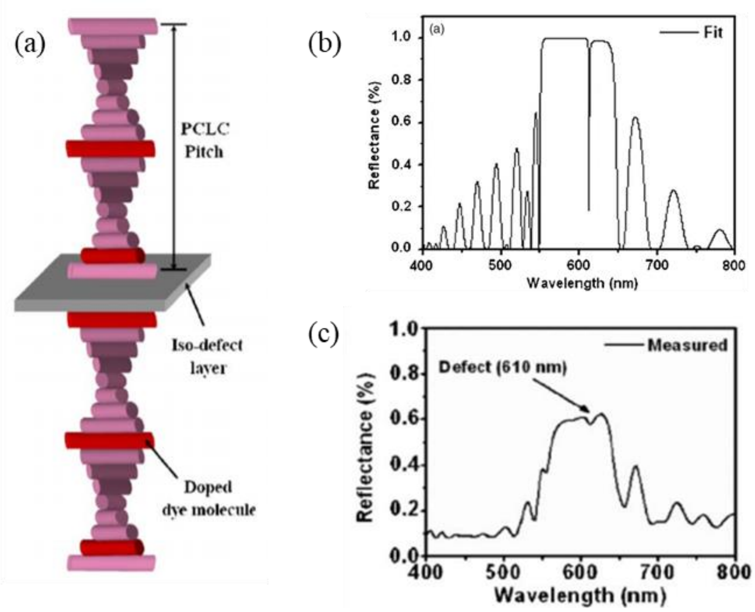

Figure1- 20 (a) Schematic diagram of layer defects mode laser (b) the simulation result of defect structure (c) the measured spectrum of defect structure

Furthermore, the density of state (DOS; refers to the states that can be occupied by a photon) under this structure is simulated, and it is found that at the same wavelength position there is a relatively larger than edge, as shown in Figure1-21(a). But, once the defect layer is removed, only the edge will have a high DOS, as illustrated in Figure1-21 (b). So, it means that the defect mode has lower threshold. Figure1-21(c) is the laser spectrum obtained after excitation of the defect. The emission appears in the photon energy gap where the dip occurs.

To summarize, I have two conclusions about edge mode laser. The first is that the dip that appears in the reflection spectrum of the defective structure will be the light-emitting position of the defective laser; the second is that owing to the high DOS value, the laser threshold at the defect location will be lower.

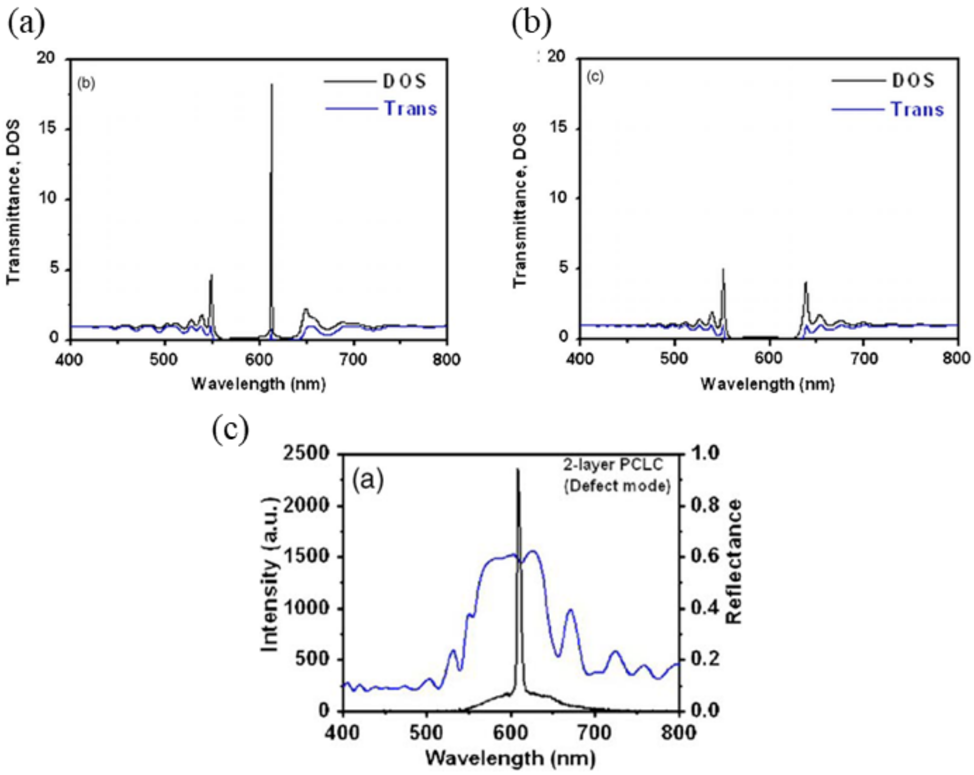

Figure1- 21 (a) the simulated results of density of state with defect structure (b) the simulated results of density of state without defect structure (c) the defect mode laser spectrum[23]

From the above literature of defect mode lasers, we can summarize different ways to modulate the laser emission wavelength. For layered defects, three-layer structures of cholesteric liquid crystals film, isotropic layer, and the other cholesteric liquid crystal film are stacked one by one by spin coating. The wavelength of the resonance place is controlled by the thickness of the isotropic layer and the films which depends on the rotation speed and the chemical concentration[23]. As for phase jump, the researchers use the alignment direction to align the liquid crystals molecules of two cells. After polymerization, the structure of two films can be fixed. Afterwards, the only need is to stack up the single-substrate liquid crystal film and make a discontinuous dislocation defect helical structure[24]. The methods above of fabricating defect mode laser has a common disadvantage- once finish stacking up the samples, the resonance wavelength is fixed. Therefore, the laser emission wavelength is also not tunable. But, for pitch jump, the tunability can be achieved after the fabrication. The liquid crystal in the structure is kept in a flow state, so that the pitch length can be controlled by the illumination time and intensity. However the disadvantage is when in the process of excitation, because the liquid crystal is still in a flow state, slightly thermal disturbance or environmental sources may disturb the helical structure of the cholesteric liquid crystal which is highly sensitive to the light and heat and cause unpredictable wavelength shifts[25]. That's why, in my research, I try to keep focus on making a stable and tunable defect mode laser.

1.3 Proposed method and scope

There has been a lot of research on cholesteric liquid crystal band edge laser as well as tunable band edge laser. But, as we know in the simulation, the threshold of defect laser will be lower than edge, which provides a better driving condition. In the past literature, the optical phenomenon of the defect structure was mainly observed by simulating or by measuring the transmission spectrum, and a few of them successfully excited the defect laser. It is needless to say to make a high quality tunable defect mode laser. That is why I try to make defect mode laser but still keep the tunable characteristic of cholesteric liquid crystal. The continuous tunability has not been fully presented, so here I hope to fully present the wavelength-tunable defect laser through simulation and experiments.

The schematic of our tunable defect mode laser sample is designed as below figure. I use mirror and cholesteric liquid crystal film as our resonant cavity. Then, I fill in liquid crystal E7 and Dye mixture. E7 is supposed to help changing phase retardation by applying different AC voltage to tune the position of the defect mode. As for dye, it acts as the gain media. After designing the cell structure, I plan to use simulation methods for checking if it is feasible to get defect mode tunable laser. Then, I will make the cell and use the experimental methods to verify the results of the tunable laser. It is expect that by applying different voltages I will obtain a laser spectrum shifted in the photon energy gap.

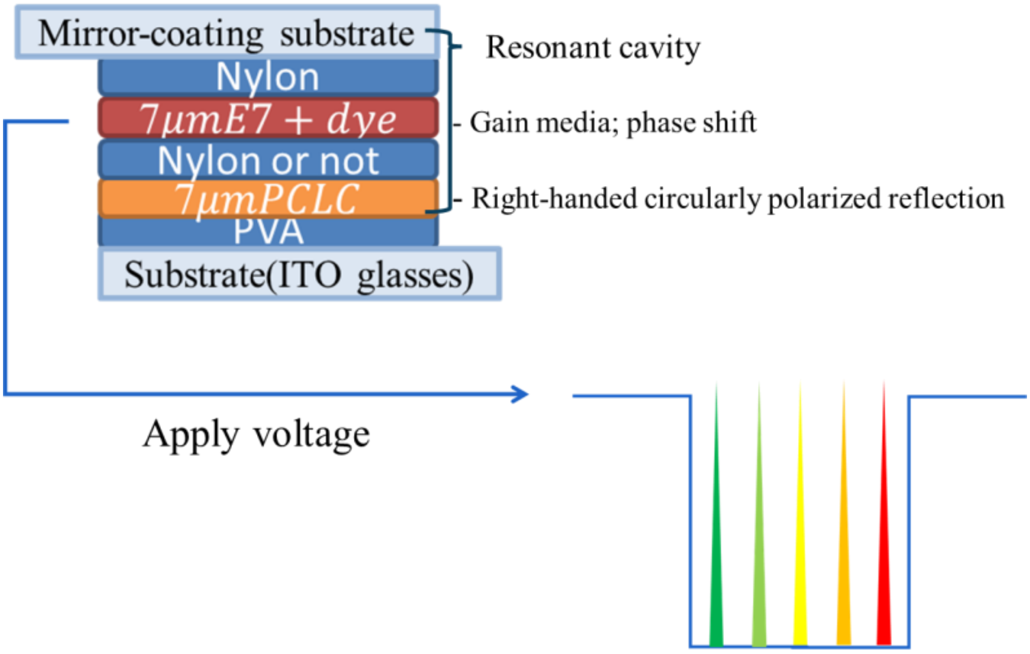

Figure1- 22 Schematic diagram of our design

Chapter 2 Simulation

From previous section, we know that there are two kinds of cholesteric liquid crystal-based laser. One is band edge mode laser, and the other is defect mode laser. From the reference, we can approach lower threshold in defect mode laser. Based on the simulation results from one of my supervisors PHD student Frederik van Acker, we believed that it is possible to make a defect mode laser according to our ideal designed structure.

By 4×4 Berreman methods[26], we are able to simulate one side substrate: transmission and reflection behavior of reflective liquid crystals film. Simultaneously, we set the different reflectivity of different materials coating as simulating the other side mirror substrate. Then, we applied the retardation property by the formula which is explained as Eq (1-9) so as to analog the liquid crystal layer (defect layer). Those conditions are brought into the laser threshold formula in Eq.1-15. The gain threshold and lasing wavelength are found by increasing the optical gain until the round trip gain equals one for a certain wavelength. To obtain a laser, we should achieve the lasing threshold condition.

The laser occurs at the position where the lowest threshold appears. Based on the simulation results, we are able to detect two kinds of lasers which are defined in previous section. We simulated with two common metal coatings which are aluminum and silver. The results are shown as below in different-coated mirror based structure. From figure2-1 and figure2-2, we found three lines and they are represented as long band edge, short band edge, and defect mode in the band gap. We demonstrated that we can obtain defect mode laser at 1/4 waveplate condition (controlled by liquid crystal layer). And, if we compare two figures below, we are able to choose one metal to reach the lowest threshold condition which is silver-coated based sample. That's why we choose to use silver-coated substrate as our mirror-based substrate in the following experiment.

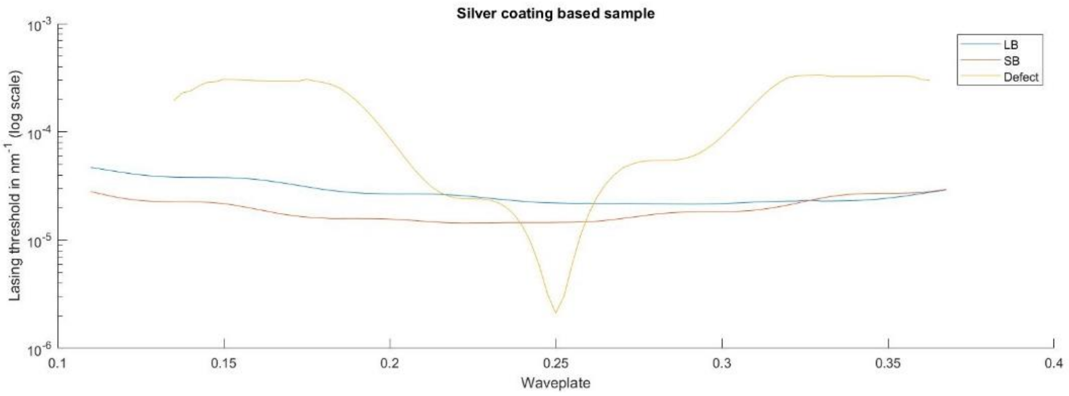

Figure 2- 1 laser threshold simulation with silver-coated based sample

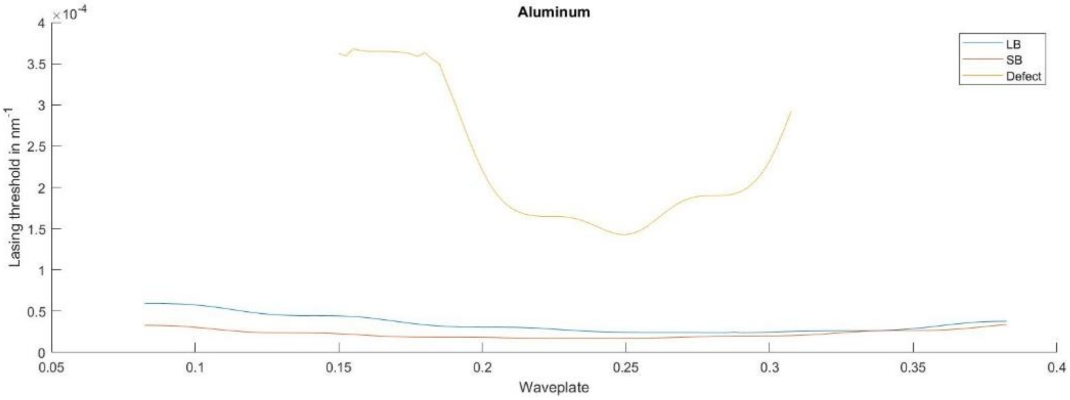

Figure 2- 2 laser threshold simulation with Aluminum-coated based sample

Also, we further simulated the position where the lowest threshold happened. X represents the position in the sample. 0 is the place where the glass substrate surface locates closed to the position of CLC film. 1 is the place where the mirror surface exists closed to the position of liquid crystal film. We detected that the lowest threshold occurs when defect mode forms and the gain are located at the edge of mirror-based substrate.

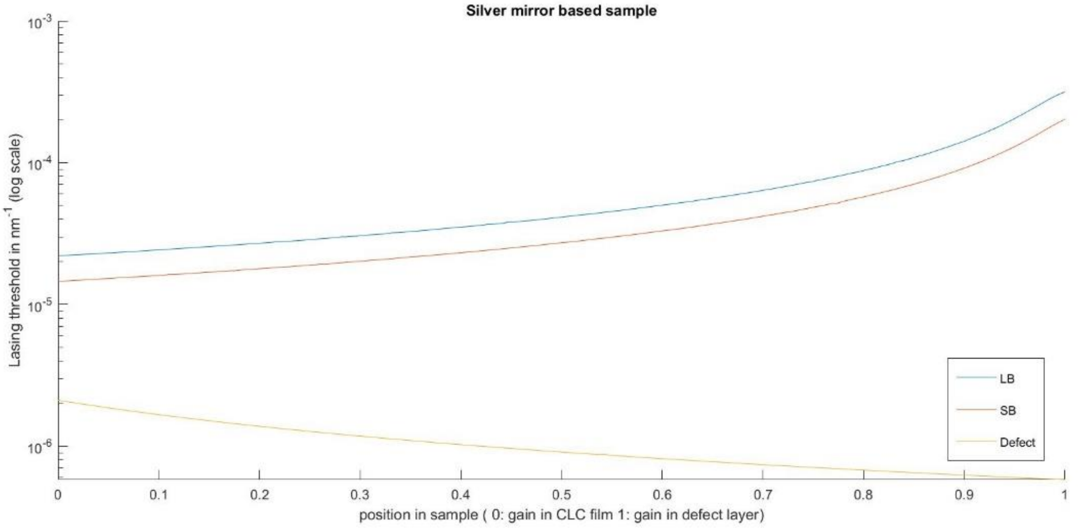

Figure 2- 3 the position where the lowest laser threshold occurs

To summarize, based on the simulation results, we are capable of detecting defect mode laser with our designed structure. We can obtain the best property of defect mode laser at the position of liquid crystal layer by silver-coated mirror-based sample. The following experiments are conducted in order to demonstrate the simulation results we get.

Chapter 3 Materials and experiment

In my research, two kinds of mixtures- cholesteric liquid crystal and dye doped liquid crystal are prepared as the table below shows. They will be discussed in detail in the following section. I divide my fabrication process into four steps: preparation of the cells, fabrication of one-side cholesteric liquid crystal film, preparation of mirror-based cholesteric liquid crystal film and filling in the cells with dye and E7 mixture. The schematic diagram is shown below. I will then introduce the measurement system that I used in this research.

Cholesteric liquid crystal	RM257,105,82	BDH	IRG	Tert	DCM
	47%,30%,20%	Suitable amount	1%	2%	Suitable amount
Dye doped liquid crystal	E7		PM597		
	99%		1%		

Table.1 The composed ratio of two mixtures in this research

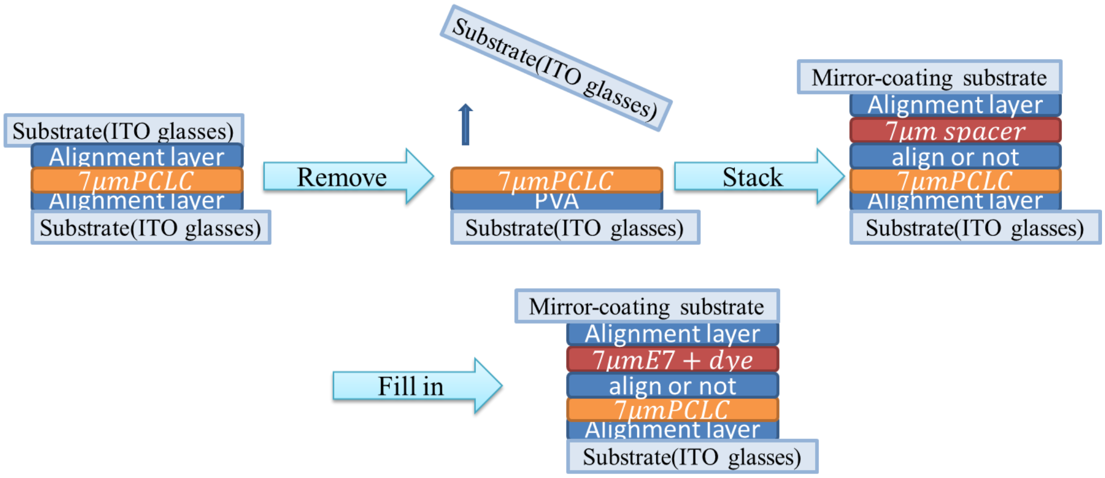

Figure 3- 1 Schematic of process flow

3.1 Introduction of materials and preparation

A. Host material- liquid crystal monomers (RM257, RM105, RM82)

The function of monomers is to form polymer branches after UV illumination which leads to the formation of the solid film. RM82 is composed of two liquid crystalline diacrylate monomers with side group of 6-carbon spacers. Similarly, RM257 is two liquid crystalline diacrylate monomers but having side groups of different lengths which is comprised by 3-carbon spacers. And, the chemical structure of RM105 is made by liquid crystalline monoacrylate monomer[27].

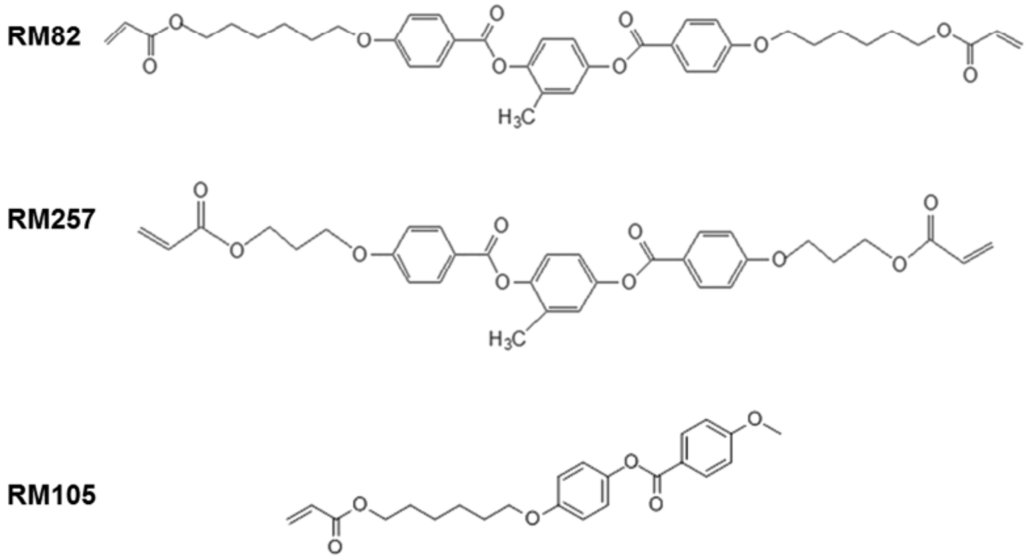

Figure 3- 2 The chemical structure of liquid crystal monomers

B. Chiral dopant (BDH1305)

BDH1305 is a kind of right-handed chiral dopant, and it cause the right-handed twist of the liquid crystal. Therefore, it is used to form cholesteric phase which offer right-handed circularly polarized reflection. Furthermore, the helical twisting power of BDH1305 is around $10(\mu m^{-1})$ for liquid crystal monomers. By modify the concentration of the chiral dopant, I can adjust the wavelength of the selected reflective wavelength. The cholesteric liquid crystal range should be made in the range of emission wavelength of dye.

C. Photo initiator (Irgacure 819)

Photo initiator helps to absorb ultra violet light and convert the light energy into chemical energy in the formation of reactive intermediate which then start off the process of polymerization.

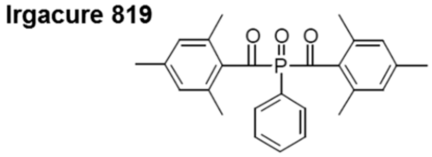

Figure 3- 3 schematic of Irgacure 819[27]

D. Inhibitor (tert-Butylhydroquinone)

Tert is an agent that slows or interferes with a chemical action of the mixture to avoid those chemicals react with each other. The chemical structure of Tert is shown as below.

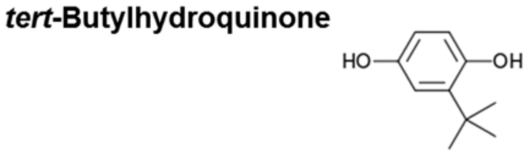

Figure 3- 4 chemical structure of tert[27]

E. Solvent (DCM)

DCM is used as the solvent to mix the liquid crystal monomers, chiral dopant, photo initiator and inhibitor uniformly. Finally, this solvent will be evaporated before filling into the sample.

F. Laser dye (Pyrromethene597, PM597)

PM597 is a kind of laser dyes which is used as laser medium in a dye laser. The chemical structure is shown as figure 3-5. The absorption range of dye is from around 450-575nm. And, it emits the light range from about 550-700nm. The dye absorption and emission spectra are shown in the figure3-6.

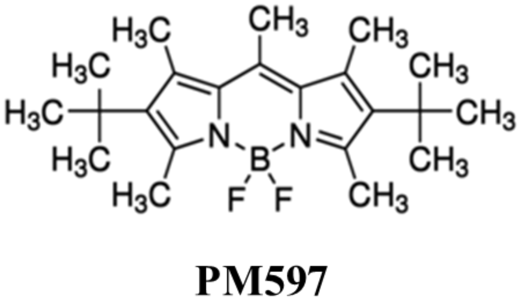

Figure 3- 5 The chemical structure of PM597

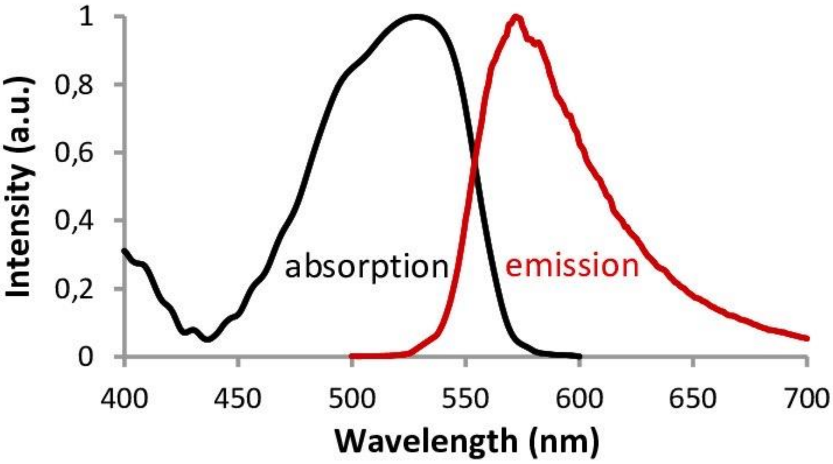

Figure 3- 6 Dye absorption and emission spectra[28]

G. Nematic liquid crystal (E7)

The E7 nematic liquid crystals possess relatively high birefringence and positive dielectric anisotropy. In my research, I use it to control the phase retardation by applying different voltages.

3.2 Fabrication of samples

In this section, I will talk about how to make the sample. The first step is to make the cholesteric liquid crystal film as one-side reflective medium which were composed of two indium-tin-oxide (ITO) coated glasses. Afterwards, I filled in Cholesteric liquid crystal and shone the UV light to photo-polymerize it into a solid film. The second step I lifted off one side of ITO glasses. Then, in the third step, I sealed the cholesteric liquid crystal film with mirror coated ITO glasses. Finally, in step four, I filled in the E7+dye mixture. In the following, the detailed fabrication process of my cells will be described.

3.2.1 Preparation of cells

I. Clean the substrates

  1. Prepare two glasses whose size is 2.5cm×2.5cm and place them in the holder.
  2. Pour the detergent which is composed of the water and neutral detergent (RBS 105) with the ratio of around 10:1 in the beaker (low concentration of neutral detergent), and put the holder in the beaker.
  3. Put the beaker in the ultrasonicator for 15 minutes so as to clean the glasses by agitating the liquid solution of water or solvent which causes the cavitation of solution molecules.
  4. Use Deionized water (DI) water wash out the remain detergent on the glasses and dry the glasses with Nitrogen gun.
  5. The detergent is replaced by acetone and the step 3. and step 4. are repeated.
  6. The detergent is replaced by isopropanol (IPA) and the step 3. and step 4. are repeated.

II. Fabricate the homogenous alignment layers (Polyvinyl alcohol, PVA and Nylon)

  A. PVA for horizontally orientation

    1. Polyvinyl alcohol is dissolved in the deionized water. Then, PVA solution is well-prepared.
    2. The cleaned glasses were put on the stage in oxygen plasma machine. The stage is heated up to 90°C and is held at this temperature for 10 minutes then press the button for oxygen discharging. This process is to do the chemical modification of the surface which turns the surface to hydrophilic surface.

3. Place the glass on the platform of spin coating machine as shown in Figure 3-7.

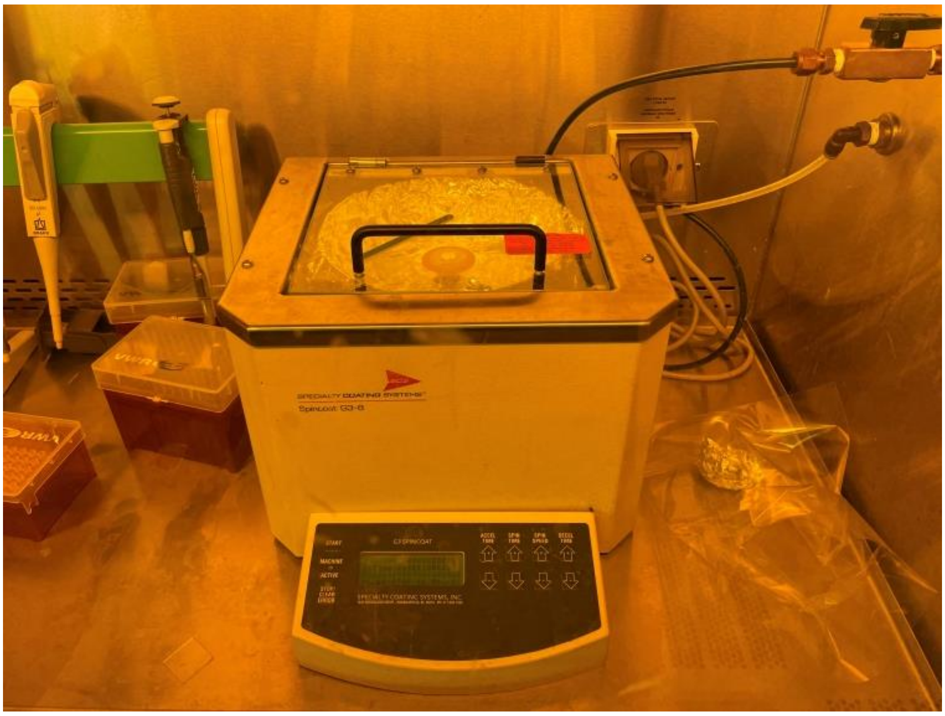

Figure 3- 7 spin coating machine in the cleanroom

4. Use micropipette to absorb the PVA solution and drop evenly on the glass.
5. The rotation speed of spinning is set at 2500rpm and the rotation time is 30 seconds. The fixed rotation speed can make the PVA alignment solution well-distributed on the surface of the ITO substrate. Therefore, a uniform thickness of PVA alignment film is formed.
6. Then, I set the temperature of hot stage at 90°C and place the coated glass on it for a soft bake for 5 minutes.
7. Place the coated glass on the platform of rubbing machine and set the moving speed of the platform and the rolling speed of the velvet cloth. Then, like the below schematic of the rubbing system, I can brush the micro-grooves direction on the alignment layer so as to give the

orientation of liquid crystal molecules.

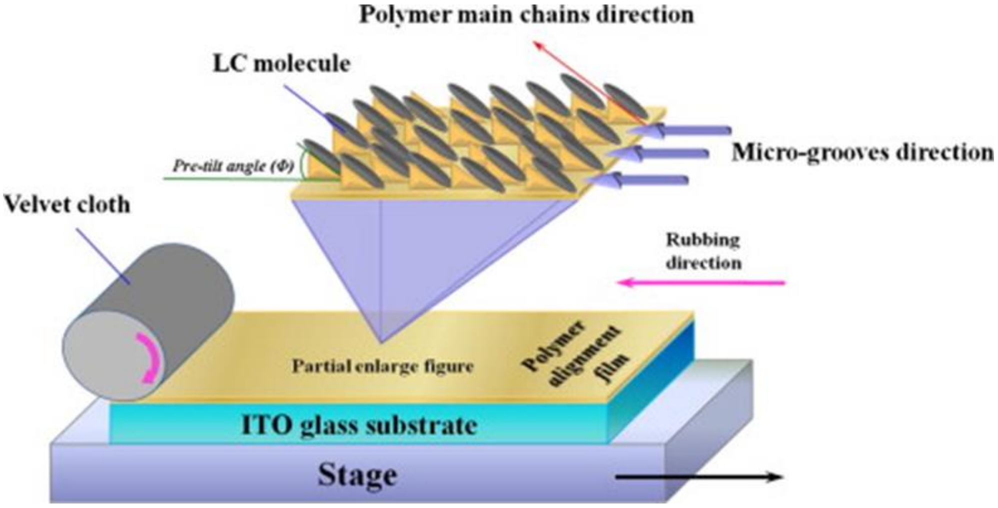

Figure 3- 8 Schematic of rubbing system[29]

B. Nylon for horizontally orientation

1. Dissolve 1wt% Nylon into Trichloroethylene (TCE) solvent.
2. Place the glass on the platform of spin coating machine.
3. Use micropipette to absorb the PVA solution and drop evenly on the glass.
4. Like PVA coating step5, I set the spin speed at 3500rpm and the rotation time 45 seconds. And, press start to spin coat the alignment film.
5. Then, I set the temperature of hot stage at 90°C and place the coated glass on it for soft bake the glass for 2 minutes.
6. The coated substrate was then put in the oven for 4 hours and the temperature was kept at 180°C.
7. Then, do the same step as PVA coating step7. The coated glass was rubbed by the rubbing machine.

III. Assembly of the liquid crystal cell

1. Take two glasses. One with the PVA coating on substrates and the other with the Nylon coating for easily lifting off the film (I will discuss in chapter 4).

2. Squeeze UV glue on a glass slide.
3. Select the suitable spacer powder size (in this experiment, I choose 6.75μm spacer) and mix the spacer with the UV glue uniformly.
4. Use slicker spoon to put the mixture in the needle and tighten the needle with the syringe.
5. Squeeze the mixture on the edge of one substrate with the dispenser.
6. Stack up two pieces of glasses.
7. Place my sample under UV light for curing UV glue and set the exposure time for 3 minutes. This step helps to seal the two glasses with the cell gap around 6.75μm.

IV. Measurement of cell gap of the cell

To make sure the cell's cell gap I use the Febry-Perot principle to measure. When white light is incident on the empty cell (two glasses sandwiched by air), multiple reflections and transmissions will be formed, as shown in Figure3-9. Due to the phase differences, two adjacent transmission lights will give rise to constructive interference. The precise interlayer thickness can be obtained by measuring the interference spectrum with spectrometer. The calculated formula will be illustrated in the following.

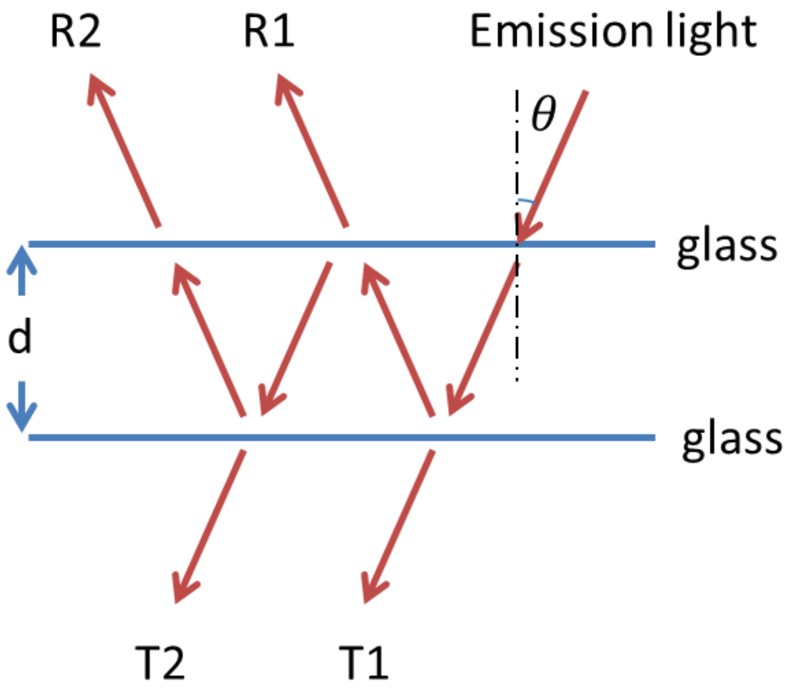

Figure 3- 9 Schematic of interference

According to Bragg law, the phase difference can be written as:

$$\frac{2\pi \times n \times d \times sin\theta}{\lambda} = 2m\pi(m \epsilon\ constant) \qquad \text{(Eq3-1)}$$

where n is the refractive index, θ is the angle between the normal direction of the substrate and direction of the incident light, d is the unknown cell gap and λ is incident wavelength. Assume that the refractive index n of air is 1and the incident angle of light source in the measurement setup is parallel to the normal direction of the substrate, so $sin\theta$ equals to 1. I can rewrite the formula as:

$$2d = m\lambda(m \epsilon\ constant) \qquad \text{(Eq3-2)}$$

If a white light source is used, the wavelengths passing through the cell will form different phases and each wavelength will interfere with each other. From the peaks of adjacent constructive interference in the spectrum as shown in Figure1-35, I can then calculate the thickness of the cell:

$$2d = m\lambda_1 \qquad \text{(Eq3-3)}$$

$$2d = (m+1)\lambda_2 \tag{Eq3-4}$$

Organized by Eq3-3 and Eq3-4, the thickness of the cell can then be obtained as shown in formula 3-10:

$$d = \frac{\lambda_1\lambda_2}{2|\lambda_1-\lambda_2|} \tag{Eq3-5}$$

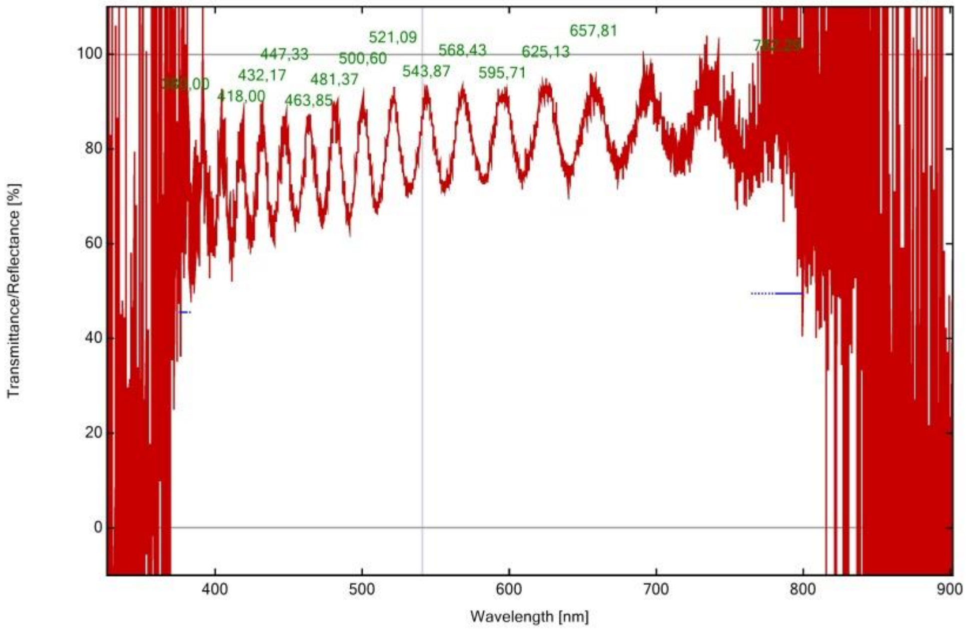

Figure 3- 10 Figure of measuring interference spectrum

3.2.2 Fabrication of one-side cholesteric liquid crystal film

The emission quality of the laser is related to the performance of resonant cavity. It is indispensable to make the cholesteric liquid crystal film uniform. If not, declination lines or the scattering of the structure may have a huge effect on the final result. Luckily, I find some ways to improve my film. The process in the following section describes how to make a cholesteric liquid crystal film.

I. Prepare cholesteric liquid crystal mixture

   1. Prepare the needed materials for cholesteric liquid crystal mixture. The composed ratio of it is listed in the beginning of Chapter 3 and the function of each material is described in 3.1.

2. Put a magnetite (stir bar) in CLC mixture and make it stir on the stirring stage for more than one hour.
3. Take out the needed amount of CLC mixture and put it on the slide glasses by spatulas.
4. Set temperature of hot stage in the vacuum injector at 90 degree. Bring slide glasses and empty cell onto hot stage. This step helps to evaporate solvent-DCM.

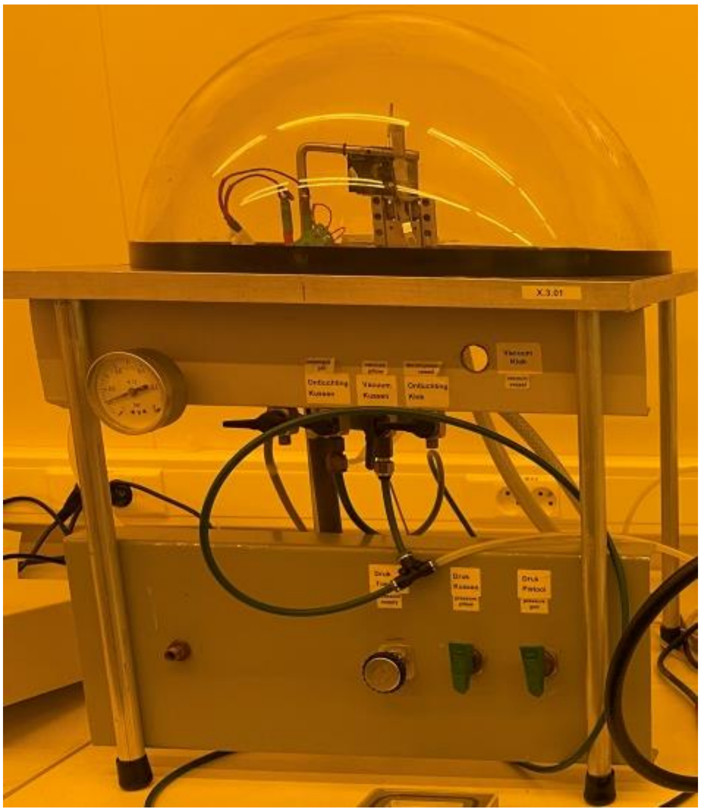

Figure 3- 11 Vacuum injector in the cleanroom

II. Get a good quality CLC sample

1. Fill the mixture by spatulas into the empty cell in the vacuum environment.
2. After filling with the CLC mixture, the sample is brought to the oven which was preheated to 90°C.
3. Turn off the oven and leave the sample in the oven for one night. When the liquid crystal molecules are disturbed by heat energy, the free energy will

increase. If the external energy is removed (cool down), the molecules would automatically be rearranged to planar state which is the lowest free energy of CLC texture. In this process, most of the declination lines and different CLC pitch structures will gradually disappear.

4. Investigate by polarized optical microscope and measure the wavelength by spectrometer.

III. Photo-polymerize the sample

1. Place the sample under the UV light and photo-polymerize with the highest intensity of UV light for 5 minutes. The polymerization is employed to prepare thin films as well to generate polymer stabilizing networks in mixtures with liquid crystal monomers.

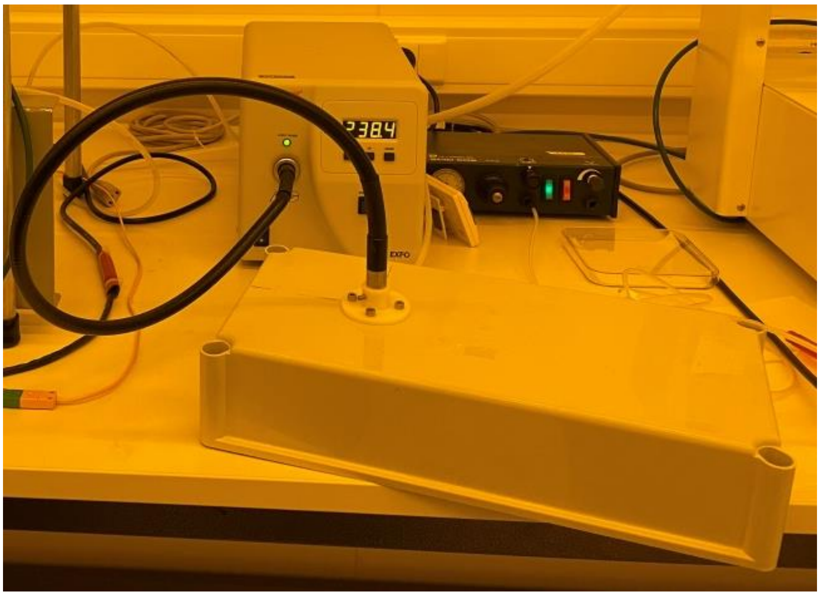

Figure 3- 12 UV light in the cleanroom

3.2.3 Mirror-based Cholesteric liquid crystal film

I. Remove one side of the cell

In order to make a single-substrate liquid crystal film, this experiment mainly uses a liquid crystal cell composed of horizontal alignment Nylon based glass substrate and PVA based substrate. The two different alignments offer different anchoring energy. I then use razor blade to separate two glasses. The glass with Nylon coating is peeled off owing to the lower anchoring energy, leaving the CLC film stick on the glass with PVA coating. The cholesteric liquid crystal film with single substrate is shown as the figure 3-13.

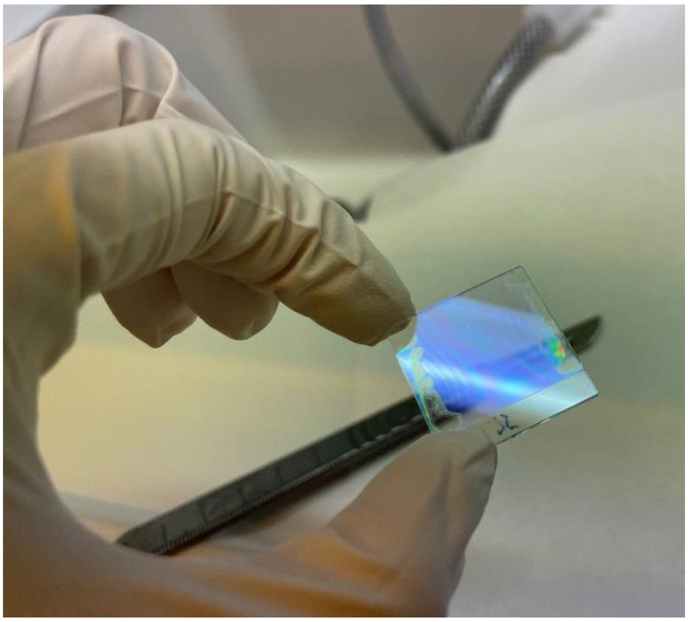

Figure 3- 13 Figure of single- substrate CLC film

II. Deposit mirror on the glass substrate

In order to make a high reflective resonant cavity, I replace one side glass with mirror coating glass. The mirror coating glass is made by two layers of metal. First, the attached layer- Chromium is deposited directly on the glass. Then, the silver layer is then deposited, providing high reflectivity in visible wavelengths. Even though the attached layer cannot act as a good mirror, it helps the second metal layer stick better on the substrate.

III. Coating alignment layer on the mirror-based substrate

1. Clean the substrate with Acetone, IPA and DI water. And, dry the substrate with the Nitrogen gas.

2. Coating Nylon or PVA alignment layer on the substrate.
3. The coated glass was rubbed by the rubbing machine.

IV. Assemble single-substrate liquid crystal film with mirror-based substrate

1. Squeeze UV glue on the glass slide. Get some 6.75μm spacer powder and mix uniformly in UV glue.
2. Use slicker spoon to put the mixture in the needle and tighten the needle with the pipe
3. Glue UV glue on the side of one substrate
4. Assemble single-substrate liquid crystal film with mirror-based substrate and do the curing process for 3 minutes by UV light.

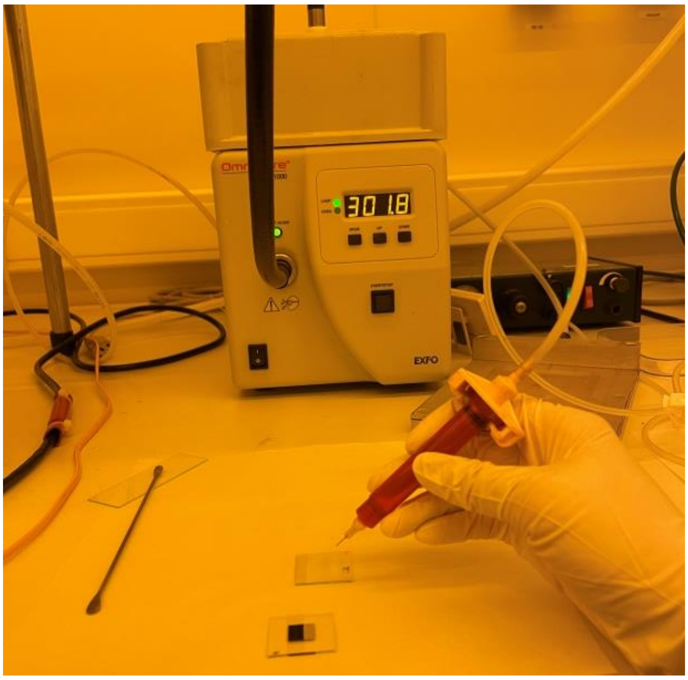

Figure 3- 14 Schematic of assembling my sample

3.2.4 Filling in with dye and E7 mixture

The goal of this experiment is to use liquid crystal layer between polymerized liquid crystal film and mirror to control the position of defect mode by tuning the voltage, thereby modulating the laser wavelength. Therefore, in this step, I fill liquid crystal layer in between two substrates.

A. Prepare the needed materials for dye doped liquid crystal mixture. The composed ratio of it is listed in the beginning of Chapter 3 and the function of each material is described in 3.1.

B. Put magnetite (stir bar) in CLC mixture and make it stir on the stirring stage for more than one hour.

C. Take out the needed amount of CLC mixture and put it on the slide glasses by spatulas.

D. Set temperature of hot stage at 90 degree. Bring slide glasses and my sample onto hot stage. Fill in the dye doped liquid crystal mixture. The schematic of fabrication process is shown as below.

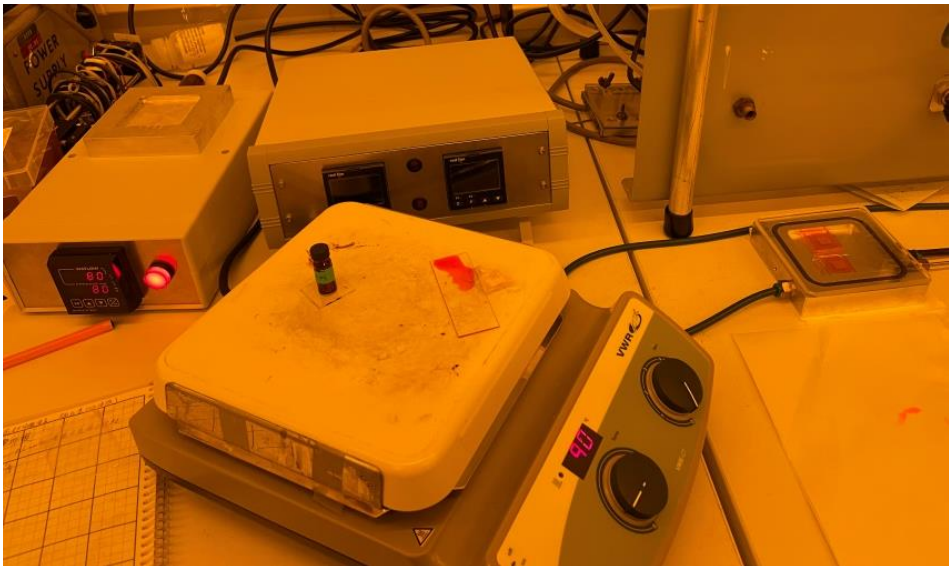

Figure 3- 15 Schematic of filling the dye doped liquid crystal mixture

E. Then, glue AB glue on the side of my sample to avoid water and air destroying the sample.

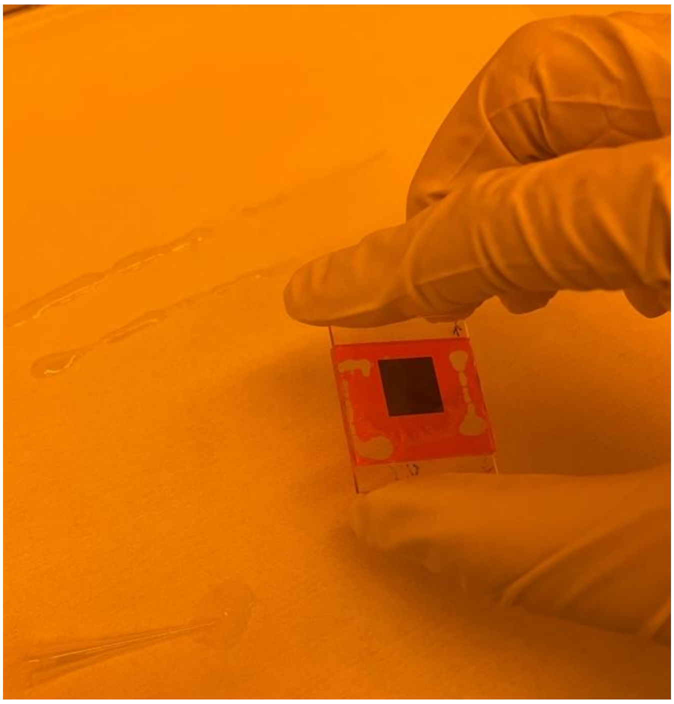

Figure 3- 16 Figure of gluing AB glue on the side of my sample

3.3 Experimental setup

In this research, my objective is to discuss about making a tunable defect mode laser by the designed structure. I not only investigate the optical performance of the sample itself but I also expect to detect the laser wavelength shift or the different optical performance according to voltage difference refer to simulation. I observe the reflective/ transmission appearance of the sandwiched sample by polarized optical microscope. Furthermore, I utilized two main systems to measure my sample. One is a laser system, and the other is spectrometer. To avoid the non-uniform optical performance in large spot size, I further improve my measurement by building microscope-based spectrometer. The signal of the reflection/transmission of my sample was investigated by a fiber spectrometer which was set at the same position of microscope CCD. Additionally, in each system, I apply a function generator equipped with an amplifier to apply special electrical treatment on the sample. I will then describe the experimental setup that mentioned above in details in the following section.

3.3.1 Measurement of optical characteristics under polarized optical microscope

Figure 3- 17 Schematic of polarized optical microscopy with CCD

The manufactured sample is observed through the system shown above. In each step of fabrication, I observed by this system to check if my sample is in good condition. The influence of adding any layers of different materials can be investigated through this system.

3.3.2 Laser measurement setup

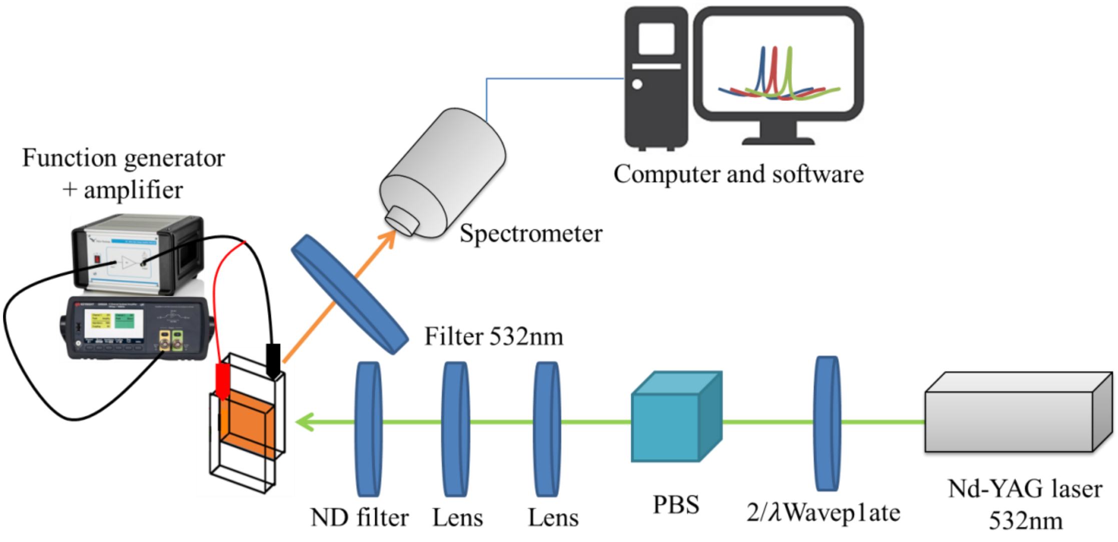

Figure 3- 18 defect mode laser measurement system

The measurement setup in this study is shown above. From Figure 3-6, I realize that the maximum absorptive wavelength of laser dye-PM597 is around 532nm. Therefore, I select Nd-YAG (neodymium-doped yttrium aluminum garnet) pulsed laser which generates polarized laser light at 532nm as the pumping laser source. The laser beam is then passing through the half wave plate, and polarized beam splitter. Polarizing Beam splitter is designed to split light by polarization state so as to transmit p-polarized light while reflecting s-polarized light. Half wave plate and polarized beam splitter are combined to modulate the intensity of laser beam. After these two components, the beam is then incident on two lenses followed by a 532nm filter. Lenses benefits from focusing the laser on my sample and exciting the laser dye. By the filter, the emission laser beam can be blocked. The spectrometer detects only the signal from the excitation of my sample.

Finally, to investigate the variation of applying different voltages, I utilize function generator to apply voltage. The upper voltage limit of function generator itself can only reach to 10 volts. Thus, I connect function generator output with function amplifier input and link the amplifier output with my sample with crocodile clip wire. The cell is sticked with copper foil tape for easily applying voltage.

3.3.3 Large area reflection signal measurement

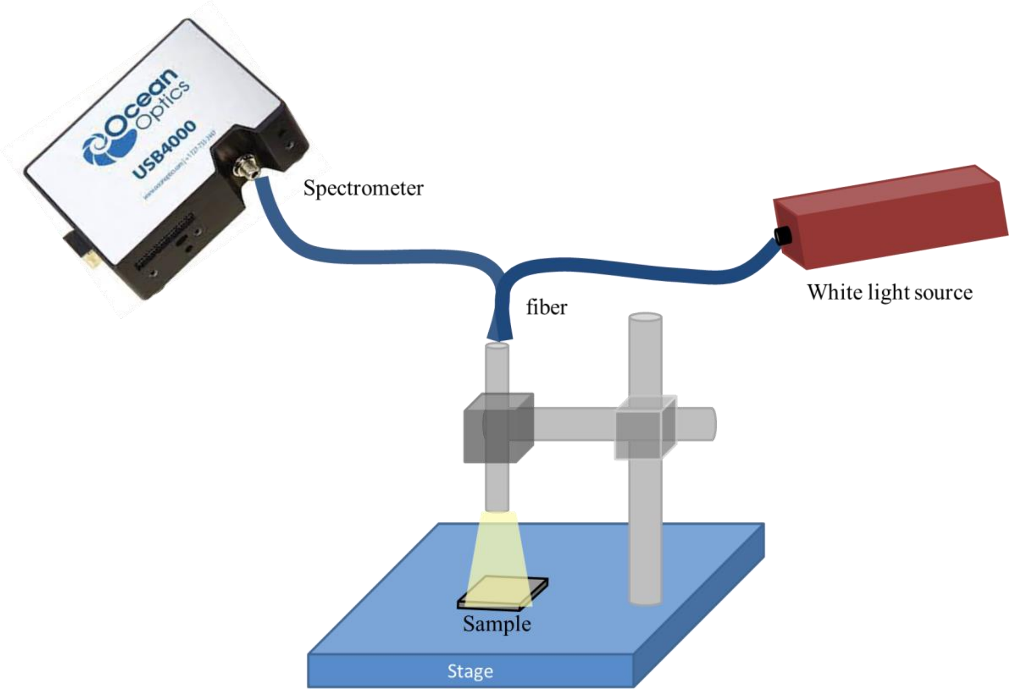

Figure 3- 19 Schematic diagram of reflection spectrum measurement system

To achieve reflective spectrum measurement, a spectrometer, light source, optical fiber, reference sample, and measurement software are required. A Y-shaped reflective fiber is used in the measurement. White light transmits through one port of the fiber and shine on the sample. At the same time, the fiber receives signal from the sample and gather to the other port of the fiber. The spectrometer is used to detect and analyze the distribution of wavelengths. Before starting the measurement, I first place the aluminum-coated glass on the stage to define the reference spectrum. And, switch off the light source to define the environment disturbance as dark signal. Then, I am able to detect the sample reflection spectrum though the system. The disadvantage of the system is that light spot covers almost the whole sample. It is possible that I gather the signal from huge area of my sample. Then, in turn, I measure non-uniformity of sample.

3.3.4 Small area reflection/transmission signal measurement based on polarized optical microscopy

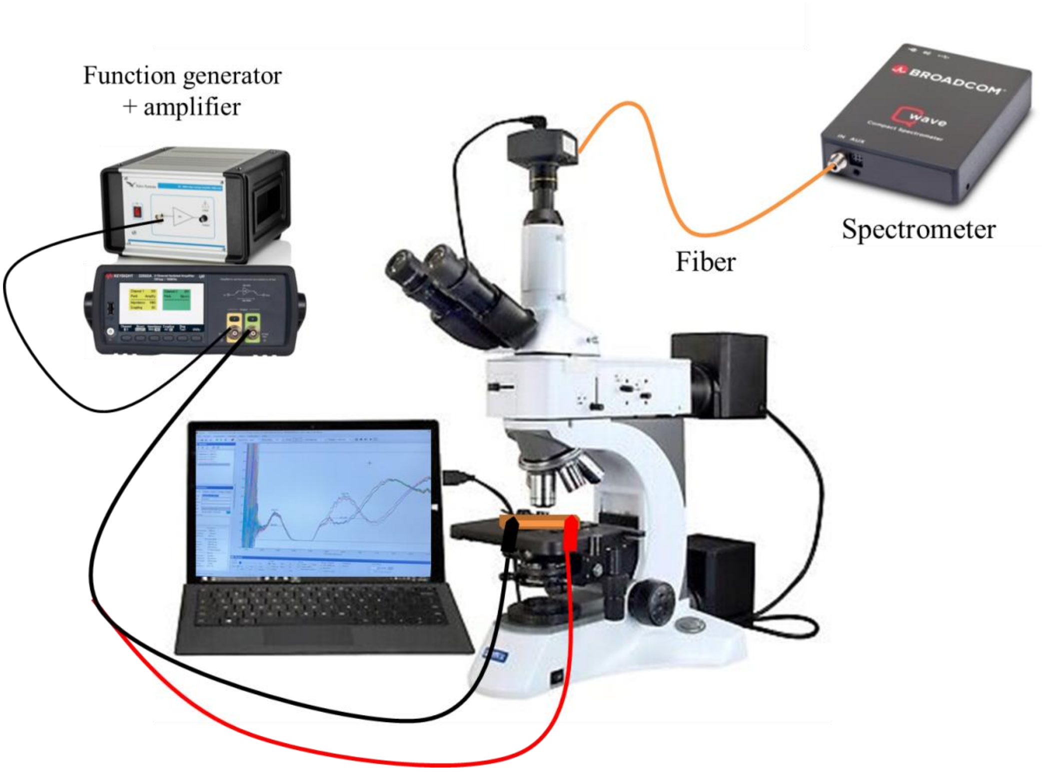

Figure 3- 20 Schematic of transmission/reflection measurement with electrical treatment

To detect the reflection/transmission signal measurement in small area, I further build my system on polarized optical microscopy. The signal I get from the spectrometer will be the same position as the CCD I observe. By checking the uniformity of the area with microscopy, I can avoid detecting disordered liquid crystal and then receive the better reflection and transmission spectrum.

Chapter 4 Results and discussion

4.1 Sample Fabrication and Optimization the sample process

It is important to form the uniform and complete cholesteric liquid crystal film. The better the resonant cavity I make, the better the quality of the laser emission I may get. In the fabrication steps, I make many improvements to optimize my cholesteric liquid crystal film. Also, I sandwiched my film with dye doped liquid crystal. The stack-up procedure should also be improved to form a well-arranged sample.

4.1.1 The effect of different alignment layers in CLC cells

For observation of the optical properties and microscopy image is it important to align the molecules in the same orientation. By spin-coating the alignment layer and rubbing it, the polymer chains on a surface are aligned in the referenced direction. This structure benefits liquid crystal molecules from aligning them to the same orientation[30]. There are several kinds of commonly used alignment layers, for example polyvinyl-alcohol (PVA), polyimides (PI), Nylon and so on. In the lab, I have two kinds of polymer for horizontal alignment- PVA which is dissolved in the deionized water and Nylon which is dissolved into Trichloroethylene (TCE) solvent.

At first, I used the cell with two PVA coating substrates and filled in cholesteric liquid crystal, the schematic figure as shown in Figure 4-1(a). After photo-polymerization, I formed my cholesteric liquid crystal film. By using razor blade, I was able to remove one side of substrate. Because I applied the stress on the film by using razor, I found that my film was separated into two films and each of them attached on one substrate as shown in Figure 4-2(a). The destroyed film is not good at acting a perfect resonant cavity and also it is hard to investigate its physical and optical properties in small area. Then, I came up with the idea that trying to fill in cholesteric liquid crystal in different substrates that are coated with different alignment layers. Based on the difference of alignment layers, chemical interactions between the alignment layers and liquid crystal molecules are supposed to differ from each other and give rise to the different anchoring energies. So, I replaced one PVA based substrate with Nylon based substrate. The structure of my sample is shown in Figure1-46(b). I discovered that after the removal of the one side substrate, I then get a prefect and complete film without damaged parts, as shown in Figure 4-2(b).

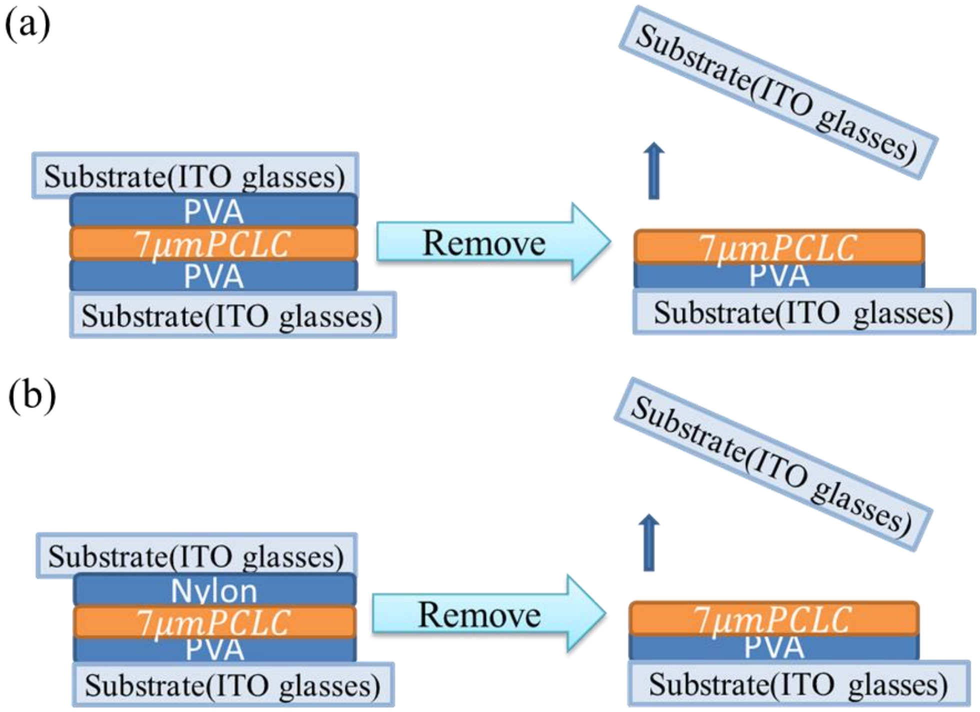

Figure 4- 1 Schematic of the removal of different coating alignment layers of the cells

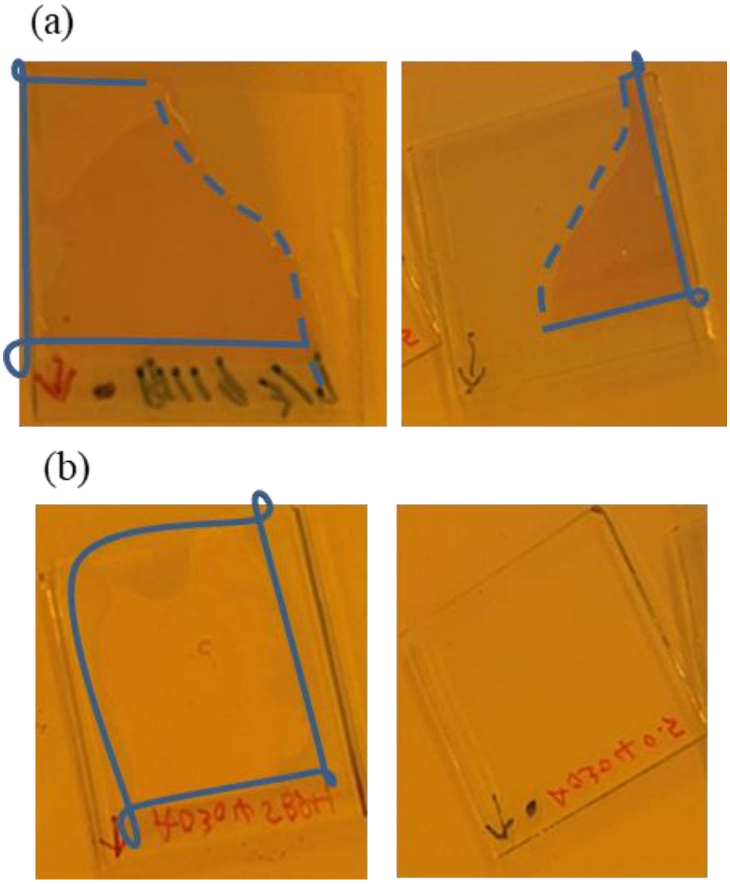

Figure 4- 2 (a) Films with two PVA coating substrates (b) Films with PVA & nylon coating substrates

4.1.2 The method to solve investigation problems of CLC

It is not enough to get the complete cholesteric liquid crystal film. In my experiment, perfect CLC planar texture film without inclination lines to act as a good reflective material is indispensable. If there are many defects in the liquid crystal film itself, the laser emission will be affected by internal defects and cause scattering and affect the resonance quality, so that the full width at half maximum (FWHM) of the laser is not narrow enough to affect the color purity. Therefore, I should investigate my film under polarized optical microscopy to check the optical performance of my film. As the figure 4-3 shown, there are a lot of declination lines on my first made CLC film. The defects are localized because the director distortion occurs [31]. I decide to fill in the cholesteric liquid crystal in vacuum environment to avoid the air bubbles formed in the cell. And, according to the reference[31], the inclination lines will vanish and shrink with time. I placed my sample in the oven and cooled down my sample from isotropic phase for one night. The result reveals that the inclination lines decreased a lot, as Figure 4-4 shows.

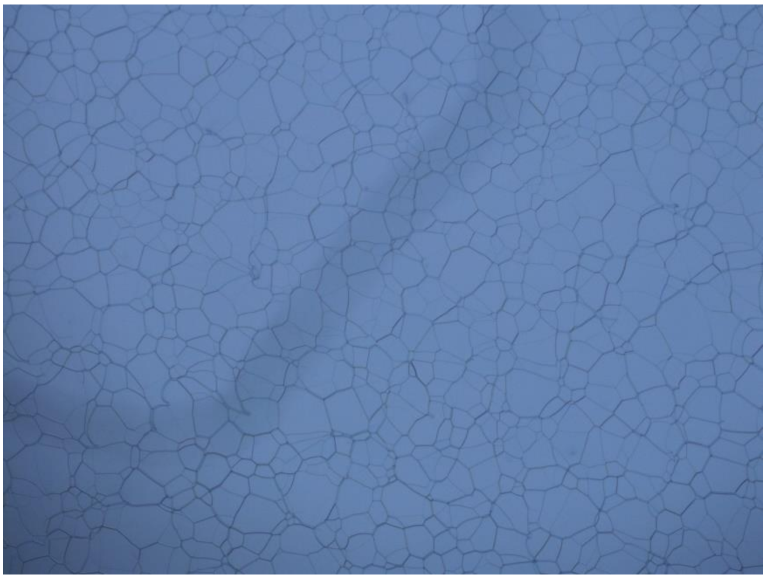

Figure 4- 3 Reflective image under POM. The scale of images is 2.33mm*1.75mm.

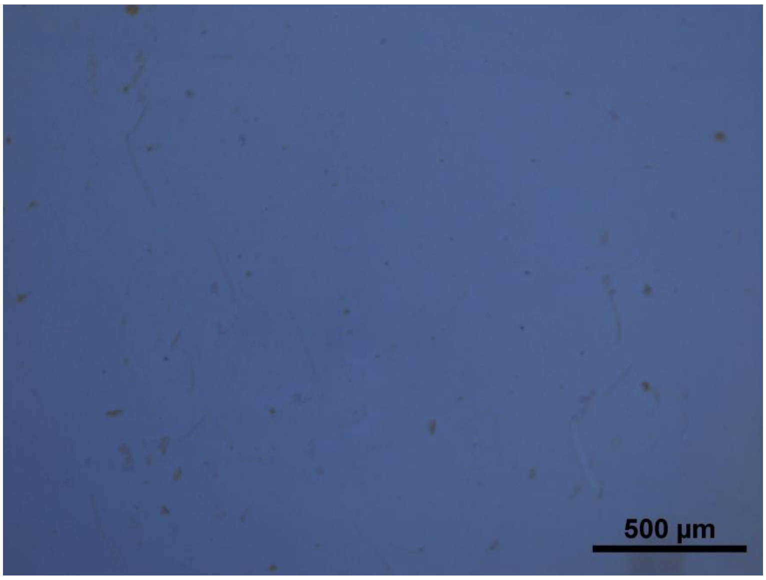

Figure 4- 4 Reflective image under POM.

4.1.3 The effect of spin coating alignment layer on CLC film and fill in the dye doped liquid crystal

In this paragraph, I discuss the variation in wavelength and microscopy image when fabricating different sandwiched layers. I will talk about the difference and optimize my fabrication steps. The schematic diagrams of four stacked-up methods are shown in Figure 4-5.

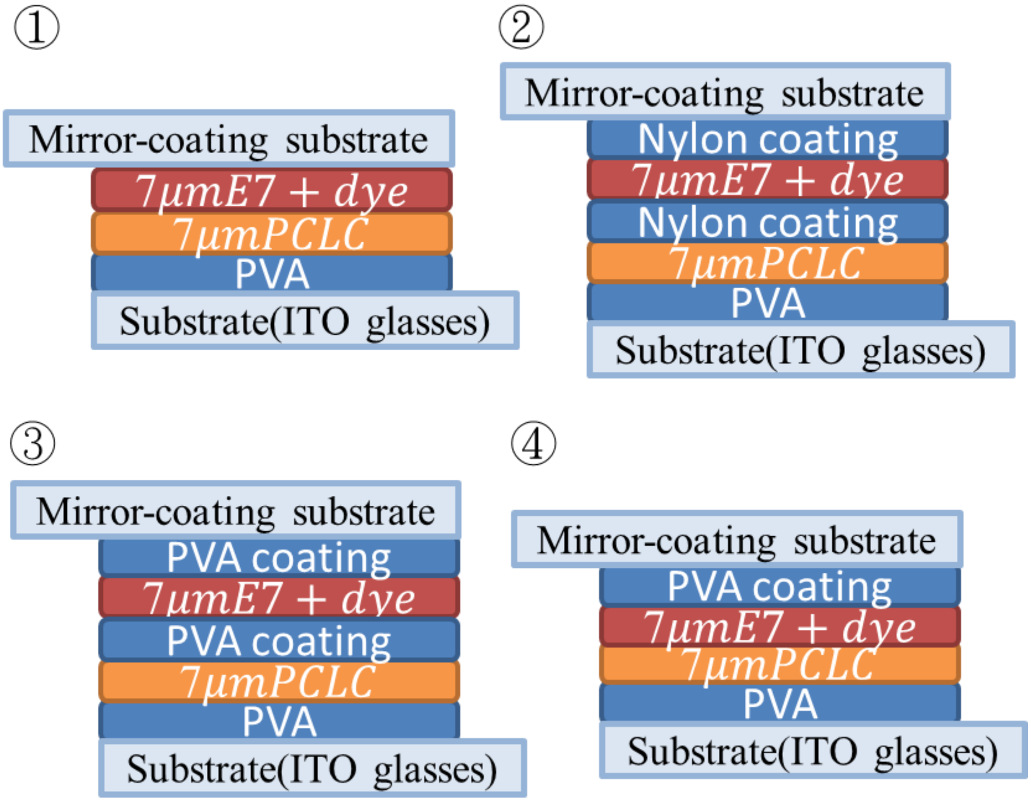

Figure 4- 5 Schematic diagram of different structures of my samples

For the first condition which is shown in Figure 4-5①, without any alignment layer on the surface of the mirror or cholesteric liquid crystal film, I directly stacked up mirror-based substrate with cholesteric liquid crystal film. After filling in the dye doped liquid crystal, I observed the image under the polarized optical microscopy (POM). The image is expressed in the figure below. I discovered that there are large amounts of big and small black dots in the microscopy image. First, I thought of unclean substrates with a lot of particles. But, when I rotated the stage of the polarized optical microscopy, I observed that these dots have brightness variations with the different rotated angles. The microscope is consisted of two crossed polarizers. Even if light blocked by passage through two crossed polarizers, it can be made to pass through crossed polarizers when a liquid crystal material is placed between the polarizers. This appearance is called birefringence in liquid crystal. It demonstrates that the black dots are liquid crystal molecules. And, because of not providing the liquid crystal molecules with alignment layers, the liquid crystal molecules in between are not presented in a high-ordered orientation. I then decided to optimize my fabrication by coating the alignment layers in between to improve the alignment.

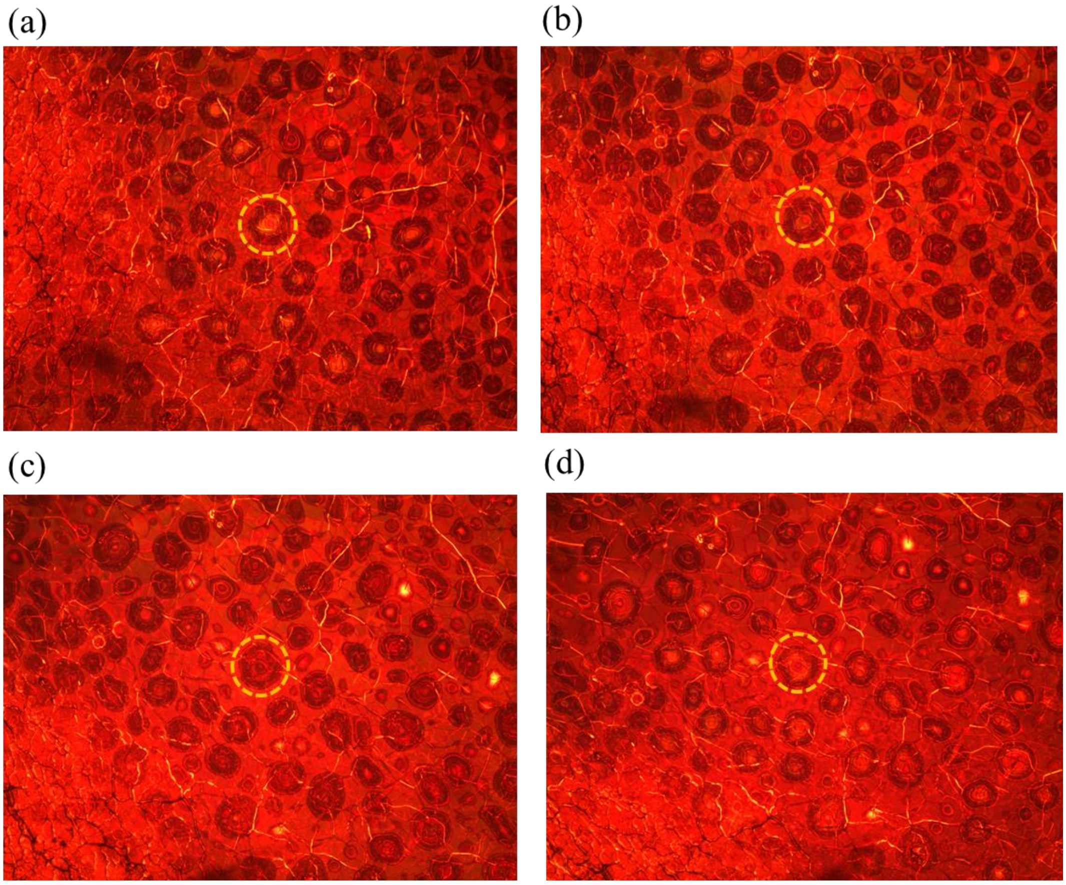

Figure 4- 6 Reflective images of my sample under POM (a) 0 degree of the stage (b) rotate stage to 20 degree (c) 40 degree (d) 60 degree. The scale of images is 2.33mm*1.75mm.

According the Figure 4-5② and ③, I coated two different alignment layers-Nylon and PVA layers on the surface of film and mirror-based substrate. Then, I compared these two conditions. No matter with which kind of alignment layers, I help the liquid crystal molecules arrange well. I successfully eliminated the black dots as shown in Figure 4-6.

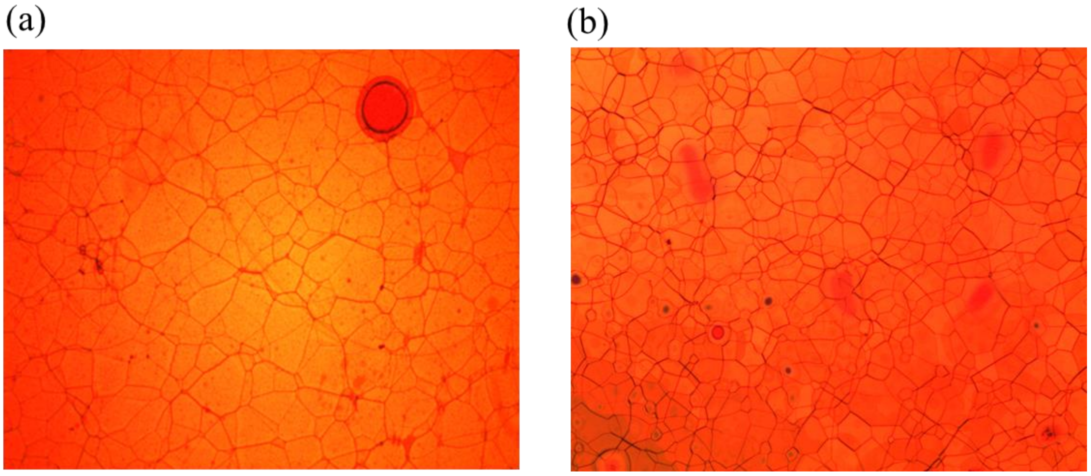

Figure 4- 7 Reflective image of my sample under POM (a) with Nylon coating layer in between (b) with PVA coating layer in between. The scale of images is 2.33mm*1.75mm.

However, when I analyzed the transmission wavelength variations of these two alignment layers, I investigated that wavelength shifts in some steps. According to the figure below, I am able to get the information of wavelength changes in each fabrication step. From figure 4-8, I measured the transmission signals of my Nylon based sample by fiber spectrometer in the cleanroom. At first, the bandgap of cholesteric liquid crystal filled in two glass substrate was detected 622nm to 679nm. And, I removed one substrate and measured cholesteric liquid crystal film. The bandgap is 625-680nm. I noticed that the removal of the substrate made no substantial effect on the wavelength. Then, I recorded the transmission spectrum after I coated Nylon alignment layer and assembled sample. I recognized in this step wavelength blue shifts a lot around 50nm.

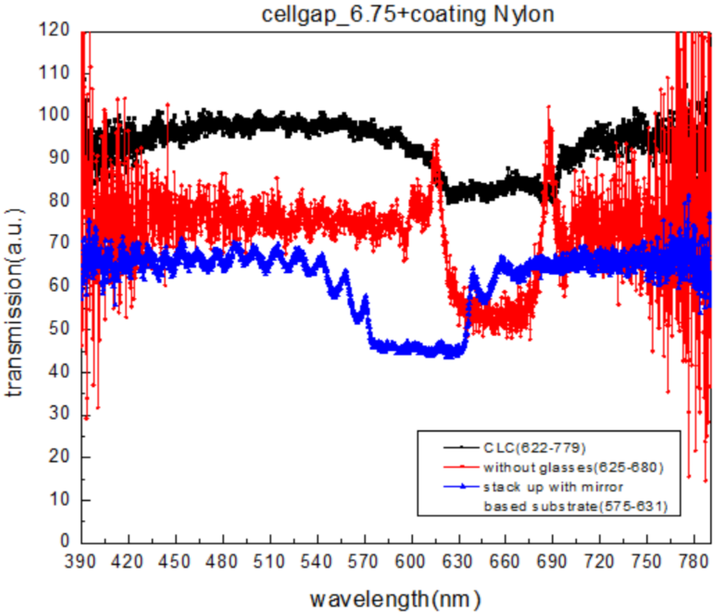

Figure 4- 8 Transmission spectrum of fabricating Nylon coating based structure

Also, I measured the PVA based sample. After I coated the PVA on my cholesteric liquid crystal film, I investigated wavelength variation around 20nm, as the figure 4-9 shows. And, I also discovered the second wavelength displacement occurred when I filled in dye doped liquid crystal. This shifts about 120nm.

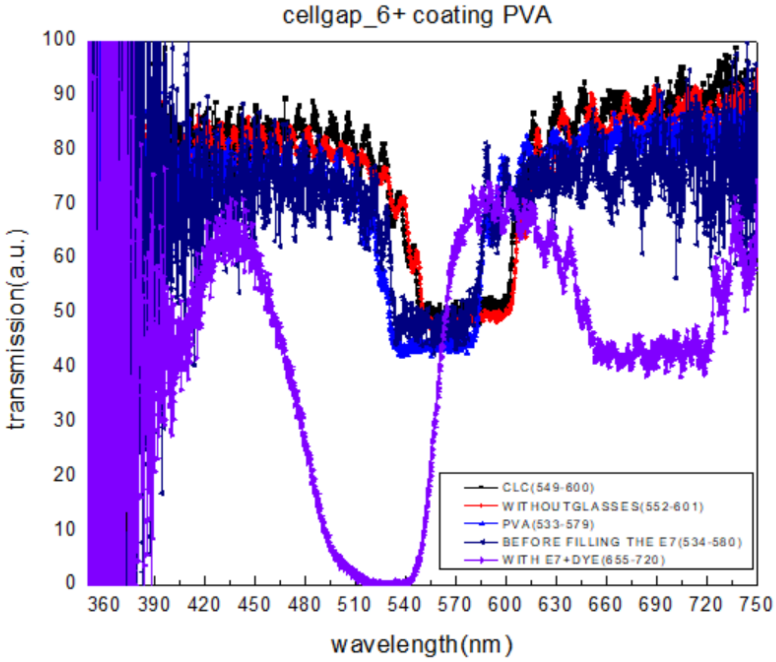

Figure 4- 9 Transmission spectrum of fabricating PVA coating based structure

To solve the shift problem, I have to find out what reason gives rise to wavelength shift. Derived from the transmission spectrum, the first shift happened when I spin coat the alignment layer. The alignment layers are consisted of two kinds of polymer dissolved in solvent TCE or DI water. I then presumed that the solvent results in the wavelength shift. I did the research by directly spin coating the solvent on my cholesteric liquid crystal film. From figure 4-10 and figure 4-11, I demonstrated that the solvents for dissolving polymer alignment material truly affect the structure of my film. DI water leads to 10nm difference in wavelength and also gives rise to several holes on CLC film. As for TCE, it results in more than 40nm wavelength shift and the appearance of CLC film is destroyed seriously. The solvent not only dissolved the polymer alignment material but also dissolved well-fabricated CLC film.

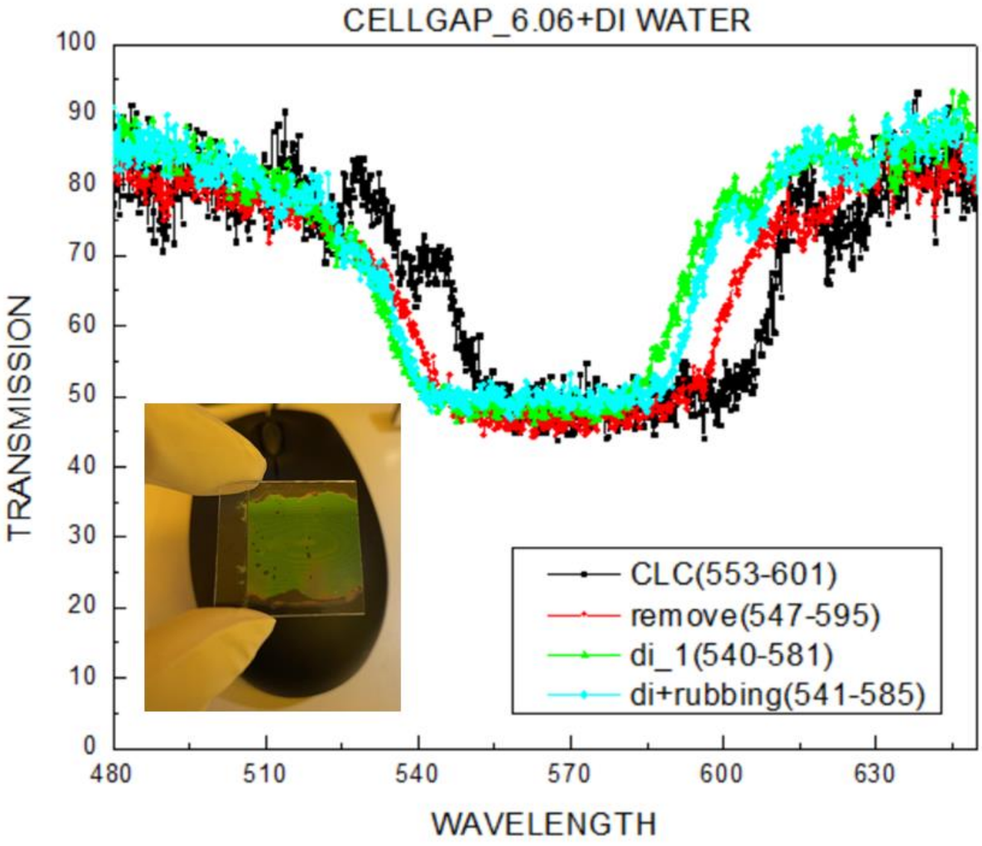

Figure 4- 10 the transmission spectrum variation when coating DI water and the film after coating

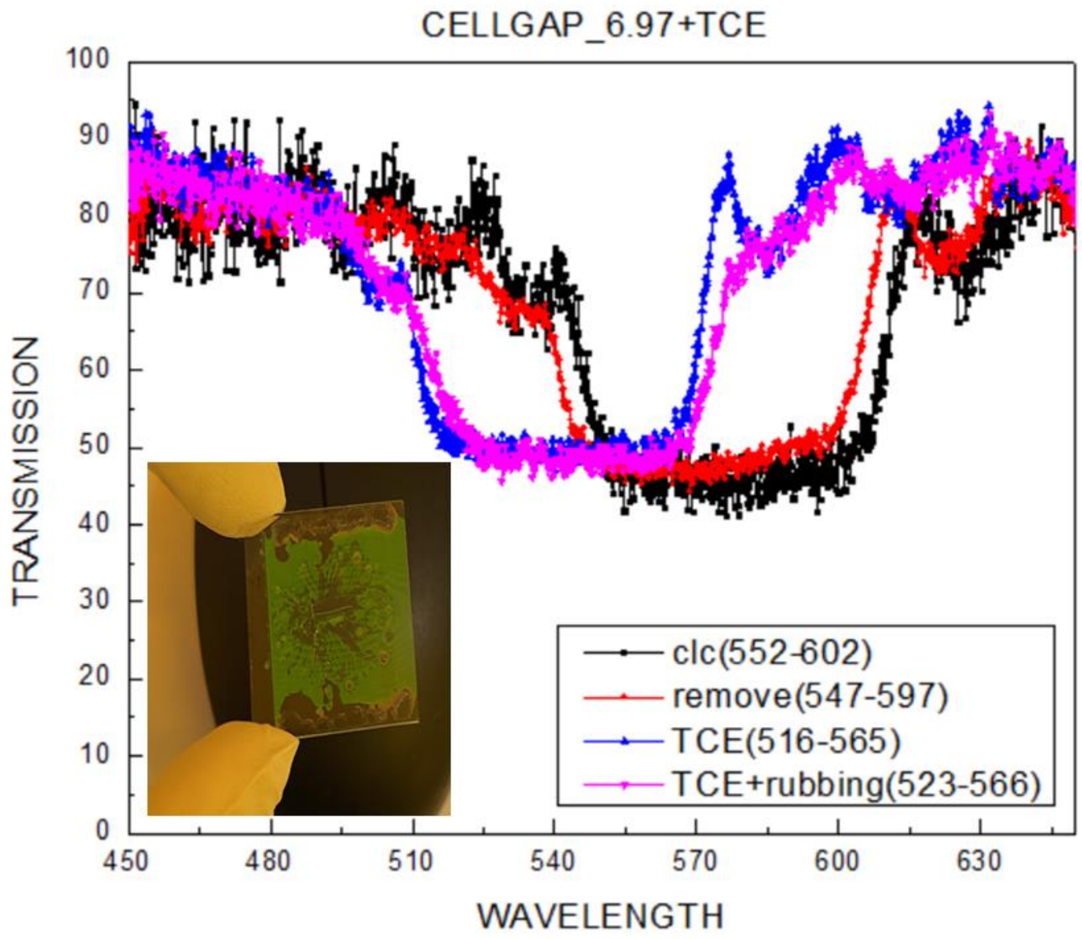

Figure 4- 11 Transmission spectrum variation when coating TCE and the film after coating

There are tradeoffs between coating the alignment layer or not. I further made a compromise for coating the alignment layer on only mirror-based substrate, as the figure 4-5④. I then eliminated the problem that the CLC film would be destroyed but I also offered a better alignment for liquid crystal molecules. The results are displayed as figure 4-12 and Figure4-13. From transmission spectrum, it indicated that there is no wavelength shift when stack-up my sample.

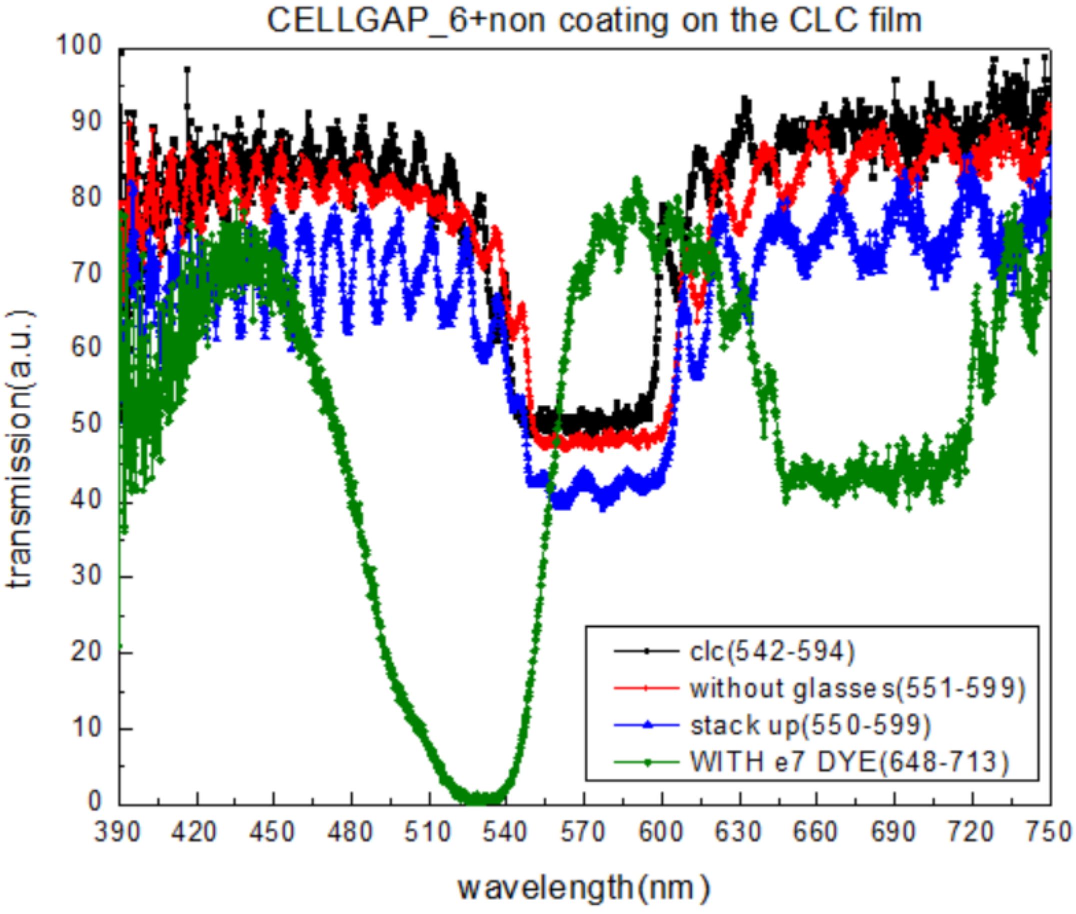

Figure 4- 12 Transmission spectrum variation when fabricating the sample

From Figure4-9 and Figure4-12, no matter with the isolation layer (with the alignment layer or not), I both discovered that the wavelength changed when I filled in dye doped liquid crystal. With the alignment layer on the surface of CLC film, it shifted 120nm. Without the alignment layer, it still shifted 113nm. In the fabrication step, I need to take account of this variation. I will then present the results in the next section. In this paragraph, I talk about the methods I modified to optimize fabrication steps. With the improvement, I am able to receive a better quality CLC film which may lead to higher reflective resonant cavity.

4.2 Optical performance measurement

Finally, I made my CLC film at around 442-482nm. Then, after filling the dye doped liquid crystal, the CLC reflective band edge shifted to the emission range of the dye as Figure1-31 (located at around 590nm). From the reflective image under POM, as Figure 4-13 shows, I observed that the most parts of black dots are removed. Due to the high reflectivity of mirror, it is not possible to directly measure the reflective bandgap of my CLC film. I then made the same structure but without depositing the mirror on the substrate, as the upper left (corner) in figure 4-15. From the reflective spectrum in Figure4-14, the reflective bandgap is around 540nm-595nm. The sample is well-prepared, and I will then measure the laser emission of my sample in the next section.

Figure 4- 13 Microscopy reflective image under POM. The scale of images is 2.33mm*1.75mm.

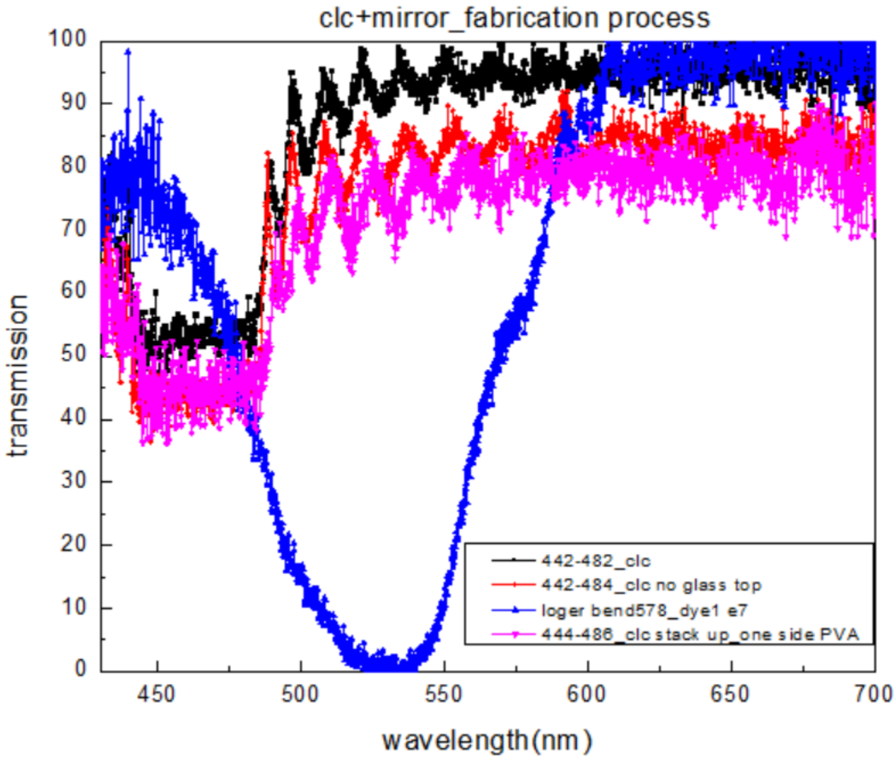

Figure 4- 14Transmission spectrum in each step of fabricating the final sample

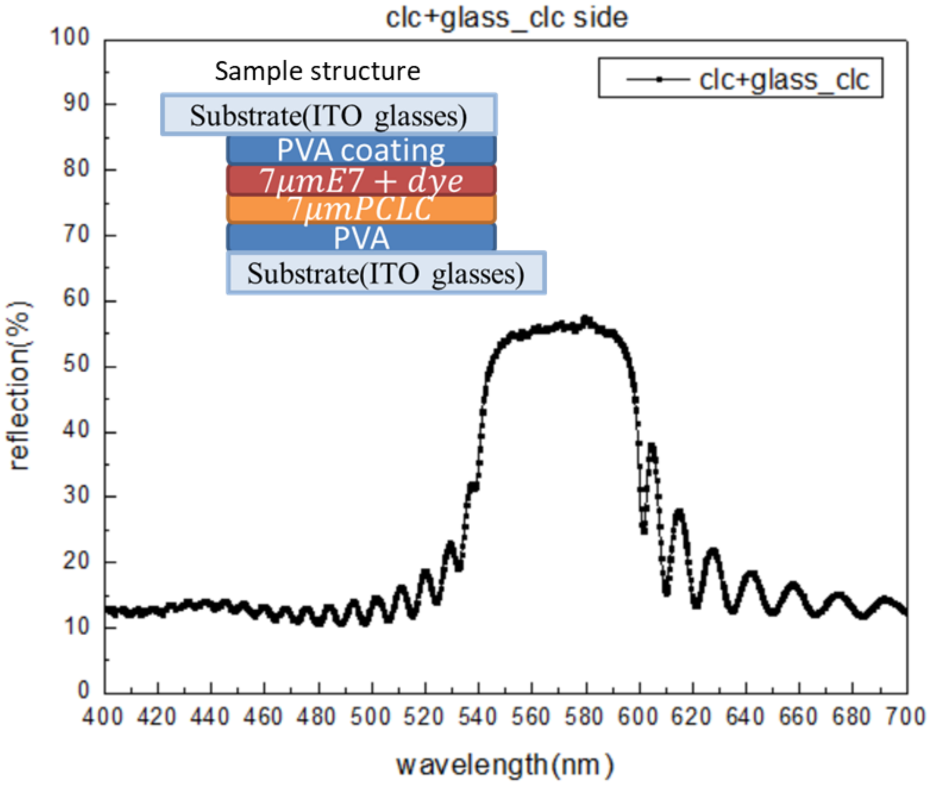

Figure 4- 15 Reflective spectrum of glass based sample and schematic structure is shown in upper left (corner)

4.3 Laser measurement of sample

In this paragraph, I will use the well-prepared samples to measure the laser signals and do the analysis.

4.3.1 Laser emission wavelength and wavelength drift

I measured my sample with laser measurement setup which I mentioned in 3.3.2. I use a 532 nm pulsed laser for pumping multiple random points in the sample. The results are shown in Figure 4-16. The figure recorded the longest and shortest edge of the wavelength drift. From the figure, I observed the laser emission happened at wavelength around 586-593nm. And, the full width at half maximum (FWHM) at 586nm is 4.8nm and at 593nm is 5.5nm, respectively.

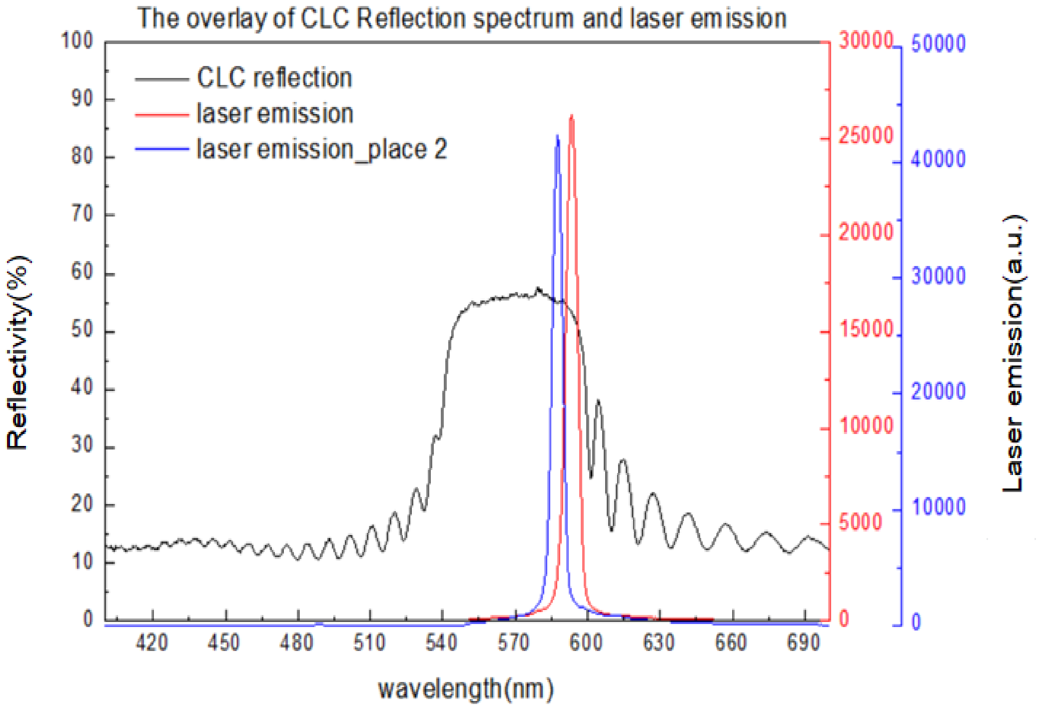

Figure 4- 16 Overlay of CLC Reflection spectrum and laser emission

There are two reasons that results in laser wavelength shift:

A. Cell thickness difference

As I mentioned in introduction, cholesteric liquid crystal molecules are continuous elastomers. For cholesteric liquid crystals, a slight change in cell thickness will cause the cholesteric liquid crystals to change the width of each pitch on the helical axis to equally share the effect of thickness changes. Once the pitch changes, the position of the photon energy gap will also be shifted, and the resonance wavelength of the defect mode will also shift slightly.

B. The orientation of liquid crystal molecules on the surface of liquid crystal film

The alignment direction of the liquid crystal molecules depends on the rubbing alignment. Although I try my best to maintain the accuracy and consistency of each position, I may still make some difference in the whole sample. The final recorded laser results will be different due to a slight difference in different position.

4.3.2 Laser measurement

To check if I am measuring the spontaneous amplification or lasing emission, I further measure input pump intensity and output light emission signal of the sample. The measurement setup is depicted in chapter 3.3.2. For the preliminary measuring setup, I use spectrometer to detect the relative value of light intensity. I measured the laser emission threshold at two different positions of the sample. As shown in Figure 4-17 and Figure 4-18, I measured the dependence of the lasing pulse energy on pump pulse energy at 532 nm. From the figure, I suppose that I get the low spontaneous emission at low pump intensity. Then, with the increasing of the pumping energy, I further got extra high laser emission. By analyzing the peak of the laser, the threshold would be detected. Before achieving the threshold, the points have low slope. After reaching threshold, the laser intensity increased dramatically and the slope became steep we may assume that the laser is produced after the threshold energy. The results point out that I am measuring laser action. These two images recorded at different place reveals roughly the same threshold. I assume that I measured the laser action inside the band gap where is referred as defect mode. This is a preliminary result. And, the further experiment should be done to c the laser emission and the corresponding input power of the threshold of laser.

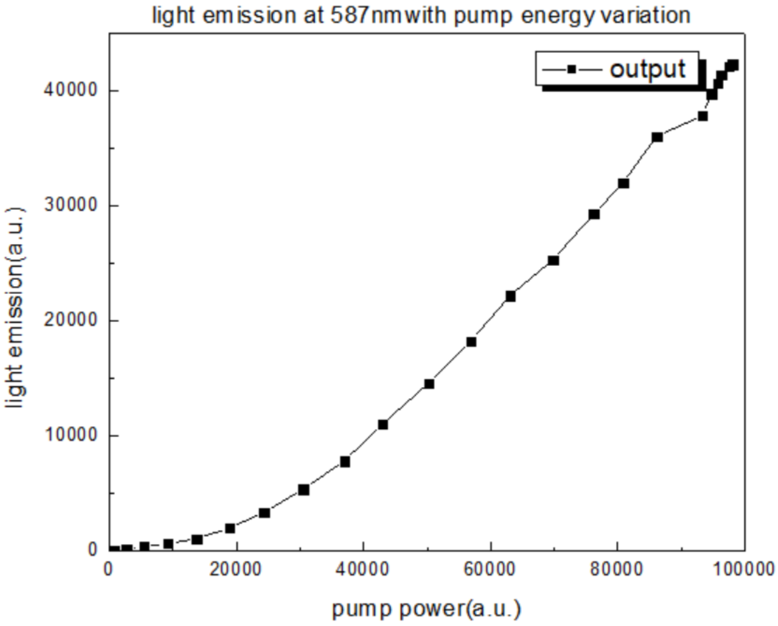

Figure 4- 17 Dependence of the lasing pulse energy on pump pulse energy at 532 nm. The estimated area of the pumping spot is of about 0.1 mm^2.

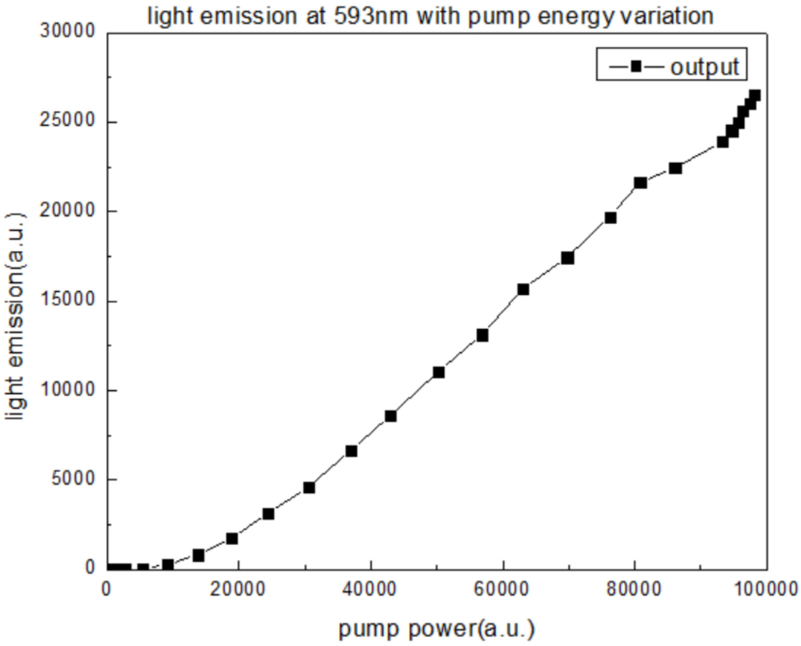

Figure 4- 18 Dependence of the lasing pulse energy on pump pulse energy at 532 nm. The estimated area of the pumping spot is of about 0.1 mm^2.

4.3.3 Mirror application for higher laser intensity

In fabrication process, I deposited the silver on the glass substrate as a mirror. Silver reflects more than 99% of the emission light. To confirm the importance of the amplitude of reflection in the cavity on light emission performance, samples with and without silver layer at the back surface are evaluated. The results of the output energy measurements based on pump energy variation are shown in figure4-19. The slope of the curve corresponds to the slope efficiency but the absolute value could not be obtained. The black line (with silver mirror) has higher slope efficiency. The laser emission of the sample with silver substrate increases faster compared to the sample without silver. In this way, I demonstrate that the sample with the mirror truly enhances light amplification.

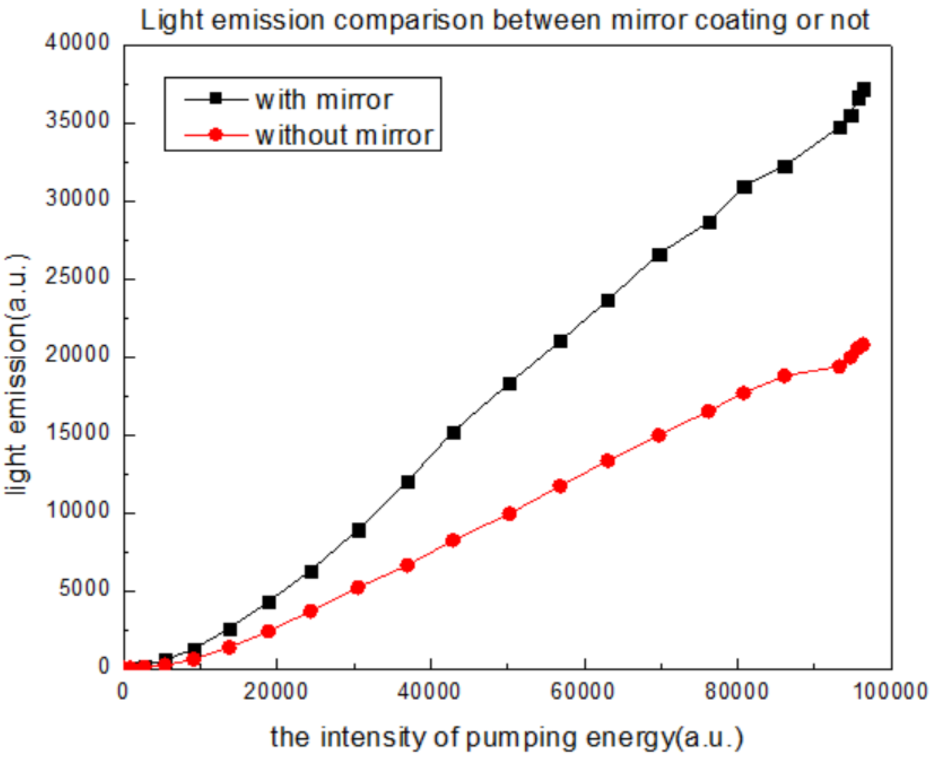

Figure 4- 19 Laser performance comparison between the samples with silver or not

4.4 Lasing wavelength modulation by voltage control

For the purpose of making a tunable laser, I applied a voltage to my sample by a function generator and 10X amplifier. I measured two points at different locations in the cell. At point1, the lasing wavelength was located at 588.7nm without voltage and shifted to 586.1nm when 1kHz 10 Volt was applied. At point 2, the laser wavelength was located at 588.7nm without voltage and shifted to 586.5nm with 1kHz 9 Volt and to 586.1nm with 1kHz 10 Volt, as shown in Figure4-20. By applying 10Volt, the lasing wavelength blue shifts 2.6nm accompanied by a decay of light emission intensity. Liquid crystal in the sample acts as a phase retarder. By applying the voltage, the liquid crystal molecules rotate and give rise to a phase shift. Further, they change the resonance condition in the resonant cavity. Finally, I detect the light emission wavelength shift.

I discovered that the wavelength shift only occurred in specific places which are near the edge of the patterned coating mirror. In the center of the patterned mirror, I could not observe the wavelength shift of the output light emission by the electric field. This experiment had a problem with stability. Initially, I could observe the laser wavelength shift when I applied the voltage. However, after several repetitions, the shift of the wavelength was reduced and finally disappeared. Repeatability is important to make a reliable component.

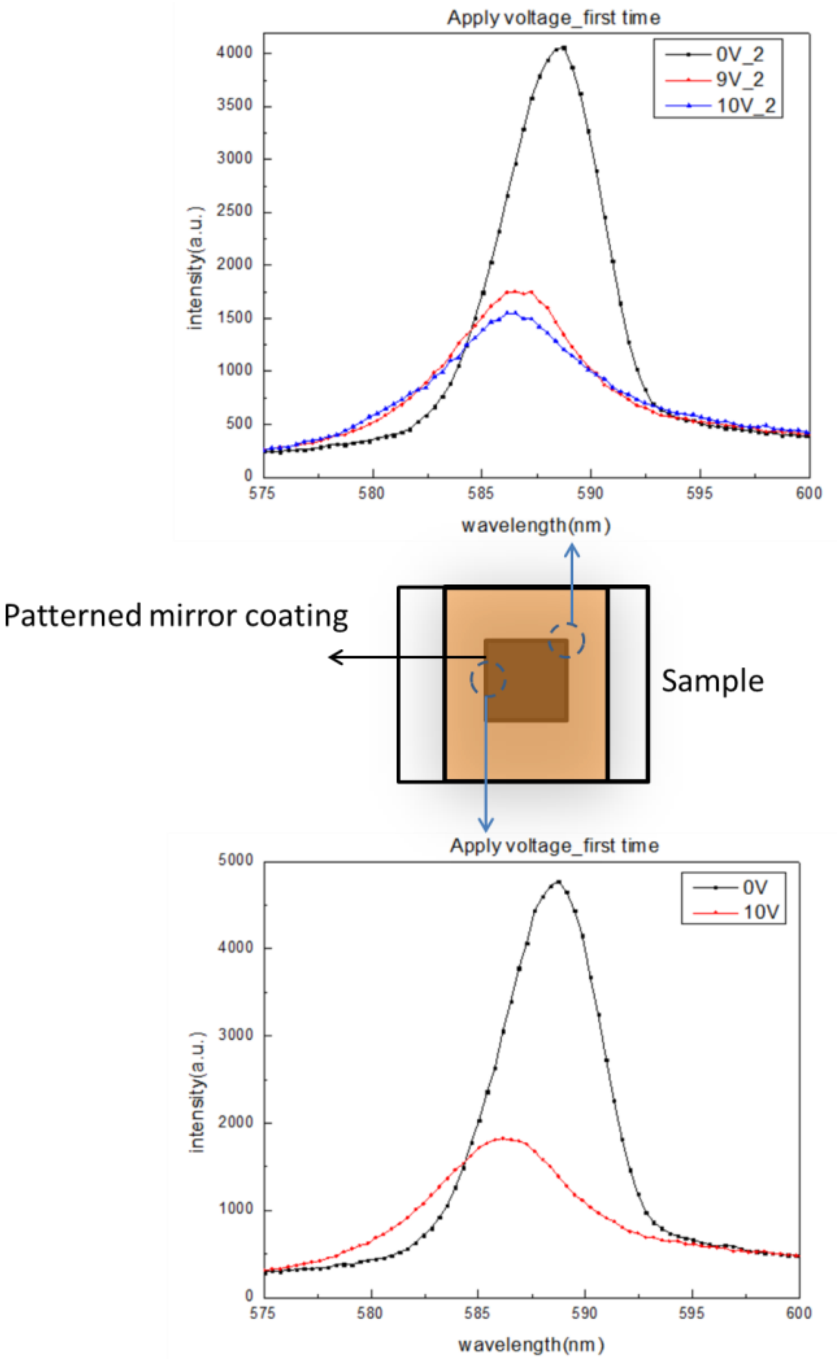

Figure 4- 20 Schematic diagram of sample and the laser shift with different voltages

The problem in voltage application should be solved. Multi-frequency LCR meter is microprocessor-based impedance measuring instrumentation. This device offers LCR components or electronic circuits tested under actual working conditions. I use this device to check the problem in my sample under the working voltage and frequency. The device revealed that the cell without applying voltage has the capacity value about

603pF, as shown in Figure4- 21. But, when I connected the sample which had already applied voltage for several times, I investigated that the capacity dropped to 11pF as Figure 4- 22 shows which means that the contact with the electrodes is lost. Simultaneously, I tested the sample without coating mirror on the glass substrate and with the voltage application. The capacity value I obtained is about 924pF, as shown in the figure4-23. It seems that the mirror coating on the substrate plays an important role on the voltage application.

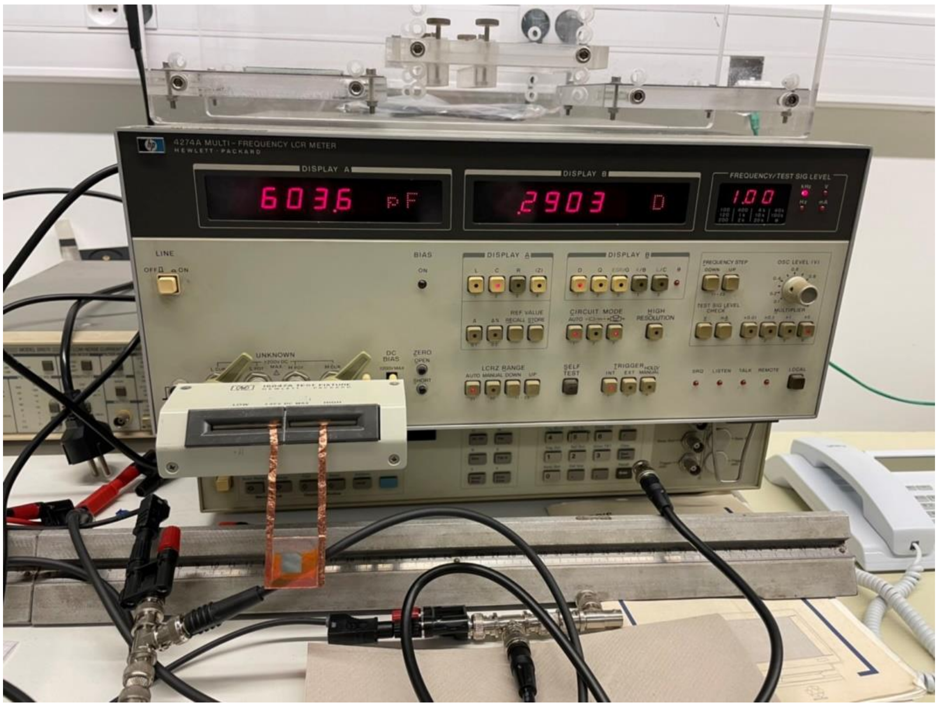

Figure 4- 21 LCR meter Measurement result of the sample with mirror before applying 20 volts

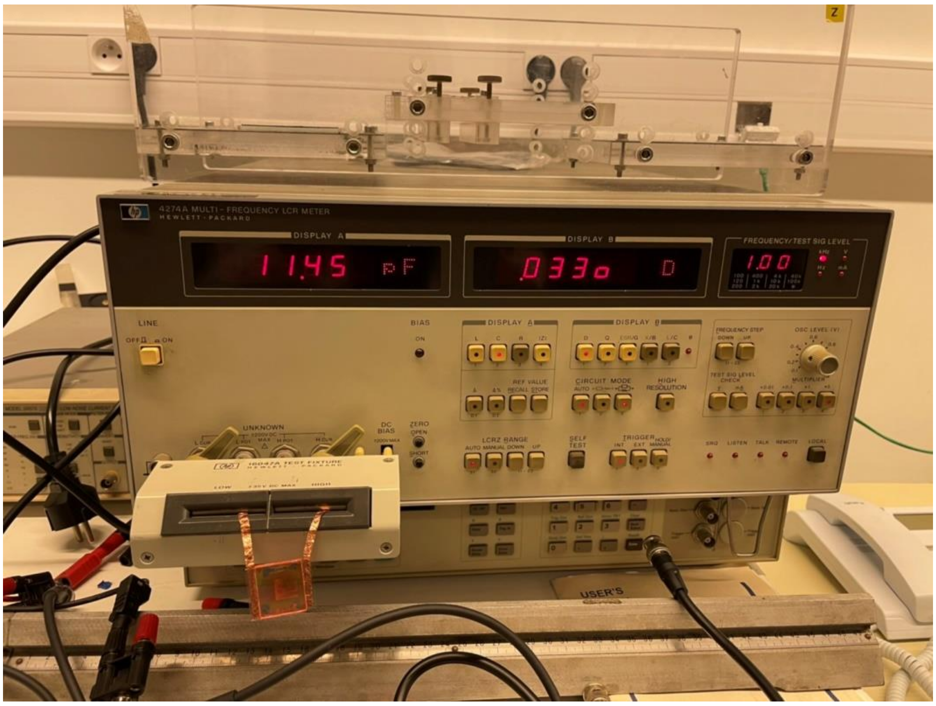

Figure 4- 22 LCR meter Measurement result of the sample with mirror after applying 20 volts

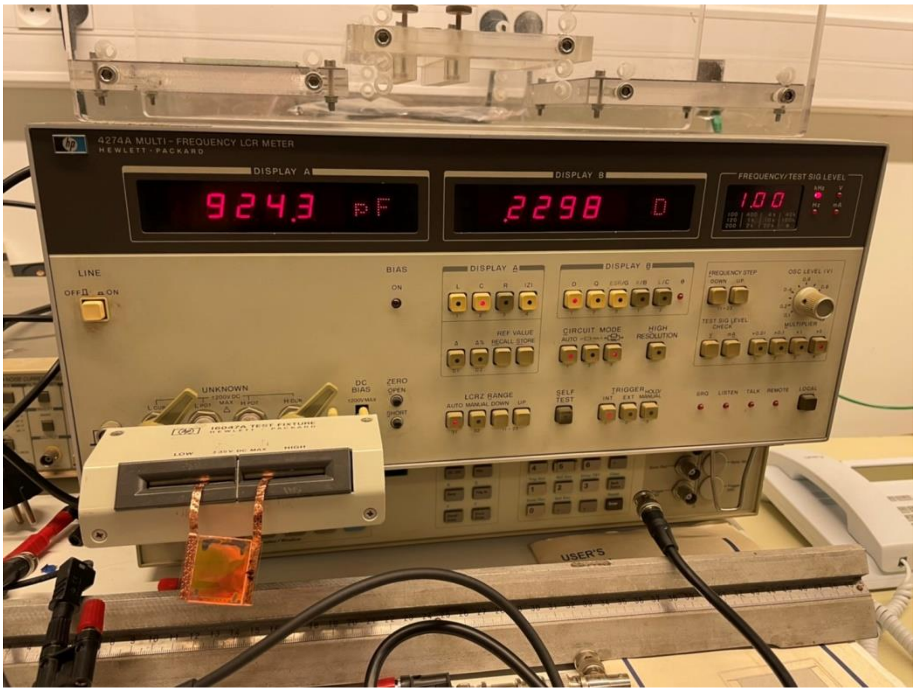

Figure 4- 23 LCR meter Measurement result of the sample without mirror

4.5 Light emission polarization dependence measurement

I placed the polarizer in front of light emission of the sample and I detected that the output signal has polarization dependence. If the director of the polarizer is parallel to the rubbing orientation of the substrate, I would measure the maximum of laser emission. And, if the director of the polarizer is perpendicular to the rubbing orientation of the substrate, I would measure the minimum of light emission, as the below figure shows. The reason is the tendency of the dye. The long axis of the dye will arrange in parallel with the long axis of the liquid crystal. This direction of the dye absorbs the maximum pump energy.

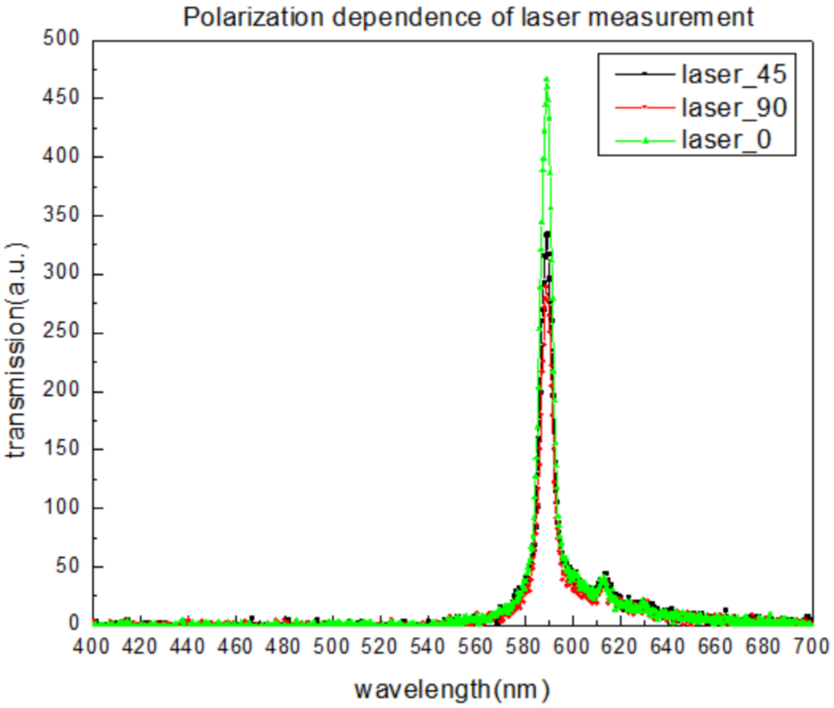

Figure 4- 24 polarization dependence of laser measurement

Chapter 5 Conclusion and prospect

I designed the stack of chiral and nematic dye-doped liquid crystal and I was convinced that it is possible to obtain defect mode laser based on the simulation results by my supervisor Frederik Van Acker. In my research, I improved and optimized the process of making the Cholesteric liquid crystal film so as to obtain high quality resonator. And further, I filled in the dye-doped liquid crystal layer at proper reflective wavelength and solved several fabrication problems. After several trial and error, I made a good-quality sample and successfully measured laser emission signal by laser measurement system.

From the results, I assumed that I measured the photo-luminescence and lasing of my sample. Furthermore, by applying electric field, I investigated the several nanometers wavelength shift. However, there are still some problems when it comes to wavelength modulation. The voltage cannot be continuously applied for a long time.

In the future, it would be interesting to conduct further experiments to confirm the results and solve the modulation problems.

Bibliography

1. McColl, J.R. and C. Shih, *Temperature dependence of orientational order in a nematic liquid crystal at constant molar volume.* Physical Review Letters, 1972. **29**(2): p. 85.
2. Algorri, J.F., et al., *Recent advances in adaptive liquid crystal lenses.* Crystals, 2019. **9**(5): p. 272.
3. Khoo, I.-C. and S.-T. Wu, *Optics and nonlinear optics of liquid crystals*. Vol. 1. 1993: world scientific.
4. Maune, B., et al., *Liquid-crystal electric tuning of a photonic crystal laser.* Applied Physics Letters, 2004. **85**(3): p. 360-362.
5. Collings, P.J. and M. Hird, *Introduction to liquid crystals chemistry and physics*. 2017: Crc Press.
6. Goodby, J.W., et al., *Handbook of liquid crystals, 8 volume set*. Vol. 1. 2014: John Wiley & Sons.
7. Kozawaguchi, H. and M. Wada, *Helical twisting power in cholesteric liquid crystal mixtures. I. Experimental results.* Japanese Journal of Applied Physics, 1975. **14**(5): p. 651.
8. Fergason, J.L., *Cholesteric structure-1 optical properties.* Molecular Crystals and Liquid Crystals, 1966. **1**(2): p. 293-307.
9. De Vries, H., *Rotatory power and other optical properties of certain liquid crystals.* Acta Crystallographica, 1951. **4**(3): p. 219-226.
10. Frank, F.C., *I. Liquid crystals. On the theory of liquid crystals.* Discussions of the Faraday Society, 1958. **25**: p. 19-28.
11. Matos, R., et al., *High-efficiency solar laser pumping by a modified ring-array concentrator.* Optics Communications, 2018. **420**: p. 6-13.
12. Yariv, A., *Quantum Electronics. 3^ rd ed.* New York: John Wiley& Sins, 1989.
13. John, S., *Strong localization of photons in certain disordered dielectric superlattices.* Physical review letters, 1987. **58**(23): p. 2486.
14. Chen, Y., et al., *Recent advances in opal/inverted opal photonic crystal photocatalysts.* Solar RRL, 2021. **5**(6): p. 2000541.
15. Joannopoulos, J.D., R. Meade, and J.N. Winn, *Photonic crystals.* Molding the flow of light, 1995.
16. Joannopoulos, J., R. Meade, and J. Winn, *Photonic Crystals: Molding the Flow of Light.-Princeton, NJ: Princeton Univ.* 1995.
17. Dowling, J.P., et al., *The photonic band edge laser: A new approach to gain*

enhancement. Journal of applied physics, 1994. **75**(4): p. 1896-1899.

18. Dierking, I., *Chiral liquid crystals: structures, phases, effects.* Symmetry, 2014. **6**(2): p. 444-472.
19. Chilaya, G., et al., *Different approaches of employing cholesteric liquid crystals in dye lasers.* Materials Sciences and Applications, 2011. **2**(02): p. 116.
20. Mysliwiec, J., et al., *Liquid crystal lasers: the last decade and the future.* Nanophotonics, 2021.
21. Lu, H., et al., *Wide tunable laser based on electrically regulated bandwidth broadening in polymer-stabilized cholesteric liquid crystal.* Photonics Research, 2019. **7**(2): p. 137-143.
22. Song, M.H., et al., *Effect of phase retardation on defect-mode lasing in polymeric cholesteric liquid crystals.* Advanced Materials, 2004. **16**(9-10): p. 779-783.
23. Jeong, S.M., et al., *Defect mode lasing from a double-layered dye-doped polymeric cholesteric liquid crystal films with a thin rubbed defect layer.* Applied physics letters, 2007. **90**(26): p. 261108.
24. Matsui, T. and M. Kitaguchi, *Finite-Difference Time-Domain Analysis of Twist-Defect-Mode Lasing Dynamics in Cholesteric Photonic Liquid Crystal.* Japanese Journal of Applied Physics, 2012. **51**(4S): p. 04DK02.
25. Matsui, T., M. Ozaki, and K. Yoshino, *Tunable photonic defect modes in a cholesteric liquid crystal induced by optical deformation of helix.* Physical Review E, 2004. **69**(6): p. 061715.
26. Stallinga, S., *Berreman 4× 4 matrix method for reflective liquid crystal displays.* Journal of applied physics, 1999. **85**(6): p. 3023-3031.
27. Mohammadimasoudi, M., et al., *Hybrid fluorescent layer emitting polarized light.* Apl Materials, 2017. **5**(7): p. 076104.
28. Nys, I., J. Beeckman, and K. Neyts, *Electrically tunable Fabry–Perot lasing in nematic liquid crystal cells.* JOSA B, 2014. **31**(7): p. 1516-1524.
29. Lin, F.-H., C.-Y. Ho, and J.-Y. Lee, *The electro-optical characteristics of liquid crystal device in multi-component liquid crystal mixture system with non-contact photo-induced vertical alignment mode.* Optical Materials, 2012. **34**(7): p. 1181-1194.
30. Ishihara, S., et al., *The effect of rubbed polymer films on the liquid crystal alignment.* Liquid Crystals, 1989. **4**(6): p. 669-675.
31. Zhang, F. and D.-K. Yang, *Evolution of disclinations in cholesteric liquid crystals.* Physical Review E, 2002. **66**(4): p. 041701.
32. Inoue, Y., et al., *Improved lasing threshold of cholesteric liquid crystal lasers*

with in-plane helix alignment. Applied Physics Express, 2010. **3**(10): p. 102702.

33. Palto, S., et al., *General properties of lasing effect in chiral liquid crystals.* Opto-Electronics Review, 2006. **14**(4): p. 323-328.